國立臺灣大學生命科學院生化科技學系

博士論文

Department of Biochemical Science and Technology
College of Life Science
National Taiwan University

Doctoral Dissertation

菸草毛狀根的生長與其尼古丁高量累積之研究

Study on the Growth and the Hyper-accumulation of Nicotine in Hairy Roots of *Nicotiana tabacum*

王榮顥

Jung-Hao Wang

指導教授：李昆達 博士

劉啟德 博士

Advisors: Kung-Ta Lee, Ph.D.

Chi-Te Liu, Ph.D.

中華民國 104 年 6 月

June 2015

國立臺灣大學博士學位論文
口試委員會審定書

菸草毛狀根的生長與其尼古丁高量累積之研究

Study on the Growth and the Hyper-accumulation of Nicotine in Hairy roots of *Nicotiana tabacum*

本論文係 王榮顥 君（學號 F97B47114 ）在國立臺灣大學化學系完成之博士學位論文，於民國 104 年 6 月 23 日承下列考試委員審查通過及口試及格，特此證明。

口試委員：

李昆達（簽名）

（指導教授）

劉啓德

張英峯　　賴爾珉

楊健志　　靳宗洛

系主任、所長 黃慶樂（簽章）

誌謝

終於到了要寫致謝詞的時候了。在我大學時沒想到自己會唸研究所，更沒想到有一天會寫博士論文的致謝。完成這篇論文，要感謝的人與事太多了。大三時，李平篤老師教授植物次級代謝時引發我對主題的興趣，大四時林白翎老師與張英峯老師開授的基因體學和蛋白體學讓我對做研究有了興趣。在一開始設計題目時，劉啓德老師跟李昆達給了很多方向的指引，老師正面積極的態度建立我對做研究的信心，讓我能夠一直做到現在。在論文題目上，感謝李昆達老師給我對於決定題目很大的自由，也讓我知道要對自己所感興趣的研究內容負責。感謝李昆達老師與劉啓德老師的支持我進行博士研究。不論在研究上或是在生活上老師都給我很多的照顧。在博士班的歲月中，感謝李昆達老師的全力支持，能夠讓我們在這些昂貴的實驗中不斷的嘗試。在初步設計上，感謝我的大學同學也是現在的博士班同學派，能夠在很多時候跟我討論並給我建議。在一開始的實驗充滿的不順遂，感謝學姊念杰與同學兼室友大仔給我信念上的支持與鼓勵，給了我繼續做下去的信心。從阿拉伯芥換到菸草系統的過程，還好有你們的支持，不然我可能就放棄了。在實驗初期，感謝筱涵、舒晴、子耕、鏡介的努力。我們在一開始跌跌撞撞中能一起找到方向。也很感謝大中、海彥、松輝、以則、科錦的加入，讓研究能更順利與更多面向。跟你們一起工作是我的榮幸。感謝學長阿蘇對實驗室大家的照顧。感謝學弟小宏在實驗上討論、在質體建構上的幫忙，以及論文撰寫討論與校訂。感謝資格考委員李昆達老師、劉啓德老師、楊健楊健志老師、靳宗洛老師、張英峯老師、常怡雍老師、賴爾珉老師的建議，讓實驗能夠大幅改進。感謝楊健志老師在生物資訊分析上的指導與在酵母菌雙雜交試驗的經驗分享。感謝靳宗洛老師在原生質體實驗技術上的指導。感謝劉力瑜老師在統計上的幫忙，並給了我們許多關於性狀分析與轉錄體分析的建議。感謝陳亦然老師提供對蛋白體與代謝體的實驗嘗試。感謝生科院共儀的技術員在轉錄分子與代謝物的定量上的幫助。真的很感謝大家，千言萬語話不盡。最後，我要感謝我的家人與筱涵的支持。從我大學畢業一直到現在這麼長的歲月中，不求回報的容許我追求自己的夢想。謝謝你們。

中文摘要

毛狀根是植物受到根毛農桿菌感染產生的特化組織，常用於根生理的研究中。此外，毛狀根具有快速生長與高次級代謝物累積的特性，故可用於生產植物的次級代謝物。目前人們對於毛狀根誘發、生長調控與次級代謝物累積之機制仍然未知。在本研究論文中，我們利用菸草、能感染菸草的根毛農桿菌 A4，以及菸草著名的次級代謝物尼古丁作為研究模型，希望透過研究毛狀根的生長與次級代謝物累積之機制，來增進毛狀根的應用性。在生長調控的部分，我們聚焦於根毛農桿菌 A4 之 T_L-DNA 中的四個 *rol* 基因，分別是 *rolA*、*rolB*、*rolC* 和 *rolD*。目前已知這些基因對於促進毛狀根形成有關，但他們參與在形成或是維持毛狀根型態中所扮演的角色仍未知。本篇研究中，我們在農桿菌中分別剔除了四個 *rol* 基因，並利用這些 *rol* 缺陷農桿菌來誘導毛狀根。我們發現，當農桿菌缺少 *rolB* 或 *rolC* 時，會延遲發根並減少發根率。而缺少 *rolA* 或 *rolD* 時沒有這個現象。此外，由缺少 *rolB* 或 *rolC* 農桿菌感染所得的毛狀根會產生較少的側根數，且無法在長時間繼代中存活。而 *rolA* 或 *rolD* 時則不具有這些現象。我們認為 *rolB* 和 *rolC* 是主要調控生長的因子。藉由寡核苷酸微陣列分析，缺少 *rolB* 或 *rolC* 的毛狀根中脂質轉移蛋白與活性氧分子相關基因表現量顯著低於由野生型農桿菌感染生成的毛狀根。我們也發現側根越多的毛狀根，就會擁有越高的脂質轉移蛋白表現量。我們也比較了由野生型農桿菌感染產生的毛狀根與菸草原生根的轉錄體差異，發現這些脂質轉移蛋白的表現量確實在毛狀根中大量累積。除脂質轉移蛋白外，我們利用 ROS 染劑對缺陷 *rolB* 或 *rolC* 的毛狀根染色，發現缺失 *rolB* 或 *rolC* 時會有較低量的活性氧分子。藉此我們推論在毛狀根的生長調控中，脂質轉移蛋白與活性氧分子含量的改變是重要的因子。在次級代謝物的調控方面，我們發現隨機挑選出來的菸草毛狀根含有的尼古丁量都遠大於菸草原生根，而且尼古丁的含量與新菸鹼具有正相關，顯示在毛狀根中的次級代謝路徑可能整體被提高：尼古丁的代謝路徑以及儲存相關的運送蛋白在毛狀根中大量表現，造成尼古丁的累積。此外，我們發現生長較快速的菸草毛狀根含有較多的尼古丁，顯示毛狀根的生長與尼古丁的累積可能受

到相關因子調控。而尼古丁在毛狀根中的累積非受到茉莉花酸訊息傳遞路徑的誘導，但依舊提升由茉莉花酸路徑啟動之乙烯反應因子 189 和 199 的表現量，進而增加關鍵酵素腐胺-N-甲基轉移酶與 N-甲基腐胺氧化酶的表現。我們的發現提供了一個簡單篩選高次級代謝物毛狀根的方法：測量毛狀根的生長速率。我們認為，這個結果可以大幅促進毛狀根在次級代謝物生產的研究與其應用性。

關鍵詞：根毛農桿菌、菸草、毛狀根、*rol* 基因、次級代謝物、尼古丁。

Abstract

Hairy root, which resulted from T-DNA transformation of *Agrobacterium rhizogenes*, is widely used in studying root biology. It is also applied in producing diverse plant secondary metabolites due to its fast-growth and metabolite-accumulating abilities. However, the regulatory mechanisms of hairy root initiation, growth, and metabolite accumulation are largely unknown. To expand the applicability of hairy roots, we used *Nicotiana tabacum* L. var Wisconsin 38, its pathogen *A. rhizogenes* A4, and its well-known metabolite nicotine as a study model to unveil the mechanisms that regulate hairy root growth and secondary metabolite accumulation. In the part of growth regulation, we focused on four *rol* genes, including *rolA*, *B*, *C*, and *D*, which are located on T_L-DNA of *A. rhizogenes* A4. These *rol* genes are known to participate in rooting; however, the means by which the *rol* genes contribute to the initiation and the maintenance of hairy roots remain unknown. In this study, we knocked-out these *rol* genes in *A. rhizogenes* A4 respectively, and used for inducing hairy roots. We found that *A. rhizogenes* lacking *rolB* or *rolC* induced hairy roots with less rooting ability than wild-type *A. rhizogenes*, whereas lacking *rolA* or *rolD* showed no significant differences. Moreover, tobacco hairy roots lacking either *rolB* or *rolC* exhibited fewer branch roots and lost their growth ability after long-term subculture than wild-type-induced hairy roots, whereas lacking of *rolA* or *rolD* did not show significant differences. We considered *rolB* and *rolC* involved mainly in the regulation of hairy root growth. Our microarray analysis revealed that the expression of several groups of genes encoding lipid transfer proteins (LTP) and reactive oxygen species (ROS)-related genes was significantly suppressed in *rolB*- or *rolC*- deficient hairy roots. We also found that

hairy root clones that exhibited greater branching also had higher levels of RolB, RolC, and the microarray-identified LTP genes. In addition, we compared the transcriptomic difference between hairy roots and un-infected intact roots by microarray, and the expression levels of the above mentioned LTP-encoding genes were dramatically higher in the hairy root. Moreover, ROS staining showed that ROS level were lower in *rolB*- or *rolC*- deficient hairy roots. We therefore suggest that up-regulating LTP and increasing the level of ROS are important for hairy root growth. In the part of secondary metabolite regulation, we found that tobacco hairy roots accumulate much more nicotine than the intact roots, and the nicotine contents were positively correlated with the amount of another metabolite anabasine, indicating hairy roots had higher secondary metabolic flux. By real-time PCR analysis, hairy roots had more abundant expression of genes encoding enzymes in nicotine biosynthetic pathway and storage transporters, indicating the accumulation of nicotine in hairy roots is via transcriptional regulation. Moreover, hairy roots with a higher growth rate had greater nicotine content, suggesting that growth and nicotine production are regulated synchronically. Nicotine up-regulation in hairy roots was regulated by ethylene response factor (ERF)189 and ERF199 to activate the key enzymes putrescine N-methyltransferase and N-methylputrescine oxidase with a jasmonic acid (JA)-independent signal. However, the possible regulator has not been identified. These findings indicate high secondary metabolites accumulated hairy root clones can be simply selected by measuring their growth rate, which expand the hairy root researches and applications in secondary metabolites.

Key words: *Agrobacterium rhizogenes*, *Nicotiana tabacum*, hairy root, *rol* genes, secondary metabolites, nicotine.

Contents

誌謝 i

中文摘要 iii

Abstract v

Contents vii

Contents of Tables xiii

Contents of Figures xv

Abbreviations xvii

Chapter 1: Introduction

1. *Agrobacterium* 1

1.1. T-DNA transferring mechanism (infection mechanism) 2

1.1.1. Attachment 2

1.1.2. T-DNA processing and exporting from bacterium 4

1.1.3. Nuclear targeting and chromosomal integrating 4

1.2. Crown gall 6

1.3. Opine 8

1.4. Hairy root 8

2. Genes on *Agrobacterium rhizogenes* T-DNA 9

2.1. *rolA* 12

2.1.1. *rolA* affects plant morphogenesis 12

2.1.2. *rolA* and plant hormone 13

2.1.3. *rolA* promoter 13

2.1.4. RolA biological functions 14

2.2. *rolB* 15

2.2.1. *rolB* affects plant morphogenesis 16

2.2.2. *rolB* and auxin 16

2.2.3. *rolB* promoter 18

2.2.4. RolB biological function 20

2.3. *rolC* 20

2.3.1. *rolC* affects plant morphogenesis 21

2.3.2. *rolC* and auxin 22

2.3.3. *rolC* and cytokinin 22

2.3.4. *rolC* and gibberellins 23

2.3.5. *rolC* promoter 23

2.4. *rolD* 24

2.5. *orf3n* 25

2.6. *orf8* 25

2.7. *orf13* and *orf14* 27

2.8. *orf13a* 29

3. Plant secondary metabolites 29

3.1. Secondary metabolites in hairy root 31

3.2. *rolA* affects secondary metabolites 32

3.3. *rolB* affects secondary metabolites 33

3.4. *rolC* affects secondary metabolites 34

4. Nicotine regulatory mechanism 36

5. Objectives 39

Chapter 2: Materials and Methods

1. General DNA manipulation 41

1.1. DNA quantification 41

1.2. Plasmid DNA extraction from *E. coli* 41

1.3. Polymerase chain reaction (PCR) 42

1.4. DNA purification 43

1.5. Cloning by restriction-ligation method 44

1.6. Cloning by Gateway system 45

1.7. Total DNA isolation from *A. rhizogenes* 45

1.8. Plasmid DNA extraction from yeast 46

2. General RNA manipulation 47

2.1. RNA quantification and quality control 47

2.2. RNA extraction from plant tissue 47

2.3. First-strand cDNA synthesis 48

2.4. Quantification reverse transcription polymerase chain reaction 49

3. General protein manipulation 50

3.1. Protein quantification 50

3.2. Total protein extraction from yeast 50

3.3. Total protein extraction from plant tissue 51

4. Microorganisms transformation 51

4.1. *E. coli* transformation by heat shock 51

4.2. *A. rhizogenes* transformation by electroporation 52

4.3. Yeast transformation by lithium acetate (LiAc) mediated method 53

5. Individual *rol* genes deficient strains generation 54

5.1. Generation of individual *rol* genes deficient strains 54

5.2. Confirmation using Southern blot 56

6. Transcriptional and translational fusion 57

6.1. Generation of destination vector pGWYFP 57

6.2. Expression clones establishment 58

7. Hairy root induction 59

7.1. N. tabacum W38 growing 59

7.2. Hairy root induction 60

7.3. Hairy root confirmation 61

8. Microarray assay and data analysis 62

9. Quantification of alkaloids 63

10. Yeast two-hybrid 64

10.1. Bait protein construction 64

10.2. Poly A+ RNA purification 64

10.3. cDNA synthesis and amplification 65

10.4. Gal4 DNA activation domain fused cDNA library of hairy root 66

11. Phosphatase activity assay 66

Chapter 3: Results and Discussion

Transcriptomic analysis reveals that ROS and genes encoding LTPs are associated with tobacco hairy root growth and branch development

Results

1. *rol* genes deficient *A. rhizogenes* mutants grew faster than wild-type. 69

2. Δ*rolB* and Δ*rolC A. rhizogenes* mutants have decreased hairy root induction ability 71

3. Aberrant hairy roots induced by *rol*-deficient *A. rhizogenes* mutants 73

4. Microarray data analysis 78

5. The expression levels of genes encoding LTPs were related to hairy root growth 83

6. ROS accumulate in hairy roots but decrease when either *rolB* or *rolC* is knocked out 85

Discussion 87

Fast-growing *Nicotiana tabacum* hairy roots accumulate more nicotine than slow-growing hairy roots due to systematic up-regulation of nicotine biosynthetic genes

Results

1. Nicotine accumulated in *N. tabacum* hairy roots 92

2. Positive corrections were found between the contents of nicotine and nornicotine and between the contents of nicotine and anabasine in hairy roots 93

3. Transcripts of the nicotine biosynthetic gene were up-regulated in hairy roots 94

4. Growth rate and nicotine content were positively correlated in hairy roots 97

5. The jasmonic acid pathway is not the activator of nicotine biosynthesis in hairy roots 99

Discussion 100

Chapter 4: Perspectives

1. Functional exploration of LTPs 107

2. Exploring the biochemical function of RolB and RolC proteins 108

3. The mechanism of secondary metabolite accumulation in hairy roots 113

Chapter 5: Conclusion 117

References 119

Appendix 155

Contents of Tables

Table 1-1. Secondary metabolites accumulations in hairy root tissues. 31

Table 1-2. Secondary metabolites affected by *rol* genes. 32

Table 3-1. GO results for transcripts down-regulated in HRΔ*rolB* compared with HRWT. 80

Table 3-2. GO results for transcripts down-regulated in HRΔ*rolC* compared with HRWT. 81

Table 3-3. GO results for transcripts up-regulated in HRWT compared with tobacco intact roots. 82

Table 3-4. The expression levels of *rolB*/*C* and LTPs in hairy root clones with different branch root densities. 84

Supplementary Table S1. Reference genes for qRT-PCR. 155

Supplementary Table S2. PCR conditions. 156

Supplementary Table S3. Primer used in this study. 158

Contents of Figures

Figure 1-1 The *rol* genes and the other loci on *A. rhizogenes* A4 T_L-DNA. 10

Figure 1-2 The overview of *rolB*-mediated plant responses. 15

Figure 1-3 Biosynthetic pathway, transportation, and storage of nicotine. 37

Figure 2-1 Mechanism of homologous recombination. 55

Figure 2-2 pGWYFP vector for *rol* gene complement. 58

Figure 2-3 Inducing tobacco hairy root. 61

Figure 3-1 Southern blot confirmation of respective *rol* gene deficient strains. 70

Figure 3-2 The growth curves of wild-type and respective *rol* genes deficient *A. rhizogenes*. 70

Figure 3-3 The day of the first root emergence post infection (DREPI). 72

Figure 3-4 Primary root number per leaf disc (R/L ratio). 73

Figure 3-5 Morphology of hairy roots at 18 days post-subculture. 74

Figure 3-6 Population distribution of the different hairy root architecture parameters. 76

Figure 3-7 Box plot analysis of hairy root architecture. 77

Figure 3-8 ROS content of HRWT, HRΔ*rolB*, and HRΔ*rolC*. 86

Figure 3-9 Nicotine contents in intact roots, excised roots, and hairy roots. 92

Figure 3-10 The correlation between the contents of (A) nicotine and nornicotine and (B) nicotine and anabasine in tobacco hairy roots. 94

Figure 3-11 Transcripts analysis of the nicotine biosynthetic genes. 96

Figure 3-12 The relationship between (A) nicotine content and growth, (B) the expression levels of *rolC* and growth, and (C) expression levels of *rolB* and *rolC*. 98

Figure 3-13 The transcript levels of AP2/ERFs in intact roots and hairy root clones 9, 22, and 3. 100

Figure 4-1 Sequence clustering of LTPs identified from microarray. 108

Figure 4-2 RolC has transcriptional activity in yeast. 112

Abbreviations

A. belladonna	*Atropa belladonna*
A. rhizogenes	*Agrobacterium rhizogenes*
A. rubi	*Agrobacterium rubi*
A. tumefaciens	*Agrobacterium tumefaciens*
A. vitis	*Agrobacterium vitis*
aa	amino acid
ABA	abscisic acid
AbA	aureobasidin A
ACC	1-aminocyclopropane-1-carboxylic acid
AD	activation domain
adc	arginine decarboxylase
ADE2	gene encoding Phosphoribosylaminoimidazole carboxylase, involving in adenine synthesis
ANOVA	analysis of variance
ao	aspartate oxidase
AP2 domain	APETALA2 domain
At	*Arabidopsis thaliana*
AUR1-C	inositol phosphorylceramide synthase
BD	binding domain
BiFC	bimolecular complementation
bp	base pair
bZIP	basic lucine zipper
C. roseus	*Catharanthus roseus*
CaMV	*Cauliflower mosaic* virus promoter
cDNA	complementary DNA
CDPK; CPK	calcium-dependent protein kinase
chv	chromosomal virulence genes
DAD	diode array detector
DF	deleting fragment
Dof	DNA binding with one finger
dpi	day post induction
dps	day post subculture
DMSO	dimethyl sulfoxide
DREPI	the day of the first root emergence post induction
dsDNA	double-stranded DNA
EDTA	Ethylenediaminetetraacetic acid
ef-1α	elongation factor 1α
ERF	ethylene response factor
GA	gibberellic acid
GAL4	galactose induced gene
GST	glutathione transferase
HA	hemaglutinin
HIS3	gene encoding Imidazoleglycerol-phosphate dehydratase, involving in histindine synthesis
HRΔ*rolA*	hairy root induced by Δ*rolA A. rhizogenes* A4
HPLC	high-performance liquid chromatography
IAA	indole-3-acetic acid
iaaH	gene encoding indole acetamide hydrolase

iaaM	gene encoding tryptophan 2-monooxygenase
IAM	indole-3-acetamide
ILA	indole-3-lactate
ipt	isopentenyl transferase
IPTG	Isopropyl β-D-1-thiogalactopyranoside
JA	jasmonic acid
JAs	jasmonic acid and its derivates
JAT1	jasmonate-inducible alkaloid transporter 1
JAZ	JASMONATE-ZIM DOMAIN
k. daigremontiana	*kalanchoë daigremontiana*
L25	L25 ribosomal protein
LB	left border
LB medium	Luria-Bertani medium
LRD	first-order lateral root densities per centimeter of main root
LRN	first-order lateral root numbers per main root
LTP	lipid transfer protein
LPS	lipopolysaccharide
M. sexta	*Manduca sexta*
mate	multi-drug and toxic compound extrusion
meJA	methyl-jasmonic acid
MEL1	gene encoding alpha-galactosidase
mpo	methylputrescine oxidase
MRL	main root length
MS	Murashige and Skoog medium
N. tabacum	*Nicotiana tabacum*
Nt	*Nicotiana tabacum*
NtBBF1	*Nicotiana tabacum rolB* domain B factor 1
NtBRF1	*Nicotiana tabacum rol* binding factor 1
Ntcp-23	*Nicotiana tabacum* circadian protein 23
Ntubc2	*Nicotiana tabacum* ubiquitin-conjugating enzyme E2
ODC	onithine decarboxylase
ORF	open reading frame
P. ginseng	*Panax ginseng*
phi-2	phosphate-induced gene 2
pmt	putrescine N-methyltransferase
*p*NPP	*para*-nitrophenylphosphatase
pp2A	protein phosphatase 2A
PR	pathogen-related
qpt	quinolinic acid phosphoribosyl transferase
qs	quinolinic acid synthase
R. cordifolia	*Rubia cordifolia*
rat	resistant to *Agrobacterium* transformation
RB	right border
Ri plasmid	root-inducing plasmid
RL ratio	primary root numbers per leaf disc on 21 day post induction
rol	root loci
ROS	reactive oxygen species
SA	salicylic acid

samdc	S-adenosylmethionine decarboxylase
sams	S-adenosylmethionine synthase
SD medium	synthetic defined medium
SOEing PCR	Splicing by overlap extension polymerase chain reaction
spds	spermidine synthase
ssDNA	single-stranded DNA
SSH	suppression substrative hybridization
T-DNA	transfer-DNA
tac-9	tobacco actin 9
Taq	*Thermus aquaticus*
TC	transcriptional fusion
Ti plasmid	tumor-inducing plasmid
TL	translational fusion
TLRL	total first-order lateral root lengths per main root
tubA1	α-tubulin
uidA, GUS	β-D-glucuronidase
UPP	unipolar polysaccharide
UTR	untranslated region
V. amurensis	*Vitis amurensis*
vir	virulence
WT	wild-type
YFP	yellow fluorescent protein

Chapter 1: Introduction

1. *Agrobacterium*

Agrobacterium, which belongs to the family Rhizobiaeae, is a genus of gram negative soil bacteria. Some species of *Agrobacterium* are plant pathogens which can cause a variety of neoplasm symptoms after infecting plant. For example, *A. tumefaciens* and *A. vitis* cause crown gall disease, *A. rubi* causes cane gall disease, and *A. rhizogenes* causes hairy root disease. It is believed that these disease symptoms are caused by inter-kingdom gene transfer from *Agrobacterium* to host plant. These transferred genes were located on the transferred DNA (T-DNA), which is harbored in the tumor-inducing plasmid (pTi) of *A. tumefaciens* and *A. vitis*, or the root-inducing plasmid (pRi) of *A. rhizogenes*.

pTi and pRi are approximate 200-300 kbp in size. In addition to T-DNA, these plasmids encode genes with function in plasmid conjugation, T-DNA processing and transfer, and opine catabolism. T-DNA is the region of approximate 10-30 kbp flanked by two border sequences, which are called left border (LB) and right border (RB). In general, the border sequences are 25 bp in length with directly repeated orientation (Yadav et al. 1982; Zambryski et al. 1982). The RB is essential for tumorigenesis and rhizogenesis, and it directs T-DNA replication for transfer from RB to LB (Shaw et al. 1984; Wang et al. 1984). In contrast, the LB is dispensable for tumorigenesis and rhizogenesis; therefore, some of the transformation might lose the sequences near the left border and some would carry plasmid sequences out of the LB (Joos, H. 1983). In addition, some of bacterial chromosome sequences could be transferred into plant genome (Ulker et al. 2008). These *Agrobacterium*-mediated DNA transfer events promote inter-kingdom gene flow.

Due to the ability of gene transfer, *Agrobacterium* species are widely applied in plant genetic transformation via binary vector strategy to study gene function, promoter trapping, and metabolic engineering (Hoekema et al. 1983). Moreover, *Agrobacterium* could transfer gene to many other eukaryotic cells, including fungi and animal cells (Lacroix et al. 2006). DNA transferring mechanism and the characterizations of hairy root are described in the following sections.

1.1. T-DNA transferring mechanism (infection mechanism)

There are three major steps occurring during T-DNA transfer process. First, the bacteria attach to the host cell. Second, the *vir* operon of *Agrobacterium* is activated by plant-derived phenolic compounds, and the T-DNA is processed and transferred to plant cell by Vir proteins. Finally, the T-DNA is transferred into plant nucleus and integrated into chromosome DNA with the aid of host plant proteins. These processes have been reviewed in many articles (winans 1992; Costantino et al. 1994; Ziemienowicz 2001; Tzfira and Citovsky 2002; Cascales and Christie 2003; Brencic and Winans 2005; Chen 2005; Christie et al. 2005; McCullen and Binns 2006; Rodriguez-Navarro et al. 2007; Gelvin 2010a, b; Pitzschke and Hirt 2010). The brief introduction of T-DNA transportation from *Agrobacterium* to plant cell is presented below.

1.1.1. Attachment

Microorganisms attach to their host plants before symbiosis or pathogenesis. In *A. tumefaciens*, several attachment strategies have been identified: flagellum-dependent attachment, pili attachment, and unipolar polysaccharide (UPP) adhesin (reviewed by Heindl et al. 2014). Before attachment, *Agrobacterium* forms biofilm with a hydrated macromolecular matrix that consists of exopolysaccharides,

extracellular DNA, and proteins (Costerton et al. 1995; Flemming and Wingender 2010). To date, six biofilm-forming polysaccharide species have been identified in *A. tumefaciens*, these are UPP adhesin, cellulose, succinoglycan, cyclic β-1,2-glucans, β-1,3-glucans, and membrane lipopolysaccharides (LPS). UPP mediates polar attachment of *A. tumefaciens* to plants or other surface (reviewed by Matthysse 2014). Presence of bacterial cellulose enhances the attachment, and the lose of cellulose shows a slightly reduced ability of tumor formation (Matthysse et al 1981; Matthysse, 1983; Mattysse et al. 2005). Cyclic β-1,2-glucans is required for biofilm formation and virulence (Dougals et al. 1982; Xu et al. 2012). Succinoglycan and β-1,3-glucans have little effects on biofilm formation and tumor formation (Tomlinson et al. 2010; Ruffing and Chen 2012; Xu et al. 2012). No conclusive result to date has demonstrated the LPS affects biofilm formation and bacteria-plant attachment. Overall, some forward genetic approaches have indicated kinds of polysaccharides participate in attachment, but the detail mechanism of bacterial attachment remains unclear.

On the other side, plant surface molecules provide recognition for pathogen. A group of *Arabidopsis* resistant to *Agrobacterium* transformation (*rat*) mutants were isolated, and some of them were poorly bound with *A. tumefaciens* (Zhu et al. 2003). A well-characterized mutant, *rat1*, which showed a reduced expression level of the cell wall arabinogalactan protein, decreases the binding of bacteria (Zhu et al. 2003; Gaspar et al. 2004). Further studies are needed to unveil the interaction between *Agrobacterium* and host cells.

1.1.2. T-DNA processing and exporting from bacterium

Plant signals initiate the T-DNA processing step. Naturally, phenolic compounds activate the VirA/VirG two component system, which is constitutively expressed at a basal level and is highly induced in a positive feedback manner by plant signals (Stachel et al. 1985; Winans et al. 1988). The VirA is a membrane bound sensor kinase, which perceives phenols, aldose monosaccharides, low pH, and low phosphatase. Upon receiving plant signal, VirA auto-phosphorylates itself, and then the phosphate group is transferred to cytoplasmic regulator VirG. The phosphorylated VirG binds at *vir* boxes of *vir* promoter and activates transcription to initiate T-DNA processing (reviewed by Palmer et al. 2004; Brencic and Winans 2005).

After production of Vir proteins, *Agrobacterium* generates single stranded T-DNAs (Stachel and Nester 1986). In *A. tumefaciens*, VirD2 cleaves and covalently binds to the 5' end of T-DNA right border to form an immature T-complex, which is VirD2-ssT-DNA complex. This complex would be recruited and translocated into plant cells by bacterial type IV secretion system, which is composed of 11 different VirB proteins and the VirD4 (reviewed by Chen et al. 2005). In addition to VirD2-ssT-DNA complex, other Vir factors, including VirE2, VirE3, VirF, and VirD3, from *Agrobacterium* are translocated into plant cells during infection (Vergunst et al. 2000; Vergunst et al 2005).

1.1.3. Nuclear targeting and chromosomal integrating

After VirD2-ssT-DNA imported into the plant cell, VirE2 coats the single stranded T-DNA to form a mature T-complex, which is VirD2/VirE2/T-DNA complex. This VirD2/VirE2/T-DNA complex is a highly ordered structure to facilitate transport through the nucleopore complex (Duckely and Hohn 2003). VirD2 and

VirE2 occupy the surface of single stranded T-DNA to resist nuclease, and both VirD2 and VirE2 contain nucleus localization signals for plant importin recognition. The mature T-complex is transported into host nucleus with the aid of plant alpha type importin (Koncz et al. 1989; Tinland et al. 1995; Deng et al. 1998; Bakó et al. 2003; Bhattacharjee et al. 2008). VirE2 has been suggested to have an additional function as a transmembrane DNA transporter to translocate actively the ssDNA into host cell (Dumas et al. 2001; Duckely et al. 2005; Grange et al. 2008). In addition, VirE3 is suggested to interact with VirE2 and plant importin to help nucleus translocation of mature T-complex (Lacroix et al. 2005).

In plant nucleus, VirF activates the host proteasome machinery to degrade the proteins surrounding the T-DNA to release the T-DNA from mature T-complex. The T-DNA is subsequently for chromosomal integration (Schrammeijer et al. 2001; Tzfira et al. 2004). The T-DNA integration is completed by illegitimate recombination (Gheysen et al. 1991). There is little known about the mechanisms and the proteins involved in this process. Some histone proteins as well as histone modifying proteins were proposed to be capable of interacting with T-DNA and therefore T-DNA could be targeted to chromosome (Zhu et al. 2003; Crane and Gelvin, 2007). Overexpressing *Arabidopsis* histone *HAT1* enhances the transformation efficiency in *Arabidopsis* and rice (Yi et al. 2002; Yi et al. 2006; Zheng et al. 2009). Besides, proteins participating in recombination and DNA repair are essential for T-DNA integration (Sonti et al. 1995; Nam et al. 1998). The detail about how these genes involved in T-DNA integrating should be further elucidated.

Although the studies of T-DNA processing and transportation mechanisms are focused on *A. tumefaciens*, it is believed that *A. rhizogenes* shares the same infection

mechanism with *A. tumefaciens.* However, *A. rhizogenes* does not encode VirD2 and VirE2. Instead, full-length and split C-terminal region of GALLS proteins, encoded by a GALLS gene, are the functional homologs to VirD2 and VirE2 respectively (Hodges et al. 2006; Hodges et al. 2009).

1.2. Crown gall

Agrobacterium tumefaciens T-DNA expression in transformed plant results in crown gall formation. Genes located on the T-DNA are so-called oncogenes, including the most common six ones, gene *5*, *iaaM*, *iaaH*, *ipt*, gene *6a*, and gene *6b*.

A. tumefaciens losing *iaaM* or *iaaH* produces tumors with differentiated shoots, and the tumor has reduced auxin levels (Garfinkel and Nester 1980; Akiyoshi et al. 1983). *iaaM* and *iaaH* encode a tryptophan monooxygenase and an indole-3-acetamide hydrolase, respectively. These two enzymes convert tryptophan to auxin indole-3-acetic acid (IAA) (Schröder et al. 1984; Thomashow et al. 1984; Thomashow et al. 1986; van Onckelen et al. 1986). The expression of these two genes results in more than 10-fold greater free form IAA level in crown gall tumors than in the periphery (Weiler and Spanier 1981; Veselov et al. 2003). The auxin overproduction is considered to promote tumorigenesis and maintain tumor morphology.

Mutation of *ipt* causes tumor with small, rooty morphology and a decreased level of zeatin-type cytokinins (Garfinkel and Nester 1980; Akiyoshi et al. 1983). *ipt* encodes an isopentenyl transferase, which condenses a molecule of adenosine monophosphate with an isoprenoid unit, the rate-limiting step of cytokinin synthesis (Astot et al. 2000). Therefore, cytokinin levels in crown gall are 100-fold higher than those in periphery (Weiler and Spanier 1981). Bedises, *A. tumefaciens* encodes an

additional *ipt*-homologous gene, *tzs*, located on *vir* operon. It allows bacteria to synthesize cytokinin after activation of VirA/G two component system, and the expression of *tzs* enhances virulence (Gaudin et al. 1994), which indicates that cytokinin production is closely related to the tumorigenesis.

Gene *6a* encodes an opine permease with little effects on tumorigenesis (Messens et al. 1985). The gene *6b* of octopine-type strains is capable of inducing small tumors on *Kalanchoë*; however, it showed no effects on tobacco (Garfinkel et al. 1981). In gene *6b*-transgenic plants, several abnormal growth phenotypes were found, including tubular leaves, thicker roots, and ectopic shoots (Tinland et al. 1992; Wabiko and Minemura 1996; Grémillon et al. 2004). The detailed biochemical and cellular function of gene *6a* and *6b* in tumorigenesis should be further elucidated.

Mutation of gene *5* has no phenotypic effect on tumor. However, co-mutation of gene *5* with *iaaM* or *iaaH* causes more shoots than *iaaM* or *iaaH* mutant (Leemans et al. 1982). Gene *5* encodes an enzyme converting tryptophan into indole-3-lactate (ILA), which competes with IAA for the auxin-binding proteins (Körber et al. 1991; Sprunck et al. 1995). The expression of gene *5* was positively regulated by auxin, but negatively regulated by ILA (Korbor et al. 1991). These indicate gene *5* play a non-essential role in tumorigenesis.

It is believed that hormone regulation causes crown gall formation. The stem inoculated with *A. tumefaciens* produces high levels of auxin and cytokinin followed by increases in ethylene and abscisic acid (Veselov et al. 2003). The ethylene insensitive tomato mutant *Never ripe* generates smaller crown gall tumor than wild-type tomato, and the tumor from mutant contains 50-fold lower ethylene level (Aloni et al. 1998). These indicated the tumorigenesis is regulated by multiple endogenous

hormone biosynthesis, and *iaaM*/*iaaH* and *ipt* from *A. tumefaciens* contribute dominantly to the hormone re-balance.

1.3. Opine

Besides neoplastic growth related genes, T-DNA encodes opine biosynthetic genes that allow host plant to produce opine in crown galls or hairy roots. Opines are low molecular weight compounds consisting of nitrogen and carbon, and serve as nutrient sources for *Agrobacterium* (Hong et al. 1997). Nowadays, over 30 kinds of opines have been found. Each *Agrobacterium* strain produces one specific opine compound; therefore, the types of opine have been used for classification of *Agrobacterium* (Petit et al. 1983). Each set of opine catabolism gene is found in non-T-DNA region of pTi/pRi in corresponding strain. Opine can be utilized by only a little groups of soil organisms, which offers a competitive advantage to *Agrobacterium* (Wilson et al. 1995).

1.4. Hairy root

Unlike crown gall, there has not been a generally agreed mechanism of hairy root formation. The expression of *A. rhizogenes* T-DNA genes in infected plant results in adventitious root disease syndrome (Chilton et al. 1982; Tepfer 1984; Cardarelli et al. 1987). The hairy roots can emerge from most types of plant tissues, such as shoots, roots, and calli. The root emergence from plant cells is involved with cell re-programming process, which most be likely caused by hormone re-balance. Some strains of *A. rhizogenes* encode *iaaM*/*iaaH* functional homologs *aux1*/*aux2* (Gaudin and Jouanin; 1995), but these auxin biosynthetic genes are not essential for hairy root formation. Instead, *rol* genes are sufficient for hairy root formation. However, there are many controversial results in these oncogenes encoded by *A.*

rhizogenes. Due to the highly potential applicability of hairy root, we aimed to understand the mechanism of the formation of hairy roots. The advantages of hairy root in biotechnology will be briefly described in next paragraph, and the studies about oncogenes encoded by *A. rhizogenes* will be stated in the next section.

Hairy root is characterized by high growth rate and genetic stability, and it could maintain these characteristics in hormone-free medium (Benvenuto et al. 1983). Unlike tumor induced by *A. tumefaciens*, hairy root is only composed of transformed cells (Bercetche et al. 1987). Hairy root is widely applied in root biology because it can harbor interested nucleotide fragment homogeneously with root physiology. Furthermore, hairy root provides a route to plant genetic engineering for producing heterologous proteins and for secondary metabolites. For the past three decades, many researches have proposed hairy root could accumulate much higher plant secondary metabolite levels compared with intact plant tissues. Furthermore, the secondary metabolites production could be enhanced via expressing structural genes of synthetic pathway, down-regulating competitive pathways, controlling the environmental factors such as light and sucrose, or treating with plant hormone such as methyl jasmonate (MeJA) or salicylic acid (SA) (reviewed by Giri and Narasu 2000; Srivastava and Srivastava 2007; Mehrota et al. 2010; Zhou et al. 2011). Furthermore, hairy root culture could be scaled up to industrial level (Mehrotra et al. 2008; Baque et al. 2011). These advantages of hairy root make it is getting attention.

2. Genes on *Agrobacterium* T-DNA

After T-DNA integrated into plant chromosome, the expression of T-DNA gene would cause the neoplastic effects on plant, such as tumorigenesis in the case of *A. tumefaciens* and rhizogenesis in the case of *A. rhizogenes*. The well-studied gene loci

are opine synthesis genes and hormone-related genes functionally homologs with the above-mentioned ones among *Agrobacterium* species. In addition to these genes, there are some unique genes in *A. rhizogenes,* including *rol* genes and other T-DNA loci. These genes affect plant in a wide diversity and result in rhizogenesis.

White and coworkers generated several deletions and transposon insertion-mutations on the T_L-DNA of Ri plasmid A4, and they found that four of the potential 18 open reading frames on the T_L-DNA affect the induction of roots on *Kalanchoë daigremontiana.* Therefore, these four loci were then named root locus A-D (*rolA-D*) genes (1985). Slightom and coworkers demonstrated these genes are corresponding to open reading frame (ORF) 10, 11, 12, and 15, respectively (1986). The diagram of genes on T_L-DNA is shown in Figure 1-1. Many researchers have been interested in how these gene affect plant due to their extremely strong effects on plant growth, hormone balance, and metabolic flux.

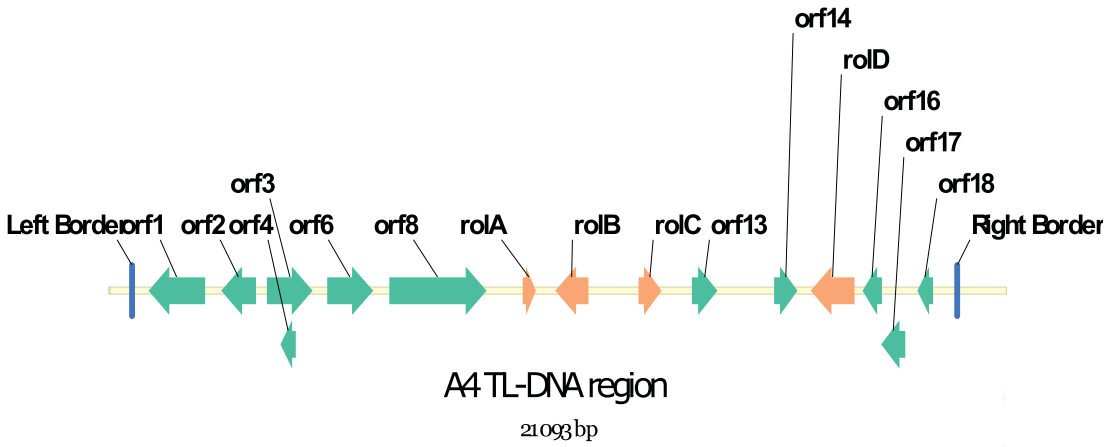

Figure 1-1 The *rol* genes and the other loci on T_L-DNA of *A. rhizogenes* strain A4. The open reading frames were predicted by ORF finder of VectorNTI 10 (Life technologies) and the results were checked by nucleotide database of NCBI website.

A. tumefaciens harboring each one of *rolA*, *rolB*, or *rolC* is sufficient to induce root formation on tobacco leaves, and *rolB* or *rolC* alone is able to stimulate rooting on *K. daigremontiana* leaves (Spena et al. 1987; Vilaine et al. 1987). However, each pairwise combination of *rolA, B, and C* genes driven by their own promoters showed more efficient rooting abilities than any single gene, and three genes all together could promote the root production with the greatest efficiency (Spena et al. 1987). These different degrees in root-promoting abilities suggested that these *rol* genes have different biological functions and act synergistically in hairy root formation.

The root emerging from leave cell is certainly caused by cell re-differentiation. Auxin is the first considered hormone participating in root growing. Compared with intact roots, tobacco hairy roots accumulate approximately 2.5-fold higher auxin concentration (Spanò et al. 1988). Moreover, *Lotus comiculatus* hairy roots showed 100- to 1000-fold increase in auxin sensitivity compared with intact roots (Shen et al. 1988). By measuring the transmembrane potential differences between single *rol* gene transformed tobacco mesophyll protoplast and non-transformed cells, Maurel and colleagues discovered that *rolB* transformed cells could increase the auxin sensitivity up to 10000-fold, while the *rolA* up to 1000-fold, and the *rolC* up to 10-fold; whereas the T_L-DNA transformed cells only raise the sensitivity to 30-fold (1991). These data demonstrate that hairy root growth closely relates to auxin responses with the fact that hairy root accumulates higher auxin and has enhanced auxin perception at the same time. In addition, *rol* genes act in a synergistic manner in rhizogenesis, but they did not act synergistically in raising auxin sensitivities.

In addition to promoting abnormal growth of plants, *rol* genes have strong effects on stimulating secondary metabolite accumulations. These indicated *rol* genes

alter plant physiology in a diverse range. I will introduce the biochemical and genetical studies of *rol* genes in plant in the introduction section 2.1~2.4, and the effects of *rol* genes on secondary metabolites in the next introduction section.

Besides *rol* genes, there are many other predicted ORFs on T-DNA. In transposon-mutagenesis experiment, these ORFs did not affect rooting (White et al. 1985). However, plant transformed with these genes would show diversified morphologies and altered hormone sensitivity. More details about these genes, including *orf3n*, *orf8*, *orf13*, *orf13a*, and *orf14*, will be introduced in the introduction section 2.5~2.9.

2.1. *rolA*

*rol*A encodes a small protein of approximate 11 kDa molecular mass. Oligonucleotide sequences of *rolA* gene in all type of Ri plasmids share high homology (Nilsson and Olsson 1997). *rolA* was initially demonstrated as a gene related to rhizogenesis; however, later research discovered that *rolA* is a minor factor in rooting. In addition to rhizogenesis, *rolA* has been proposed to stimulate secondary metabolites in many types of plant tissues. The detailed descriptions are presented below.

2.1.1. *rolA* affects plant morphogenesis

A. tumefaciens harboring *rol*A with its promoter was able to induce rooting on tobacco leaf discs (Spena et al. 1987; Vilaine et al. 1987), but not on *Kalanchoë* leaves (Spena et al. 1987). *rolA*-deficient *A. rhizogenes* induced thicker and more curled hairy roots (White et al. 1985). The phenotypic changes in *rol*A-transgenic tobacco include highly wrinkled leaves, shorter internodes, and more condensed inflorescences with larger flowers (Schmülling et al. 1988; Sinkar et al. 1988); by

contrast, it was also reported to have smaller flowers with lower male fertility (Sun et al. 1991; Martin-Tanguy et al. 1993; Michael and Spena 1995). *rol*A-transgenic tomato had longer internodes, a smaller root system, smaller wrinkled leaves, smaller flowers, and lower pollen germination rate (van Altvorst et al. 1992).

2.1.2. *rolA* and plant hormone

rolA could increase the sensitivity to auxin in transgenic plant (Maurel et al. 1991; Vansuyt et al. 1992). Besides, *rolA*-expressing tobacco showed a similar phenotype with wild-type plant treated with gibberellic acid (GA) biosynthesis inhibitor; however, treating GA with *rolA*-transgenic tobacco only partially restored the phenotypic change (Dehio et al. 1993). Mortiz and Schmülling discovered that two active GAs, GA1 and GA20, were reduced in *rolA*-transgenic tobacco plant, and the precursors GA53 and GA19 were accumulated, indicating blocking GA synthetic pathway partially explains the phenotypic change caused by *rolA* (1998). Other hormone levels were measured in *rolA*-transgenic tobacco (Dehio et al. 1993), but no conclusive result could be proposed from the above reports.

2.1.3. *rolA* promoter

Transformation of *rolA* along with its 473-nucleotide upstream sequence, which is similar to some upstream sequences of auxin-responsible genes, was sufficient to cause the phenotypic change in tobacco (Carneiro and Vilaine 1993). In the same report, they demonstrated that stem had the most abundant *rolA* mRNA level, which was 5-fold and 50-fold higher than those in leaf and in root, respectively. *rolA* transcripts containing a 5'-untranslated region (5'-UTR), which would be spliced in *Arabidopsis*, was proposed to be an indispensable fragment to *rolA* expression, and it might act as a *cis*-acting regulatory factor (Magrelli et al. 1994). Pandolfini and

coworkers found that *rolA* mRNA could be transcribed in bacteria. However, the *rolA* transcripts were abolished while the 5‘-UTR was deleted (2000). This 5’-UTR has been proposed as a bacterial promoter. In 1996, Guivarc’h and coworkers expressed *rolA* driven by its 477 bp or 366 bp long upstream fragments, and they discovered the longer promoter would induce wrinkled leaves and short internodes in transgenic tobacco, whereas the shorter promoter only cause a dwarf phenotype with normal leaves (1996). In summary, *rolA* driven by its own promoter expresses in both prokaryotic and eukaryotic cells under the regulation of 5’-UTR, and the tissue-specific activation pattern is regulated by its 477 bp long promoter sequence.

2.1.4. RolA biological functions

Through sequence analysis and structure modeling, RolA was proposed to be a DNA- binding protein owing to the fact that it is a alkaline protein structurally homologous with papillmavirus E2 DNA-binding protein (Levesque et al. 1988; Rigden and Carneiro 1999). However, the RolA-GUS transgenic tobacco cells showed the lowest GUS activity in nucleus and the highest in plasma membrane system (Vilaine et al. 1998). There is no transmembrane signals in RolA protein, which indicated RolA is a non-integrated membrane protein. Moreover, RolA might expresses in not only plant but also bacterial cell (Guivarc’h et al., 1996). These studies propose that RolA might possess multiple functions. From these evidence, we could hypothesize that RolA is a membrane-associated protein in plant cell, and it might be a transcriptional factor in bacterial cell. Combining these evidence, we proposed a possible role of RolA in plant. RolA is associated with plasma membrane in ground state, and it could be translocated into nucleus to regulate transcription process via unknown signaling stimulation. Nevertheless, RolA is still an functionally

known protein with the positive effects on rhizogenesis, development, and hormone homeostasis.

2.2. *rolB*

rolB encodes a protein of 259 amino acids in *A. rhizogenes* strain A4. It is discovered in all types of Ri plasmids. *rolB* is the most well-studied gene among the *rol* genes; however, rather conflicting results have been obtained. Recently, studies of *rolB* have been focused on its ability to induce secondary metabolites in plants. The way how *rolB* affects plant is illustrated in Figure 1-2, and the details are presented as follows.

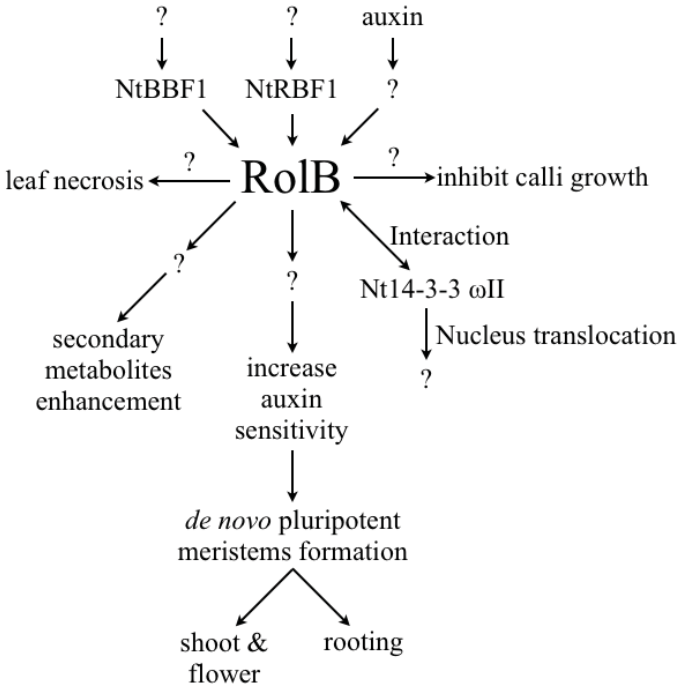

Figure 1-2 The overview of *rolB*-mediated plant responses. *rolB* can be activated by auxin-dependent signals or auxin-independent transcript factors BBF1 and RBF1. The RolB expression would inhibit the growth of *R. cordifolia* calli and induce tobacco leaf necrosis. The RolB can interact with tobacco 14-3-3 protein which resulting in nucleus translocation; however, abolishing the interaction by several point mutations only make little damage on the rooting. Besides, RolB can enhance the secondary metabolites and increase the auxin perceptions in transformants. Increasing the auxin perceptions promotes plant *de novo* pluripotent meristem formation, resulting in rhizogenesis and other organogenesis.

2.2.1. *rolB* affects plant morphogenesis

rolB is the earliest research of interest among the *rol* genes. By deleting *rolB* from *A. rhizogenes* A4, the ability to induce hairy root on *K. daigremontiana* was abolished (White et al. 1985). Besides, *rolB* alone was capable of inducing tobacco rhizogenesis with almost the same efficiency as wild-type *A. rhizogenes* (Cardarelli et al. 1987; Spena et al. 1987). These reports indicated that *rolB* was the most important gene in rooting among the *rol* genes. Altamura and coworkers reported that *rolB* could strongly promote meristem formation by bypassing the regulatory factors of all types of organs (1994; 1998), and the results suggested that *rolB* regulates plant re-differentiation toward rooting.

rolB-transgenic tobacco presented smaller leaves with lower length-to-width ratio and highly branched plentiful roots (Cardarelli et al. 1987). Tobacco expressing *rolB* driven by *Cauliflower mosaic* virus (CaMV) 35S promoter showed bigger flower and early necrotic leaf (Schmülling et al. 1988). *rolB*-transgenic tomato showed reduced internode length and apical dominance with smaller flowers, lower pollen viability, and smaller fruits (van Altvirst et al. 1992; Arshad et al. 2014). On the other hand, *rolB* induces apical dominance in rose (van der Salm et al. 1997). These indicate *rolB* functions in a species-dependent and tissue-dependent manner.

2.2.2. *rolB* and auxin

The phenotypic change in *rolB*-transgenic plants suggest that *rolB* is an-auxin responsive protein which mediates auxin signaling. Membrane potential measurement showed that *rolB*-transformed cells could increase auxin sensitivity up to 10000-fold (Maurel et al., 1991), and the polarization of auxin in *rolB*-expressing protoplast

could be blocked by a larger number of anti-auxin binding protein antibodies (Venis et al. 1992).

RolB was at first characterized as a glucosidase that hydrolyses indole glucosides *in vitro*, and *rolB*-transformed plant would increase auxin sensitivity by increasing IAA directly (Estruch et al. 1991c). However, two independent research groups invalidated the hypothesis later. Nilsson and coworkers demonstrated that wild-type and *rolB*-transformed tobacco showed the same contents of free IAA, and they had the same capacity of hydrolyzing IAA conjugates (1993a). Increasing auxin sensitivity in *rolB*-transformed tobacco was independent to intracellular auxin concentration because neither the accumulation nor the metabolism of endogenous auxin was affected; instead, *rolB* might increase the auxin perception (Delbarre et al. 1994; Maurel et al. 1994). This hypothesis was consistent with the experiment that the plasma membranes of *rolB*-transformed tobacco cells had additional auxin binding ability (Filippini et al. 1994).

There is other evidence supporting that *rolB* has a close connection with auxin. Expressing *rolB* in tomato ovary by the tissue-specific promoter results in fruit parthenocarpy (Carmi et al. 2003), which has the similar effect with accumulating auxin in ovary by expressing bacterial auxin synthetic gene *iaaH* (indole acetamide hydrolase) driven by the same ovary-specific promoter along with treating its substrate (Szechtman et al. 1997). Expression of *rolB* in tobacco anther cells reduces stamen elongation and delays dehiscence (Cecchetti et al. 2004), which is considered as the result of lacking auxin polar transport system (Okada et al. 1991). In 1994, Altamura and coworkers demonstrated *rolB* promotes *de novo* primordia formation from tobacco thin cell layer in not only root but also flower (1994), which is

consistent with the reports that auxin controls the development of tobacco cells toward roots and flowers (Smulders et al. 1988; Smulders et al. 1990). In addition, auxin plays a crucial role in floral meristem formation and subsequent flower primordia formation (reviewed by Cheng and Zhao 2007). All in all, *rolB* has the auxin-like effects on plant fruit, ovary, and flower development, which supports the concept that *rolB* enhances the auxin perception in transformants.

Besides auxin, *rolB* was reported to have the correlation with cytokinin in promoting shoot formation from thin cell layers (Altamura et al. 1998). However, little connection between *rolB* and cytokinin has been proposed.

2.2.3. *rolB* promoter

rolB and *rolC* share a bidirectional promoter. Respective *rolB* and *rolC* native promoters drive *uidA* (β-D-glucuronidase) showed a similar expression pattern in shoot phloem but distinguishably in roots. *rolB* promoter activity shows mainly in the root primordia, including both primary and lateral primordia, and root cap, whereas *rolC* promoter activity does in phloem and in the apical meristems (Schmülling et al. 1989). The expression pattern of *rolB* indicates it has a close relation to cell differentiation and proliferation in the root. Overall, these two genes share a bidirectional promoter but they are regulated distinguishably.

rolB seems to be an auxin-regulated gene. In tobacco mesophyll protoplast, the expression level of *rolB* could be stimulated 20- to 100-fold by auxin treatment, whereas *rolC* expression increases only 5-fold (Maurel et al. 1990). In the same report, they discovered that treating exogenous auxin makes *rolB* express not only in root primordia but also in root vascular tissue and pericycle cells. Maurel and coworkers proposed the full activation of *rolB* by auxin is 12 to 18 hours after

treating, indicating that *rolB* belongs to an auxin late responsive gene. On the other hand, *rolB* could increase auxin perception within 8 hours after auxin treatment (1994). We can hypothesize the following two points. First, a low level of *rolB* expression is enough to increase auxin sensitivity in plant, and second, the activation of *rolB* might not only participate in amplifying auxin signals but also regulate other physiological behaviors independent to auxin signals.

There is much other evidence supporting that *rolB* is responsive to auxin but regulates not only auxin-related physiology. An auxin antagonist oligogalacturonide polymer is capable of inhibiting the rhizogenesis of *rolB*, and this effect disappears while *rolB* is driven by tetracycline-inducible promoter (Bellincampi et al. 1996). Expressing *rolB* under control of its native promoter resulted in root or flower primordia formation, which is similar to treating exogenous auxin, whereas expression under CaMV 35S promoter in *Hieracium piloselloides* resulted in multi-potency (Koltunow et al. 2001). These phenomena showed the activation and the function of *rolB* have a close relationship with auxin.

Chimeric fusion of *uidA* with different lengths of upstream non-coding sequence of *rolB* shows that a 1185 bp length promoter region triggers the highest GUS activity (Capone et al. 1991; Capone et al. 1994). However, the 623 bp length promoter sequence drives a comparable activity. In addition, they identified five *cis*-elements, including regions -623 to -341, -341 to -306, -216 to -158, and the other two within regions about 70 and 80 bp around the CAAT and the TATA box, and they are so named as domain A-E, respectively. De Paolis and coworkers isolated a protein, which binds to the ACTTTA motif within domain B of *rolB* promoter via a single zinc finger structure. This protein was designated NtBBF1, representing *N. tabacum rolB*

domain B factor 1 (1996). NtBBF1 is essential for tissue-specific expression of *rolB* (Baumann et al. 1999). However, NtBBF1 is not an auxin-regulated gene, which indicates *rolB* is regulated at least by an unknown factor related to auxin and NtBBF1. In addition, another *trans*-acting element NtRBF1 (*N. tabacum rol* binding factor 1) can bind to -533 to -530 region of *rolB* promoter in non-meristem cells, and there is no differences between the concentrations of NtRBF1 in *rolB*-transformed and non-transformed tobacco plants (Filetici et al. 1997). Collectively, *rolB* is an auxin-inducible gene which increases auxin perception, but *rolB* can also be activated by an auxin-independent pathway and regulates auxin-independent responses in plants.

2.2.4. RolB biological function

Protein crude extract from RolB-expressing *Escherichia coli* has higher phosphatase activity than the extract from empty plasmid transformed *E. coli*, and the phosphatase is inhibited by tyrosine phosphatase inhibitor (Filippini et al. 1996). Moriuchi and colleagues reported that RolB was a nucleus-localized protein that could interact with tobacco 14-3-3 κI, κII, ωI, ωII, ωIII, and ε (2004). In the same report, they generated a series of point mutations in RolB, and some of them could abolish the interaction; however, these point mutation reduce, but not abolish, root induction ability. The findings indicated that the physical interaction of RolB and 14-3-3 proteins are not essential for rhizogenesis.

2.3. *rolC*

In *A. rhizogenes* A4, *rolC* is a 543 bp gene which encodes a protein of approximate 20 kDa molecular mass. RolC is proved to be a cytosolic protein via ultra-centrifugation combining with specific antibody detection (Estruch et al.,

1991b). *rolC* plays an important role in promoting rooting, increasing branching, and stimulating secondary metabolites. *rolC* can strongly promote rooting and secondary metabolite production; therefore, it has been studied for a long time. However, until now, there is no conclusion about biological function of *rolC*. The followings summarize the studies about *rolC*.

2.3.1. *rolC* affects plant morphogenesis

rolC affects plant morphology in many aspects. *rolC* could induce root in tobacco (Spena et al. 1987; Schmülling et al. 1988), belladonna (Bonhomme et al. 2000a), carnation (Casanova et al. 2004), trifoliate orange (Kaneyoshi and Kobayashi 1999), and persimmon (Koshita et al. 2002). *rolC* induces not only roots but also adventitious shoot in carnation (Casanova et al. 2003; Casanova et al. 2004) and ginseng (Gorpenchenko et al. 2006). Besides, *rolC* induces somatic embryogenesis in ginseng (Gorpenchenko et al. 2006). In tobacco, *rolC* induces more abundant branch roots than *rolA*- or *rolB*-expressing hairy roots (Schmülling et al. 1988). Furthermore, *rolC* plays a role in hairy root elongation (White et al. 1985). These results suggest *rolC* exhibits cytokinin- and auxin-like activities, and it might induce the formation of pluripotent meristematic cells as *rolB*.

rolC-transgenic tobacco reduces apical dominance, and the plant appears dwarfism with shorter internodes, smaller leaves with narrow shapes, early flowering with smaller size, lower pollen viability and seed production (Schmülling et al. 1988; Oono et al. 1990; Nilsson et al. 1993b; Scorza et al. 1994; Kaneyoshi and Kobayashi 1999; Koshita et al. 2002).

2.3.2. *rolC* and auxin

rolC was characterized as an auxin-related gene due to its ability to induce rooting and increase auxin sensitivity (Spena et al. 1987; Smulders et al. 1988; Casanova et al. 2003). However, IAA content in the *rolC*-transformed plants showed no differences (Nilsson et al. 1993b; Schmülling et al. 1993; Casanova et al. 2004) or even decreased (Nilsson et al. 1996).

rolC has a cell-autonomous behavior. *rolC* induces rooting from the transformed cell, but the neighboring untransformed cells are not affected (Schmülling et al. 1988). This indicates RolC is neither a mobile nor a diffusible factor in rhizogenesis. Besides, *rolC* transformation does not alter the growth habit of original tissues (Estruch et al. 1991b). In summary, *rolC* promotes *de novo* pluripotent meristem formation by its protein expression.

2.3.3. *rolC* and cytokinin

rolC reduces apical dominance and enhances lateral shoot development, and these were suggested to be the effects of cytokinin (Schmülling et al. 1988). Estruch and coworkers demonstrated that RolC expressed in *E. coli* had an *in vitro* β-glucosidase activity that releases the active free form cytokinin by cleaving glucosidic conjugates directly (Estruch et al. 1991a). However, the level of glucosidic conjugated cytokinin *in vivo* was not altered by expressing *rolC*, and free cytokinin levels in the plants were either the same or even lower (Nilsson et al. 1993b; Schmülling et al. 1993; Faiss et al. 1996; Nilsson et al. 1996). Furthermore, the fraction of around 20 kDa isolated by size exclusive gel chromatography from *rolC*-transformed *Panax ginseng* extract showed no β-glucosidase activity (Bulgakov et al. 2002a). Transforming with *rolC* or *ipt*, a cytokinin biosynthetic gene encoded by

Agrobacterium, shows different phenotypes in root system and leaf color (Schmülling et al. 1988; Fladung 1990; Beinsberger et al. 1991; Schmülling et al. 1993; Faiss et al. 1996). Taken together, the phenotypic alternations caused by *rolC* are not directly related to cytokinins.

2.3.4. *rolC* and gibberellins

rolC-transgenic plant showed reduced size with shorter internodes, which are GA-reduced-like effects. Tobacco transformed with 35S-*rolC* showed less GA1 and GA3 but higher GA19, so *rolC* might decrease active form of GA by blocking GA biosynthetic pathway (Nilsson et al. 1993; Schmülling et al. 1993). However, exogenous GA3 application only restore the morphological change on internode length (Schmülling et al. 1993). We can conclude GA content alternation is one of the effects resulted from *rolC* expression.

2.3.5. *rolC* promoter

rolC promoter is identified to be specifically activated in companion cells (Nilsson et al. 1996). In *rolC*-transgenic tobacco, *rolC* expresses mainly in the vascular tissues of both root and stem (Spena et al. 1987; Schmülling et al. 1988; Schmülling et al. 1989). The phloem-specific *cis*-acting element was found within -1 to -153 bp region of *rolC* promoter (Sugaya and Uchimiya 1992). However, *rolC* expression level in leaves was as high as that in roots while plant transformed with the entire T-DNA (Durandtardif et al. 1985; Leach and Aoyagi 1991). It hinted that *rolC* may be regulated by other genes localized on T-DNA.

The promoter region driving *rolC* during somatic embryogenesis is around -255 bp upstream of the transcriptional start site (Fujii and Uchimiya 1991; Fujii et al. 1994). It is shown that a sucrose-responsive *cis*-element locates between -135 and -94

bp of *rolC* promoter (Yokoyama et al. 1984). When sucrose is present in culture media, *rolC* could be activated in the whole transgenic plant (Nilsson et al. 1996). However, sucrose is responsiveness and phloem-specific expression share the same *cis*-acting element, which indicates the two phenomena are linked. High concentration of sucrose usually present in phloem of roots and stems. Therefore, the fact that the *rolC* mainly expresses in these two tissues is reasonable.

2.4. *rolD*

rolD is only found in the agropine-type Ri plasmid T_L-DNA region (Christey 2001). *rolD*-transgenic tobacco displayed early flowering and reduced rooting. Moreover, *rolD* alone cannot induce rooting (Mauro et al. 1996). *rolD* expresses mainly in elongating and expanding tissues in adult plants with temporal regulation (Trovato et al. 1997).

rolD promoter, as well as *rolB* promoter, contains an auxin-responsive *cis*-element with a zinc finger binding element. *rolD* is also a late auxin-induced gene. However, the *rolB* expression level increases with treatment of raised IAA concentration, whereas the *rolD* reaches the maximum level at approximate 1 μM of exogenous IAA and then decreases while increasing IAA concentration (Mauro et al. 2002).

In vitro enzyme reaction shows that RolD is an ornithine cyclodeaminase (OCD), which converts ornithine to proline. The result was consistent with the fact that higher proline content was detected in *rolD*-expressing flower (Trovato et al. 2001). There is no any other gene encoding OCD found in plants or in *A. rhizogenes*. According to the research, the phenotypic change in *rolD*-transgenic plant might be

related to either higher proline accumulation or decreasing pool of ornithine, limiting the polyamine biosynthesis.

rolD is the only *rol* gene which has not been reported to affect plant secondary metabolites; however, *rolD*-transgenic tomato accumulated pathogen-related protein 1 (PR-1), whose expression frequently accompanies with secondary metabolites accumulation (Bettini et al. 2003). Besides, *rolD*-transformed tomato showed increased number of inflorescences and higher fruit yield. It is the only gene which seems to increase plant reproductivity among the *rol* genes.

2.5. *orf3n*

There are several genes other than *rol* genes on *Agrobacterium rhizogenes* A4 T_L-DNA, and these genes are named *orf1-18* (Slightom et al. 1986; Figure 2). In *A. rhizogenes* strain HRI, the *orf3* homologous gene is slightly larger than the gene on pRiA4, and it was designated *orf3n* (Lemcke and Schmülling 1998). Compared with wild-type, tobacco expressing 35S-*orf3n* showed shorter internode length, different leaf morphology with necrosis on leaf tip, delaying flowering, and lower density of inflorescences. Besides, *orf3n* repressed shoot formation from callus, which indicates that *orf3n* decreased the sensitivity to cytokinin. *orf3n* was therefore suggested to suppress the dedifferentiation of tissues, which may favor the hairy root formation and maintenance (Lemcke and Schmülling 1998).

2.6. *orf8*

orf8 is the longest ORF on T_L-DNA. It encodes a protein of 780 amino acids. In addition to *rol* genes, *orf8* is the most studied ORF on T_L-DNA. The ORF8 N-terminal domain shows homology to the RolB, and the C-terminus shows a significant similarity to the *iaaM*-encoded protein (Levesque et al., 1988), which can

convert tryptophan into indole-3-acetamide (IAM) for auxin biosynthesis. In the early years of *rol* gene investigation, *rolB* was considered to be an auxin biosynthesis-related protein (refer to introduction section 2.2). Therefore, *orf8* was initially connected to auxin metabolism, transport, or perception. Lemcke and coworkers reported tobacco expressing 35S-*orf8* did not show altered phenotype but with a five-fold increase of indole-3-acetamide (IAM). Besides, *E. coli* expressing *orf8* exhibited the tryptophan monooxygenase activity (2000). It suggested *orf8* may involve in the biosynthesis of auxin. However, Otten and Helfer expressed 5'-sequence, homolog to *iaaM,* 3'-sequence, and full-length of *orf8* in tobacco, but none of them had greater IAM production. On the other hand, tobacco expressing *orf8* had dramatically greater amounts of glucose, fructose, sucrose, and starch (2001). Further experiment figured out the sucrose accumulation may be because *orf8* inhibited sucrose export (Umber et al. 2002).

orf8-transgenic tobacco cotyledon showed a similar phenotype with cotyledon treated with auxin (Ouartsi et al. 2004). Umber and coworkers observed *orf8*-transgenic tobacco showed stunted growth and rough, mottled leaves with thick, fleshy midribs (2005). The usage of different CaMV 35S promoter version seems to be the dominant factor causing different phenotypic change of *orf8*-transgenic plants.

Expressing *orf8* in plant cell can increase the tolerance of exogenous auxin and cytokinin. Plant cell expressing *orf8* can grow on media containing concentrations of auxin that completely inhibit the growth of wild-type or *iaaM*-transgenic cells (Lemcke and Schmülling 1998). Tobacco leaf discs expressing *orf8* generate fewer, but thicker, roots and more calli than un-transformed ones (Ouartsi et al. 2004). These indicated *orf8* may play a role in auxin- and cytokinin-regulated growth. In the same

work, Ouartsi and coworkers discovered ORF8 expression is dramatically up-regulated after 6 hours of treating with exogenous auxin (2004). It indicated *orf8*, as well as *rolB* and *rolD*, was a late auxin response gene.

The function of *orf8* has not been clear, but it may co-express with *rolB* gene because they both respond to auxin. Besides, the sucrose export was suppressed in *orf8*-transgenic cell, which revealed that *orf8* expression may be beneficial to plant growth and opine synthesis. Moreover, higher sucrose accumulation can induce the expression of RolC protein. It hinted that these proteins may act together to promote hairy root growth.

2.7. *orf13* and *orf14*

rolA, *B*, or *C* alone is sufficient to induce rooting in tobacco (Schmülling et al. 1988); however, an *Agrobacterium* carrying *rolABC* genes is still insufficient to induce rooting only if either *aux1*/*aux2* or *orf13*/*orf14* are present in carrot (Cardarelli et al. 1987; Capone et al. 1989). Moreover, the combination of *rolB* along with *orf13* is almost as efficient in root inducing as full-length T_L-DNA (Aoki and Syõno 1999). These indicated *orf13* and *orf14* may act as auxin biosynthesis genes. However, neither of them contains homology with auxin biosynthesis genes (Hansen et al. 1997), and unlike *aux1/aux2* genes, *orf13* and *orf14* together cannot induce rooting in tobacco (Cardarelli et al. 1987; Camilleri and Jouanin 1991).

orf13 can induce cell proliferation to produce green callus on carrot and tobacco leaf discs (Hansen et al. 1993). Tobacco expressing 35S-*orf13* showed growth reduction, short internodes, fewer developed roots, reduced apical dominance, wrinkled leaves with browning, and asymmetric flowers (Hansen et al. 1993; Lemcke and Schmülling 1998). Moreover, *orf13* inhibits cell division and elongation of apical

meristem cells, which causes reduced apical dominance (Lemcke and Schmülling 1998). These phenotypic changes of *orf13*-expressing plants are similar to those of plants treated with cytokinin. Moreover, the exogenous cytokinin, rather than auxin, increases the number of rooting in *orf13*-expressing tobacco; however, there was no obvious difference in endogenous cytokinin concentration between *orf13*-expressing tobacco and wild-type tobacco (Lemcke and Schmülling 1998). In grafting experiment, *orf13* phenotype is transmissible from transgenic scions to wild-type rootstocks (Hansen et al. 1993); however, Lempke and Schmülling cannot prove the results (1998). All in all, *orf13* was considered to be a rooting factor working synergistically with RolB, and *orf13* might regulate the cytokinin signaling to promote rooting.

Stieger and coworkers found the ORF13 protein contains a retinablastoma-binding (Rb) domain. If the Rb domain was mutated, the leaf size of transgenic plant was the same as that of wild-type; however, the reduced shoot apical dominance was not restored. These suggested ORF13 contains more than one functional domain (2004). Rb domain controls the cell cycle progression from G1 to S phase in mammalian cells, which can accelerate cell devision and proliferation. According to the above-mentioned results, Stieger et al. proposed that ORF13 activates cell division of *Agrobacterium*-infected cells and promotes dedifferentiation, which is required for the new differentiation of root organ. However, the hypothesis has not been proved.

Unlike *orf13*, there has been little research focusing on *orf14*. All known about *orf14* was mentioned above.

2.8. *orf13a*

orf13a is a small ORF encoding a protein of 75 amino acids. It is located between *orf13* and *orf14* on the opposite strand (Hansen et al. 1991). The isoelectric point of ORF13a was predicted to be 11.6, and it contains a common motif that can be regulated by phosphorylation; therefore, it is proposed to be a DNA-associated protein (Hansen et al. 1994). Transcription of *orf13a* was mainly in leaf vascular tissues (Hansen et al. 1994).

3. Plant secondary metabolites

Plant secondary metabolites are molecules irrelative to normal growth, development, or reproduction. By contrast, these compounds confer physiological advantages in resisting herbivores, insects, and pathogens, withstanding the environmental stresses, and providing ecological advantages in interspecies competitions. The plant secondary metabolites can be classified into the following three groups. The first group is alkaloids, which are nitrogen-containing molecules. The second group is terpenoids, which usually have an aliphatic structure derived from five-carbon isoprene unit. The third group is phenolic compounds, which contain basal phenol structure derived from phenylalanine or phenylpropanoids. The herbal medicines are used in traditional medicine all over the world for a long time, indicating these plant secondary metabolites are potential drugs for many kinds of diseases. In complementary drug development, the plant secondary metabolites possess biological activities including antitumor, immunosuppressant, antiprotozoal, antiviral, anti-aging, fat-lowering, and cholesterol-lowering function (Lee et al. 2011; Vaishnav and Demain 2011; Ouyang et al. 2014). Therefore, the known-functioned plant metabolites are applied to diets and drugs to enhance human health, and other

unknown-functioned compounds are good resources in natural compound library for drug screening.

The major limitation of secondary metabolite applications lies in their production in present. There are three alternative ways nowadays to produce valuable metabolites: *in vitro* synthesis, semi-*in vitro* synthesis, and *in vivo* synthesis by whole or partial tissues of plants. *In vitro* synthesis is only applied in compounds with simple structure, less chiral centers, and fewer modified carbon rings. On the other hand, the complex compounds could only be produced by the other two methods. Semi-*in vitro* method is using biological intermediate undergoing a few *in vitro* reaction steps to produce the final product. For instance, VP16-213 and VM26 are two anti-cancer drugs derived from podophyllotoxin, which is extracted from *Condyloma acuminatum* (Stähelin 1970, 1973). Alternatively, the target compounds can be produced *in vivo* and extracted for direct use. However, the compounds are usually relatively low in quantity naturally, so growing plants for extracting metabolites is not efficient. Many investigations proposed strategies to use cell cultures or tissue cultures to produce secondary metabolites (reviewed by Namdeo 2007; Hussain et al. 2012). Hairy root culture is one of the most successful methods due to its genetical stability and higher basal level of metabolites. It is believed that genes located on the T-DNA affect the production of secondary metabolites in hairy roots (Taneja et al. 2010). Much evidence indicates that *rol* genes are core regulators in plant secondary metabolites accumulation. I summarize the studies about secondary metabolites in hairy root cultures and *rol* genes-transformed cultures in this section.

3.1. Secondary metabolites in hairy root

Numerous investigations have pointed out that a variety of secondary metabolites accumulate in hairy root cultures of corresponding plant species (reviewed by Giri and Narasu 2000; Sevón and Oksman-Caldentey 2002; Guillon et al. 2006; Ono and Tian 2011; Zhou et al. 2011; Sharma et al. 2013). In Table 1-1, I show six examples, including alkaloid, phenolic, and terpenoid drugs, which hyper-accumulate in hairy roots. These metabolites, except nicotine, have been used clinically. Notably, the artemisinin is synthesized in leaves and stored in both leaves and flowers, and it is not synthesized in suspension cells and calli (Liu et al. 2011); however, it can be synthesized in hairy roots in a massive amount (Weathers et al. 1994). In addition to artemisinin, there are many other aerial tissue-synthesized metabolites, such as camptothecin, vindoline, menthol, morphine, codeine, thebaine, taxol, withanolides, vinblastine, and vincristine can accumulate in corresponding plant hairy roots (reviewed by Sharma et al. 2013). It indicates the regulation of secondary metabolites in hairy root tissue is different from that in other plant tissues.

Table 1-1. Secondary metabolite accumulations in hairy root tissues.

Plant Material	Metabolite	Effects (fold change)	Reference
Nicotiana rustica	alkaloids	2.4	Hamill (1986)
Atropa belladonna	hyoscyamine/scopolamine	75 (highest) 17 (mean)	Bonhomme (2000b)
Papaver somniferum	codeine	3.6 (highest)	Bonhomme (2004)
Linum tauricum	podophyllotoxin	15-23	Ionkova (2009)
Podophyllum hexandrum	podophyllotoxin	5-10 (than cell)	Li (2009)
Artemisia annua	artemisinin	0.38-2.9 (than leaf) 400 (than root)	Weathers (1994)

Many reports indicated plant tissue transformed with single or combination of *rolA-C* genes accelerates the production of secondary metabolites. However, the molecular mechanisms have not been elucidated. I summarized the effects of *rol* genes in Table 1-2, and more details are discussed in the following parts.

Table 1-2. Secondary metabolites affected by *rol* genes.

Gene	Plant Material	Metabolite	Effects (fold change)	Reference
rolA	*Nicotiana tabacum* root culture	nicotine	2-2.5	Palazón (1997)
	Rubia cordifolia calli	anthraquinones	2.8	Shkryl (2008)
rolB	*Vitis amurensis* calli	anthraquinones	100	Kiselev (2007)
	Rubia cordifolia calli	anthraquinones	15	Shkryl (2008)
rolC	*Atropa belladonna* root culture	scopolamine/ hyoscyamine	4-28	Bonhomme (2000a)
	Panax ginseng calli	ginsenoside	3	Bulgakov (1998)
	Nicotiana tabacum root culture	alkaloids	14	Palazón (1998)
	Nicotiana tabacum root culture regeneration	alkaloids	4.6	Palazón (1998)
	Rubia cordifolia calli	anthraquinones	1.3-1.8	Bulgakov (2002b)
	Rubia cordifolia calli	anthraquinones	2-4.3*	Shkryl (2008)

* calli were grown for 5 years with sub-culturing every three month.

3.2. *rolA* affects secondary metabolites

rolA was reported to stimulate 2- to 2.5-fold increase of nicotine directly with little positive influence on growth rate in tobacco root culture (Palazón et al. 1997). In *Rubia cordifolia* callus culture, *rolA* promotes 2.8-fold increase in anthraquinone production and 1.5-fold increase in growth rate at the same time (Shkryl et al. 2008).

These two reports show the same results that *rolA* expression positively relates with growth rates and secondary metabolite contents. However, *rolA* is the least studied gene among *rolA-C* about its effects on secondary metabolites. The available data are too limited to provide any hypothetical mechanism regarding the effects of *rolA* on secondary metabolites.

3.3. *rolB* affects secondary metabolites

rolB seems to be a strong inducer of secondary metabolites. *rolB*-transgenic *R. cordifolia* calli accumulated 15-fold higher anthraquinones than non-transform calli by enhancing the expression of the key structural gene, isochorismate synthase (Shkryl et al. 2008). The greatest record of *rolB* effects on secondary metabolites was more than 100-fold increase in resveratrol production in *Vitis amurensis* calli, which contain 3.15% resveratrol in dry weight (Kiselev et al. 2007). In addition, the resveratrol production has a positive correlation with both the transcripts of *rolB* and phenylalanine ammonia-lyase, which is the key enzyme of resveratrol biosynthetic pathway. Nevertheless, the transcript levels of *rolB* have a negative correlation with growth rates of calli (Kiselev et al. 2009). In conclusion, *rolB* seems to promote secondary metabolites via inducing the expression of genes encoding secondary metabolism pathway resulting in greater metabolic flux towards secondary metabolites. Nevertheless, the effects of *rolB* on the secondary metabolites are difficult to be connected with auxin.

In hairy root culture, *rolB* shows completely different effects from those in calli culture. *rolB*-transgenic roots showed higher growth rate with lower nicotine content (Palazón et al. 1997). This result supports the fact that *rolB* is regulated distinctly in different cell type, and the way how hairy root accumulates higher level of secondary

metabolites might be the cooperation of the genes located on T-DNA for physiological adaption.

Bulgakov and coworkers transformed *rolB* into *R. cordifolia* calli, and they treated the calli with a tyrosine phosphatase inhibitor canthridin. The growth of *rolB*-transformed calli was not affected by canthridin, but the anthraquinone contents increased with the increase of canthridin concentrations (2002). This result reduces the possibilities that RolB is a tyrosine phosphatase in plant, and the tyrosine phosphatase signaling did not participate in secondary metabolites anabolism. In 2009, Dubrovina and coworkers reported that treating with calcium channel blockers dramatically suppresses the resveratrol contents in *rolB*-transgenic *V. amurensis* calli (2009). With *AtCPK1*, *A. thaliana* calcium-dependent protein kinase 1, expressed in *R. cordifolia*, the anthraquinones are up-regulated with higher reactive oxygen species (ROS) level (Bulgakov et al. 2011). However, the *rolB*-transgenic *R. cordifolia* calli have lower ROS level (Bulgakov et al. 2012), which indicates the stimulus of metabolite accumulations of *rolB* is not only via activating CPK signaling. It needs further evidence to clarify the regulatory mechanism of *rolB* on secondary metabolism pathway.

3.4. *rolC* affects secondary metabolites

rolC strongly promotes the growth with little improvement of nicotine content in transgenic tobacco root culture (Palazón et al. 1997). On the other hand, the expression of *rolC* has a moderately negative correlation with growth and a moderately positive correlation with alkaloid productions in *Catharanthus roseus* (Palazón et al. 1998a). The result was diametrically opposite to the observation proposed by the same authors that the faster-growing *rolC*-transgenic tobacco root

contains higher nicotine (Palazón et al. 1998b). These three studies conducted by the same group showed inconsistent results in the relationships among growth rates, metabolites productions, and *rolC* expressions.

rolC-transgenic *Atropa belladonna* root tissues showed similar propane alkaloid level as *rolABC*-transformed ones with a 12-fold increase in intact roots; however, *rolC* alone only increase 17-fold of growth rate than non-transformed root tissue, which is 4.4-fold lower than *rolABC* together (Bonhomme et al. 2000a). In *P. ginseng* root and callus tissues, *rolC* promotes 1.8 to 3 times of ginsenoside accumulation without affecting growth rate (Bulgakov et al. 1998). *rolC*-transformed *R. cordifolia* calli accumulate 1.3 to 1.8 times of anthraquinone contents (Bulgakov et al. 2002). After 5-year cultivation, the calli carrying *rolC* accumulates 2 to 4.3 times of anthraquinone contents with higher isochorismate synthase expression levels (Shkryl et al. 2008).

The *rolC* might increase secondary metabolites through activating the transcription of the biosynthetic genes and the plant defense-related signals. In *rolC*-transgenic *Eritrichium sericeum*, specific cytochrome P450 monooxygenase *CYP98A3*, which is related to caffeic acid biosynthesis, is up-regulated, whereas the *CYP98A1* and *CYP98A2* were not (Inyushkina et al. 2009). β-1,3-glucanse, which belongs to the pathogen-related 2 (PR-2) gene family, is up-regulated in *rolC*-transformed *P. ginseng* (Kiselev et al. 2006). However, in *R. cordifolia* callus culture, *rolC* down-regulates reactive oxygen species (Bulgakov et al. 2008), which are stress-responsive products and are usually activated along with PR-2. On the other hand, high ROS level promotes secondary metabolites (Bulgakov et al. 2011). To sum up, *rolC* might alter plant metabolite content by up-regulating the gene expressions in

biosynthetic pathway directly and/or in a defense pathway related to PR-2 but independent to reactive oxygen species.

4. Nicotine regulatory mechanism

Nicotine is one of the most studied secondary metabolites due to the cigarette consumption. Even though it has been used for a long time, how it is regulated in tobacco plant remains unknown. In plant, nicotine functions as a herbivore-preventing agent, growth-regulating factor, and detoxification compound. Nicotine is synthesized in the roots, transported to the shoots, and then stored in leaf vacuoles (Mothes 1954; Dawson and Solt 1959; Saunders 1979). The nicotine biosynthetic pathway was clarified by a sequences of studies, and the pathway is summarized in Figure 1-3 (reviewed by Shoji and Hashimoto 2011).

Many reports indicate that hairy roots massively accumulate corresponding secondary metabolites of the host plant. In 1986, Hamill and coworkers reported that *N. rustica* hairy root culture induced by *A. rhizogenes* LBA9402 accumulated 3-fold higher nicotine levels than that of intact roots (Hamill et al. 1986). This result was further proved by Parr and Hamill. They generated hairy roots from different species of *Nicotiana,* and 4.47- to 58.8-fold increases of nicotine level in hairy roots compared with respective intact roots were observed (Parr and Hamill 1987). In the thesis, we would like to unveil the mechanism underlying huge amounts of secondary metabolites in hairy roots.

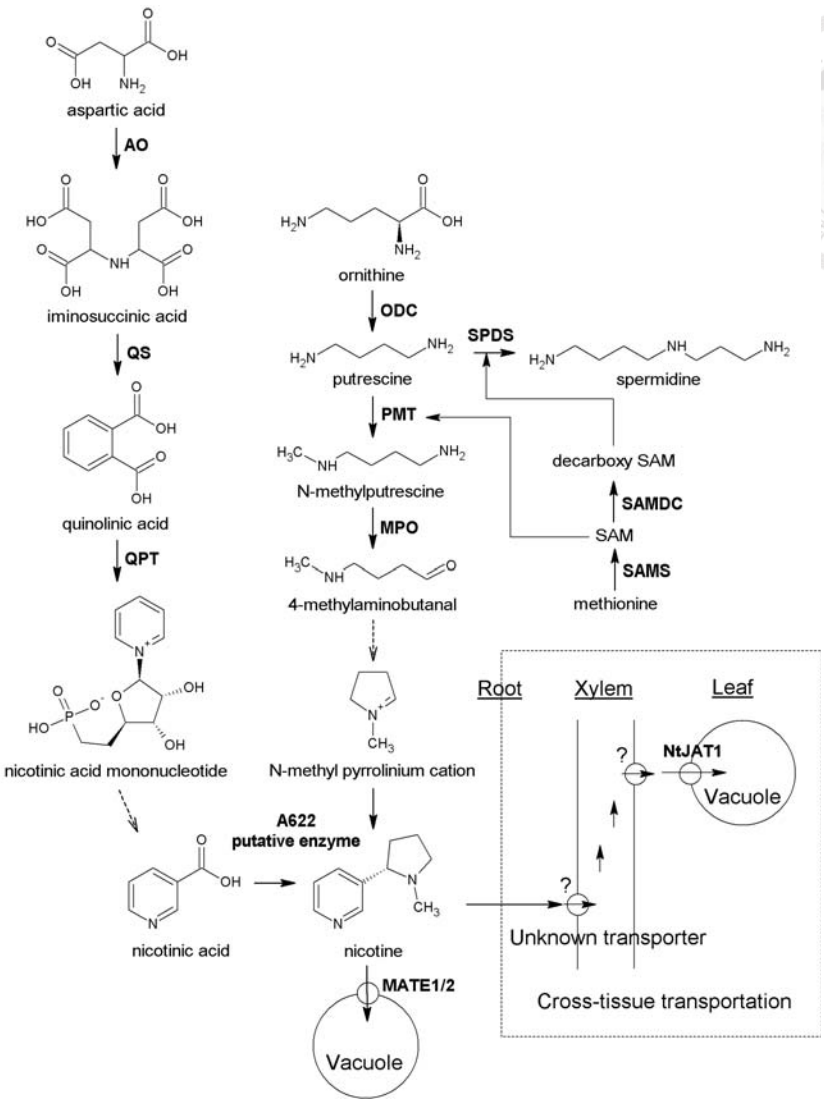

Figure 1-3 Biosynthetic pathway, transportation, and storage of nicotine. Abbreviated proteins: ODC, ornithine decarboxylase; PMT, putrescine N-methyltransferase; MPO, N-methylputrescine oxidase ; AO, aspartate oxidase; QS, quinolinic acid synthase; QPT, quinolinic acid phosphoribosyl transferase; A622, a presumable oxidoredutase; SPDS, spermidine synthase; SAMS, S-adenosylmethionine synthase; and SAMDC, S-adenosylmethione decarboxylase; MATE1/2, two homologous multidrug and toxic compound extrusion (MATE)-type transporters; JAT1; jasmonate-inducible alkaloid transporter 1. Nicotine was synthesized in root cell, and it would be either sent into root vacuole by MATE1/2-proton anti-porter or transported to leaf through xylem. Both transporters for nicotine xylem loading in root and unloading in leaf are unclear. The nicotine in leaf is sent into vacuole by the MATE like transporter JAT1.

Naturally, nicotine is a defensive toxin against insect herbivores (reviewed by Steppuhn et al. 2004). Jasmonic acid and its derivates (JAs) are closely associated

with defensive responses to stresses, including herbivory and wounding (reviewed by Wasternack 2007; Browse 2009; Wasternack and Hause 2013). Moreover, JAs elicit production of kinds of secondary metabolites (Gundlach et al. 1992). Treating jasmonic acid (JA) or methyl jasmonic acid (meJA) stimulates the nicotine contents in tobacco plants and cell suspension culture by activating genes in nicotine biosynthesis pathway (Imanishi et al. 1998; Shoji et al. 2000). The expression levels of *ODC*, *PMT*, *MPO*, *AO*, *QS*, *QPT*, *A622*, *NtMATE1/2*, and *NtJAT1*, almost all of the known enzymes involved in nicotine biosynthetic pathway, are regulated by the plant hormone JAs (Imanishi et al. 1998; Shoji et al. 2000b; Goossens et al. 2003; Xu and Timko 2004). Moreover, *nic2* mutant with low nicotine content showed reduced ethylene responsive factor (ERF) transcripts that are involved in JAs-induced nicotine biosynthesis (Shoji et al. 2010). In the promoter regions of putrescine methyltransferase (PMT) and quinolinate phosphoribosyl transferase (QPT), two key enzymes of nicotine biosynthesis, are found to contain JA-responsive G-box and GGC box motifs (Xu and Timko 2004; De Boer et al. 2011). In the absence of JA, the JA transcriptional repressors JASMONATE ZIM DOMAIN (JAZ) 1-3 might block the PMT transcription by physical interaction with MYB2, which binds to the G-box motif. In the presence of JA, the JAZs were attenuated by proteasome-mediated protein degradation, which resulted in the activation of PMT and QPT to stimulate nicotine biosynthesis (De Boer et al. 2011; Shoji and Hashimoto 2011b; Zhang et al. 2011). In addition, cDNA microarray analysis showed that some APETALA2/ ETHYLENE RESPONSE FACTOR (AP2/ERF) family genes are down-regulated in low nicotine gene mutant *nic1/2* (i.e. *aabb* genotype) (Shoji et al. 2010). In the tobacco hairy root tissues, these AP2/ERF genes are up-regulated after treating with

MeJA, while they are down-regulated after treating with ethylene precursor 1-aminocyclopropane-1-carboxylic acid (ACC) (Shoji et al. 2010). These AP2/ERF might be the transcriptional activators which bind to GGC box after JA signals (De Boer et al. 2011; Shoji and Hashimoto 2011b).

Treating ethylene decreases the nicotine levels in tobacco. Ethylene and JA interact synergistically or antagonistically in various signals. In the view of nicotine biosynthesis, ethylene down-regulates some structural genes by down-regulating the AP2/ERF (Shoji et al. 2000a; Shoji et al. 2010). *Manduca sexta* induces the ethylene production to prevent nicotine production (von Dahl et al. 2007). The antagonistic interaction between ethylene and JA responses may ensure the effective nicotine-based defense mechanism. In addition, treating auxin reduces the nicotine levels by an unknown mechanism (Tabata et al. 1971; Takahashi and Yamada 1973). To sum up, nicotine is up-regulated by JA pathway, but it is down-regulated by both ethylene and auxins signals.

There is a controversial idea that tobacco hairy root has higher auxin perceptions and greater nicotine content at the same time. Nicotine regulation in tobacco hairy root is a unique mechanism distinguished from that in normal tissue.

5. Objectives

In plants, secondary metabolites are usually tightly regulated; however, the regulatory rules seem to be broken in hairy root tissues, which leads to massive accumulations. Due to the characteristic, researchers have established hairy root culture to manufacture secondary metabolites for two decades. However, hairy root can only be induced in some dicots and few woody plants, which is a huge limitation in applying hairy root to producing more metabolites from the plant species which are

resistant to *A. rhizogenes*. To expand the applications, our eventual goals are to find out the molecular mechanisms in rhizogenesis and in metabolite accumulations. Finally, we hope we can produce plant secondary metabolites either by inducing hairy root formation efficiently or by regulating metabolic flux directly. This will hugely improve the development of pharmacology.

In the fundamental step, we focus on the *rol* genes, which have been reported to be highly related to rhizogenesis and secondary metabolite accumulations in various plants. We take *N. tabacum* as a plant model because it has been widely applied in studying hairy root formation. Besides, tobacco contains one of the most studied secondary metabolites, nicotine, and other related alkaloids, which offers a metabolomics model for metabolite accumulations. Via studying the functions of the *rol* genes in tobacco hairy roots, we may figure out how *rol* genes alter plant signals and ultimately result in rooting and secondary metabolites accumulating. In the case of rooting, we might generate root systems in pharmaceutically valuable monocots or in other plants whose hairy roots cannot be generated through altering the signals based on our findings. Besides, secondary metabolites are up-regulated by *rol* genes in many types of plant tissues. The enhancement seems to be a general phenomenon without tissue specificity. By studying how the *rol* genes regulate metabolites, we might contribute to clarify the metabolomics regulatory mechanisms in plants; furthermore, we could apply the result to enhancing the metabolite productivity and to lower production cost.

Chapter 2: Materials and Methods

1. General DNA manipulation

1.1. DNA quantification

Double-stranded DNA (dsDNA) and single-stranded DNA (ssDNA) used in this study were quantified by Quant-iT dsDNA Broad-Range Assay Kit (Life Technologies) and ssDNA Assay Kit (Life Technologies), respectively. 10 μl of sample or standard DNA was added to 0.6 ml Flat Cap PCR Tube (Sorenson BioScience), followed by adding 190 μl of working solution, composited by 99.5% (v/v) of buffer and 0.5% (v/v) of fluorescent dye from the assay kits. The sample and standard reactions were then mixed by vigorously shaking and incubated for 2 minutes at room temperature. The DNA concentration was measured and calculated by Qubit 2.0 Fluorometer (Life Technologies).

1.2. Plasmid DNA extraction from *E. coli*

The plasmid isolation from *E. coli* was carried out by alkaline lysis method. Single colony of *E. coli* was inoculated in a glass tube containing 3 ml Luria-Bertani (LB; which consists of 10 g/l tryptone, 5 g/l yeast extract, and 10 g/l NaCl, pH 7.0) and the appropriate antibiotics at 37°C with shaking overnight. The cell pellet was collected by centrifugation at 6,000 x *g* for 2 minutes. To resuspend the cells, 300 μl of solution I (25 mM Tris-HCl, pH 8; 10 mM EDTA; 10 μg/ml RNase (Sigma R-4642) was added to the cells with vigorous shaking. Then, 300 μl of solution II (0.2 N NaOH; 1% SDS) was added and mixed gently by inverting the tube and the mixture was incubated at room temperature for 5 minutes to lyse the cells completely. After incubation, 300 μl ice-cold solution III (3 M potassium acetate, pH 5.2) was added and mixed immediately by inverting the tube to precipitate the genomic DNA

and proteins. The solution was incubated on ice for another 5 minutes to precipitate potassium dodecyl sulfate to improve the purity of plasmid DNA. Centrifugation was performed at 18,000 x *g* for 10 minutes at 4°C and the supernatant containing plasmid DNA was transferred to a new centrifuge tube. The plasmid DNA was further precipitated by adding 0.6 volume (540 µl) of isopropanol and centrifuging at 18,000 x *g* for 30 minutes at 4°C. The supernatant was discarded, and the plasmid DNA pellet was washed once by adding 1 ml of 70% ethanol and centrifuging at 18,000 x *g* for 10 minutes at 4°C to remove the residual isopropanol. The supernatant was discarded and the plasmid DNA pellet was allowed air-dry for 10 minutes to evaporate ethanol. The plasmid DNA was redissolved either in deionized water for electroporation transformation or in TE (10 mM Tris-HCl, pH 8.0; 1 mM EDTA) buffer for chemical transformation, PCR analysis, sequencing, and endonuclease reaction.

1.3. Polymerase chain reaction (PCR)

In this study, five different DNA polymerases (or premix reagents) were used in PCR of different purposes. For routine PCR, *Taq* DNA Polymerase Master Mix Red (Ampliqon) was used. Phusion Flash High-Fidelity PCR Master Mix (Thermo Scientific) was applied in cloning. Expand High Fidelity PCR System (Roche) was used to synthesize DIG-labeled DNA probe. Advantage 2 Polymerase Mix (Clontech) was applied in long distance PCR for constructing Gal4 activation domain-fused cDNA library to identify the positive yeast two-hybrid clones of the library. iQ SYBR Green Supermix (Bio-Rad) was used in quantification PCR (described in the Material and Methods section 2.4, reverse transcriptase quantification polymerase chain reaction). Except the quantification PCR, all other PCR reaction mixtures containing

1x PCR buffer was supplied by the respective companies. In general, 1.5 mM of magnesium (II) chloride, 0.4 mM of dNTP (each), 200 nM of primers (each), and 1 ng/μl of genomic DNA templates or 1 pg/μl of plasmid DNA templates were used. PCR conditions were shown in Supplementary Table S2.

1.4. DNA purification

In aqueous solution such as PCR product, DNA was precipitated by adding 1/10 volume of 3 M sodium acetate (pH 5.2, adjusted by acetic acid) followed by adding 2 volumes of absolute ethanol. Centrifuging at 18,000 x *g* for 30 minutes at 4°C to pellet the DNA and the supernatant was removed by pipet tip, and the pellet was air-dried for 10 minutes to evaporate the residue ethanol. The DNA pellet is redissolved in TE buffer (10 mM Tris-HCl, 1 mM EDTA, pH 8.0). If the targeted nucleotide fragment is isolated from a polynucleotide mixture, agarose gel electrophoresis coupled with gel extraction is applied. After electrophoresis, the agarose gel containing target DNA fragment was excised and transferred to a microcentrifuge tube, and the DNA was extracted from the gel with Zymoclean Gel DNA Recovery Kit (Zymo Research). Appropriate volume (100 μl for every 100 mg of agarose gel) of ADB Buffer was added to the tube and incubated at 45°C until the agarose gel dissolved in the buffer (approximate 15 minutes). The solution was loaded onto the Zymo-Spin I Column, and the column was centrifuged at 18,000 x *g* for 30 seconds, and the flow through was discarded. The column was then washed by 200 μl of DNA Wash Buffer twice under the same centrifugation condition. After wash step, the DNA was eluted by 6 μl of TE buffer (10 mM Tris-HCl, 1 mM EDTA, pH 8.0). These DNA purification procedures were taken to obtain a single purified DNA fragment for many downstream applications in this study, such as PCR, splicing by overlap

extension PCR (SOEing PCR), endonuclease reaction, sequencing, ligation, and *in vitro* LR recombination.

1.5. Cloning by restriction-ligation method

pK18*mobsacB-rolA*, *B*, *C*, and *D* vectors for deleting respective *rol* genes, pGBKT7-*rolA*, *B*, *C*, and *D* vectors for constructing bait vector for yeast two-hybrid, and pET-21d-*rolB* and *rolC* for *in vitro* phosphatase activity assay in this thesis were cloned by restriction-ligation method. PCR product was purified by agarose gel electrophoresis, and 25 μl of eluted DNA was incubated with 1 volume of 2x Taq DNA Polymerase Master Mix Red (Ampliqon) at 72°C for 10 minutes to incorporate adenine bases to the both ends of PCR products. The products were further purified by isopropanol precipitation and resuspended in 10 μl of tris buffer. Then, 2 μl of product was added to a microcentrifuge tube containing 1 μl of yT&A cloning vector (Yeatern), 1 μl of T4 DNA ligase buffer (New England Biolab), 5 μl of deionized water, and 1 μl of T4 DNA ligase (New England Biolab). The reaction was carried out for 2 hours at room temperature to create cloning vector, and the result plasmid was transform into *E. coli* by heat shock mentioned below. The cloning and expressing plasmids were extracted and incubated with restriction enzymes respectively, and the fragments were purified by agarose gel electrophoresis. Afterward, 3:1 molar ratio of insert:vector with the total amount 100 ng of DNA were combined into a microcentrifuge tube containing 1 μl of T4 DNA ligase and 1 μl of buffer (New England Biolab), and then deionized water was added up to 10 μl. The reaction was taken for 2 hours at room temperature followed by *E. coli* transformation to obtain expression vector.

1.6. Cloning by Gateway system

For transcriptional fusion, pTC*rolB* and pTC*rolC*, with *yfp* driven respectively by *rolB* and *rolC* native promoters. For translational fusion, pTL*rolB* and pTL*rolC*, *yfp-rolB* and *yfp-rolC* driven by respective native promoters, were constructed by Gateway Technology (Life Technologies). 1 μl DNA solution containing 1 fmole purified plasmid or DNA fragment was added to a microcentrifuge tube containing 1 μl of deionized water, 0.5 μl of Salt Solution (Life Technologies), and 0.5 μl of pCR8/ GW/TOPO TA Cloning Vector (Life Technologies). The reaction was carried out at room temperature for 5 minutes. 2 μl of the reaction product was used for *E. coli* transformation to create entry clone. The transformation procedure was presented in the Materials and Methods section 4.1, *E. coli* transformation by heat shock. Then, the entry vector and the destination vector containing Gateway fragment were extracted, and 1:1 molar ratio of these two plasmids with the total 75 ng DNA were added into a microcentrifuge tube containing 0.5 μl of LR Clonase II Enzyme Mix (Life Technologies). The reaction was carried out at room temperature for an hour. Afterward, 0.25 μl of protease K (Life Technologies) was added to inactivate the reaction by incubating at 37°C for 10 minutes. 2 μl of the resulting mixture was used for *E. coli* transformation to obtain expression clones.

1.7. Total DNA isolation from *A. rhizogenes*

Agrobacterium total DNA was extracted with Wizard Genomic Purification Kit (Promega). One colony of *A. rhizogenes* was cultured in 3 ml yeast extract broth (YEB; which consists of 5 g/l beef extract, 1 g/l yeast extract, 5 g/l peptone, 5 g/l sucrose, and 0.49 g/l magnesium chloride heptahydrate) containing the appropriate antibiotics for 48 hours. One milliliter of cells (OD_{600}=1) were added to a

microcentrifuge tube. The cells were pelleted by centrifugation at 18,000 x *g* for 2 minutes. 600 µl of Nuclei Lysis Solution (Promega) was added to resuspend the cells by gently pipetting up and down, and the cells were incubated at 80°C for 5 minutes for lysis. The lysate was cooled to room temperature. 1 µl of RNase A (Sigma R-4642) was added and mixed gently by inverting the tube, and the cell lysate was incubated at 37°C for 30 minutes to reduce RNA contaminations. Then, 200 µl of Protein Precipitation Solution (Promega) was added to the RNase A-treated cell lysate and the sample was mixed by vortex vigorously for 20 seconds followed by incubating on ice for 5 minutes. Afterward, centrifugation at 18,000 x *g* for 3 minutes and the supernatant containing the genomic DNA was transferred to a new microcentrifuge tube. The genomic DNA was further purified by isopropanol precipitation and 70% ethanol wash. The air-dried genomic DNA pellet was rehydrated in TE buffer by incubating at 60°C for 1 hours, followed by incubating in 4°C refrigerator overnight. The *A. rhizogenes* genomic DNA was ready to be applied to cloning, PCR analysis, DIG-probe synthesis, and endonuclease treatment for Southern blot.

1.8. Plasmid DNA extraction from yeast

A single yeast colony was inoculated into 0.5 ml of the SD (synthetic defined) medium (6.7 g/l yeast nitrogen base without amino acids, 20 g/l dextrose) with 50 ppm kanamycin and appropriate amino acid supplement overnight at 30°C with shaking. The cells were transferred to a microcentrifuge tube and then pelleted by centrifugation at 18,000 x *g* for 30 seconds. The supernatant was removed and the pellet was resuspended in 50 µl TE buffer. 2 µl of 5 U/µl Zymolyase solution (Zymo Research) was added and incubated at 37°C for an hour with vigorous shaking to lyse

the yeast cell walls. Then, 20 μl of 10% sodium dodecyl sulfate (SDS) was added to cells and vortexed vigorously to lyse cells. To extract the DNA, the sample volume was brought to 200 μl with deionized water. Then, 200 μl of buffered phenol (pH 8.0) was added to the sample and mixed by vigorously vortexing. Centrifugation was carried out at 18,000 x *g* for 10 min and the upper aqueous phase was transferred to a new microcentrifuge tube. These phenol extraction steps were repeated until the interphase between aqueous solution and phenol was clean. To remove the phenol contamination, 200 μl of chloroform:isoamyl alcohol (24:1) was added, mixed and centrifuged as phenol extraction, and the final aqueous solution containing yeast DNA was further purified by isopropanol precipitation. The DNA pellet was redissolved in TE buffer for downstream PCR analysis or *E. coli* transformation to recover plasmid DNA.

2. General RNA manipulation

2.1. RNA quantification and quality control

All the RNA used in this study was quantified by Qubit RNA Assay Kit (Life technologies) following the instruction manual. The detail procedure was the same as which described in DNA quantification (Section 1.1). The RNA quality was examined by formaldehyde denaturing agarose gel electrophoresis. The RNA sample was treated with same volume of NorthernMax-Gly Sample Loading Dye (Life technologies) and incubated at 55°C for 30 minutes with NorthernMax Running Buffer (Life Technologies)

2.2. RNA extraction from plant tissue

Fresh plant tissue was weighted and frozen by liquid nitrogen, and the tissue was ground into fine powders with mortar and pestle. Before thawing, 1 ml of TRIzol

reagent (Life Technologies) per 100 mg of tissue powder was added to the mortar to cover the sample. The mixture thaw at room temperature. The cell debris was removed by centrifugation at 12,000 x *g* for 1 minutes. Total RNA was extracted with a Direct-zol RNA MiniPrep kit (Zymo Research) following the manufacturer's instructions. 0.5 ml of supernatant was transferred to a new microcentrifuge tube and 0.5 ml of absolute ethanol was added to the sample followed by vortexing. Then, 0.8 ml of the mixture was loaded onto Zymo-Spin IIC Column (Zymo Research). The total RNA would bind onto the column matrix by centrifuging at 12,000 x *g* for 1 minute. The column was washed by 400 µl Direct-zol RNA PreWash buffer with centrifugation at 12,000 x *g* twice, and the column was further washed by 700 µl of RNA Wash Buffer with centrifugation at 12,000 x *g* for 1 minute. The RNA was then eluted by adding 25 µl of DEPC-treated water and centrifugation at 12,000 x *g* for 1 minute. The DNA contamination was removed by adding 2.5 µl of 10x TURBO DNase Buffer and 1 µl of TURBO DNase (Life Technologies) and incubating at 37°C for 30 minutes. To remove DNase, 3 µl of DNase Inactivating Reagent was added and the sample was centrifuged at 12,000 x *g* for 2 minutes, and the pellet was discarded. The supernatant containing RNA was applied to first-strand cDNA synthesis.

2.3. First-strand cDNA synthesis

The cDNA was synthesized by GoScript Reverse Transcription System (Promega) following the manufacturer instruction. 1 µl of plant total RNA (1 mg/ml) was added to a nuclease-free PCR tube containing 1 µl of Oligo$(dT)_{15}$ and 7.5 µl of nuclease-free water. The oligo$(dT)_{15}$/RNA mixture was incubated at 70°C for 5 minutes and then chilled at 4°C. Then, 4 µl of GoScript 5x Reaction Buffer, 4 µl of 25 mM $MgCl_2$, 1 µl of PCR Nucleotide Mix with final concentration 0.5 mM each

dNTP, 0.5 μl of 20 unit/μl Recombinant RNasin Ribonuclease Inhibitor, and 1 μl of GoScript Reverse Transcriptase were added to the oligo$(dT)_{15}$/RNA mixture. cDNA synthesis was carried out by incubating the mixture at 25°C for 5 minutes followed by 50°C for an hour. The reaction was terminated by heating the mixture at 70°C for 15 minutes. The RNA template was then removed by adding 1 μl of RNase H (Life Technologies) with incubating at 37°C for 20 minutes. The resulting cDNA was ready for first-strand cDNA synthesis for quantification reverse transcription polymerase chain reaction (qRT-PCR) and cloning.

2.4. Quantification reverse transcription polymerase chain reaction

The aliquot of first-strand cDNA synthesis was diluted 100-fold to be the 4x concentration of template. The forward primer and reverse primer of interested transcripts were diluted to 800 nM respectively and mixed together with the same volume to generate 4x concentration of primer mix (400 nM each). The quantification reverse transcription polymerase chain reaction (qRT-PCR) composited with 5 μl of iQ SYBR Green Supermix (Bio-Rad), 2.5 μl of 4x concentration of template, and 2.5 μl of 4x concentration of primer mix. Depending on the numbers of samples, real-time fluorescent signals were detected by either CFX-384 or CFX-96 (Bio-Rad). The PCR program was described as following: (1) activating DNA polymerase at 95°C for 2 minutes; (2) amplifying target sequence by 40 cycles of DNA denaturing at 95°C for 20 seconds, primer annealing at 55°C for 20 seconds, and sequence amplifying at 72°C for 20 seconds. The fluorescent signals were detected at the end of every sequence amplifying step; (3) completing all the amplicons at 72°C for 5 minutes. After PCR, melting curve detection (built-in program) and DNA gel electrophoresis

were performed to check the specificity of PCR. The relative expression level were calculated by the method proposed by Yuan et al. (2006).

3. General protein manipulation

3.1. Protein quantification

In this study, protein was quantified by Bio-Rad Protein Assay, which is based on Bradford protein quantification method. The calibration was performed with bovine serum albumin (BSA). 5 μl of protein samples and protein standards (0.1 mg/ml to 1 mg/ml) were added to a 96-well microtiter plate, which was followed by adding 200 μl of 5-fold diluted Protein Assay Reagent (Bio-Rad). The reaction was completed by incubating at room temperature for 10 minutes and the optical absorption was detected at 570 nm. The protein concentrations of samples were calculated with the calibration of standards.

3.2. Total protein extraction from yeast

A single yeast colony was inoculated into 3 ml of the SD (synthetic defined) medium containing 50 ppm kanamycin and appropriate amino acid supplement at 30°C overnight with shaking, which was followed by inoculating the entire culture to a 500 ml Hinton flask containing 100 ml of medium. Until OD_{600nm} of the culture achieved 0.5, the cells were collected by centrifuging at 6,000 x *g* for 10 minutes at 4°C. The cell pellet was resuspended by 7 ml of breaking buffer (50 mM sodium phosphate, pH 7.4; one Complete Protease Inhibitor Cocktail Tablet containing EDTA (Roche) was added to 50 ml of breaking buffer), and 0.5 ml of acid-washed glass beads (Sigma G8772) was added to the breaking buffer with vigorous vortex to lyse cells. The cell debris was removed by centrifugation at 20,000 x *g*. Then, 2.5 ml of supernatant was loaded onto PD-10 Desalting Column (GE healthcare) and eluted by

3.5 ml of tris buffer (50 mM Tris-HCl, pH 7.4). The eluent was concentrated by 3 kD cut-off Vivaspin Sample Concentrator (GE Healthcare). The yeast protein sample could be quantified and analyzed by Western blot directly.

3.3. Total protein extraction from plant tissue

Whole plant tissue was frozen by liquid nitrogen and ground into fine powders with mortar and pestle. 1 ml of CelLytic P Cell Lysis Reagent (Sigma C2360) containing Complete Protease Inhibitor Cocktail (Roche; 1 tablet was added to 50 ml of CelLytic P) was added to 0.5 mg of the tissue powders. Then, the sample was desalted and concentrated by PD-10 Desalting Column (GE Healthcare) and 3 kD cut-off Vivaspin Sample Concentrator (GE Healthcare) as described above. The plant protein was applied in Western blot analysis.

4. Microorganisms transformation

4.1. *E. coli* transformation by heat shock

Single colony of *E. coli* was picked from LB plate, inoculated into 3 ml of LB medium in a glass tube and then cultured overnight. The overnight culture was diluted 1000-fold into a new 3 ml LB medium and then grown at 37°C until the OD_{600} reached 0.3-0.5. *E. coli* cell pellet was harvested by transferring the culture medium to pre-chilled centrifuge tube and centrifuging at 1,500 x *g* for 5 min at 4°C. The pellet was resuspended in one-tenth of original volume of ice-cold transformation and storage (TSS) solution (LB broth adding 10% w/v polyethylene glycol 8000 (PEG), 5% dimethyl sulfoxide, and 50 mM magnesium chloride). A 0.1 ml aliquot of cells was mixed with 100 ng of plasmid DNA for transformation, and was incubated on ice for 30 minutes. To transform *E. coli*, the mixture of cells and plasmid DNA was heat shocked by incubating at 42°C water-bath for 2 minutes, which was

followed by ice-bath for 5 minutes. Next, 250 μl of super optimal broth with catabolite repression (SOC, which consists of 20 g/l tryptone, 5 g/l yeast extract, 10 mM NaCl, 2.5 mM KCl, 10 mM $MgCl_2$, and 20 mM glucose) was added to the mixture, and the cells were incubated at 37°C with shaking at 200 rpm for an hour for recovery. To select the transformants, the cells were spread onto LB agar containing appropriate antibiotics and incubated for 16 hours. The transformants were further confirmed by colony PCR and restriction-map analysis.

4.2. *A. rhizogenes* transformation by electroporation

A glass culture tube containing 3 ml YEB was inoculated with a single colony of the *A. rhizogenes.* The cells were grown overnight at 26°C with shaking. The entire 3 ml overnight grown culture was inoculated into a flask containing 100 ml YEB, and the cells were incubated at 26°C with shaking until the OD_{600} of the culture reaches 0.5-0.8. The cells were chilled on ice for 10 minutes and transferred to pre-chilled centrifuge tube. Cell pellets were collected by centrifuging at 10,000 x *g* for 10 minutes at 4°C. Equal volume of ice-cold sterile deionized water was added to wash the cell twice, and one-tenth volume of ice-cold filter-sterile 10% glycerol was added to wash the cell once. Cells were finally resuspended in 400 μl ice-cold filter-sterile 10% glycerol and were aliquoted every 40 μl into individual microcentrifuge tubes. The cells could be either frozen by liquid nitrogen and stored at -80°C or processed electroporation directly. To perform *Agrobacterium* transformation, 100 ng plasmid DNA dissolved in deionized water was added to 40 μl aliquot of cells and incubated on ice for 30 minutes. After incubation, the cells were transferred to a 0.1 cm MicroPulser Cuvette (Bio-Rad 165-2089) and the electroporation was carried out by MicroPulser Electroporator (Bio-Rad) with built-in *Agrobacterium* transformation

program. One milliliter of YEB was added to the cuvette to rinse the cells, and the mixture was transferred to a glass culture tube. The tube was incubated at 26°C for 4 hours with shaking. The cells were selected by plating on the YEB agar plates containing the appropriate antibiotics, and further confirmed by PCR with total DNA extracted by Wizard Genomic DNA Purification Kit (Promega).

4.3. Yeast transformation by lithium acetate (LiAc) mediated method

All media used for yeast culture were supplied with 50 ppm kanamycin. Yeast transformation was performed by YeastMaker Yeast Transformation System 2 (Clontech). 3 ml of yeast peptone dextrose adenine (YPDA, which contains 10 g/l yeast extract, 20 g/l peptone, 20 g/l dextrose, and 20 mg/l L-adenine hemisulfate salt) broth was incubated with a yeast colony at 30°C for 12 hours. Then, 5 µl of the culture was transferred to a 50 ml of YPDA broth in a 250 ml Hinton flask. The culture was incubated at 30°C with shaking until the OD_{600} reached 0.15-0.3, and the cells were pelleted by centrifuging at 1,000 x *g* for 10 minutes and resuspended in 100 ml of fresh YPDA broth. The culture was incubated at 30°C until the OD_{600} reached 0.4-0.5. The cells were pelleted and washed by adding 100 ml of sterile deionized water followed by 3 ml of 1.1 x TE/LiAc (1 x TE/LiAc consists of 10 mM Tris-HCl, 1 mM EDTA, and 100 mM LiAc; pH 7.5), and finally resuspended in 1.2 ml of 1.1 x TE/LiAc solution. To introduce a plasmid into yeast cells, 100 ng of plasmid was added into 50 µl of 1.1 x TE/LiAc suspended cells. 5 µl of YeastMaker Carrier DNA and 500 µl of PEG/LiAc (40% w/v PEG 4000; 1 x TE/LiAc) was added to the cells, mixed and incubated at 30°C for 30 minutes. After incubation, 20 µl of dimethyl sulfoxide (DMSO) was added to the cells and incubated at 42°C for 15 minutes. Then, the cell pellet was collected by centrifugation at 18,000 x *g* for 30

seconds, and the cells were resuspended in 1 ml of 0.9% NaCl and the positive transformants were selected by plating onto SD agar with appropriate amino acid supplements. In addition to single plasmid transformation, library-scale transformation was performed in this study to make protein-protein interaction screening using yeast two-hybrid method. In library-scale transformation, DNA was added to 600 μl of 1.1 x TE/LiAc-suspended cells. 20 μl of YeastMaker Carrier DNA and 2.5 ml of PEG/LiAc were added, and 30°C incubation was taken for 45 minutes. Then, 160 μl of DMSO was added before 42°C incubation for 20 minutes. The cells were pelleted and resuspended in 3 ml YPD Plus Medium, and incubated at 30°C for 90 minutes with shaking to increase transformation efficiency. The cells were pelleted again and resuspended in 15 ml of 0.9% NaCl. The transformants were selected by plating onto SD agar (150 μl per 15 cm petri dish) with appropriate amino acid supplements.

5. Individual *rol* genes deficient strains generation

5.1. Generation of individual *rol* genes deficient strains

Splicing by overlap extension polymerase chain reaction (SOEing PCR) applied to delete the coding sequences of respective *rol* genes (Horton 1995). The sequences upstream and downstream of the target deletion fragment were amplified and ligated together by SOEing PCR with primers listed in Supplementary Table S3 and Phusion High-Fidelity DNA Polymerase (Thermo Scientific), and the PCR products were cloned into TA cloning vectors (Yestern). The amplified DNA fragments were subcloned into pK18*mobsacB* vector (Schäfer et al. 1994). The resulting plasmids were transformed individually into wild type *A. rhizogenes* A4 by electroporation, and the transformants were plated onto YEB agar plates with 100 ppm kanamycin.

The plates were then incubated at 26°C. Then, one of the colonies was inoculated in 3 ml YEB overnight with shaking at 26°C, and the overnight culture was spread onto YEB agar containing 10% sucrose. The colonies grown under 10% sucrose were either wild-type or target fragment-deleted strains. Southern blot was performed to distinguish them. The detail mechanism about deficient strain generation was illustrated in Figure 2-1.

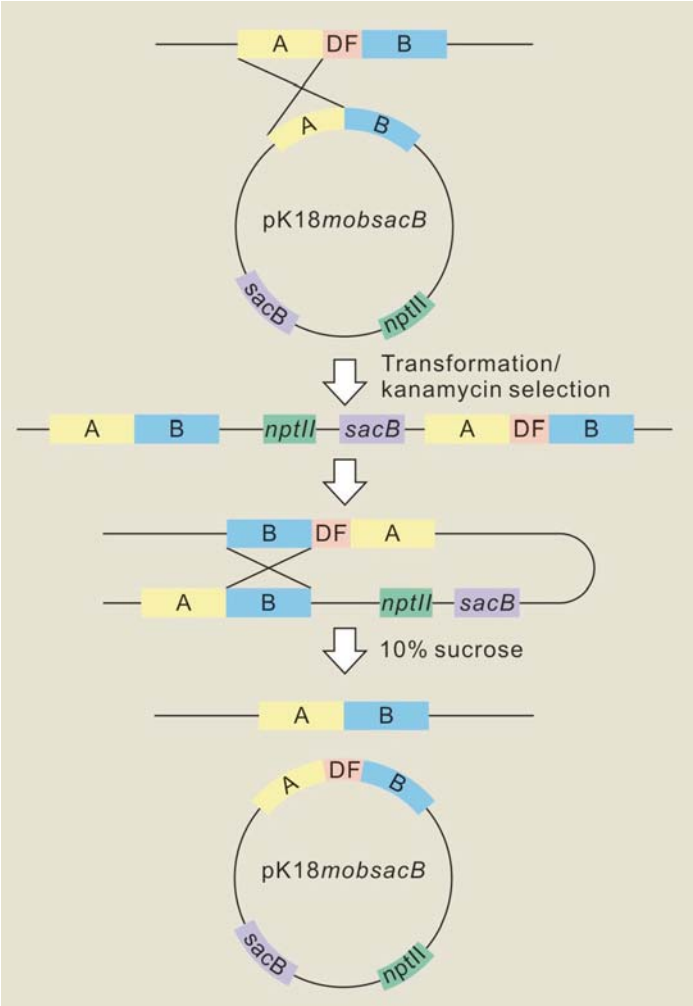

Figure 2-1 Mechanism of homologous recombination. To knock-out the target deletion fragment (DF), upstream and downstream sequences (A and B) of DF are ligated together by splicing overlap extension PCR (SOEing PCR) and cloned into pK18*mobsacB* vector, which only contains *E. coli* replicate *ori* site. The resulting vector is transformed into *Agrobacterium*. Only transformants with the vector integrated into chromosome by homologous recombination at either A or B of DF could survive under kanamycin selection (*nptII*, kanamycin-resistant gene). Then, one of the survival transformants is cultivated and further counter-selected by 10%

sucrose. The strain containing *sacB* in its chromosome cannot survive under sucrose condition; therefore, only the strain undergoing the second homologous recombination at either A or B could survive. By these two selection stages, the wild-type (the second homologous recombination at the same site) or DF deficient (at another sites) strains are harvested. These two different genotypes may be easily identified by colony PCR.

5.2. Confirmation using Southern blot

Agrobacterium total DNA was isolated by Wizard Genomic DNA Purification Kit (Promega) and treated with *Eco*RI (New England Biolabs). The resulting fragments were separated by agarose gel electrophoresis. Then, the gel was submerged with 50 rpm orbital shaking at room temperature in the following order: 250 mM HCl for 10 minutes, denaturation solution (0.5 N NaOH, 1.5 M NaCl) for 15 minutes twice, deionized water for 1 minute, neutralization solution (0.5 M Tris-HCl, pH 7.5; 1.5 M NaCl) for 15 minutes twice, and 20x SSC buffer (1x SSC consists of 0.15 M NaCl and 15 mM sodium citrate) for 15 minutes. The DNA fragments were then transferred to Immobilon-Ny$^+$ Transfer Membrane (Merck-Millipore) by capillary attraction overnight. The capillary attraction equipment was set as follows (from bottom to top): 20x SSC container, glass plate, bridge resting in a reservoir of 20x SSC, soaked 3MM filter paper, agarose gel, dried Immobilon-Ny$^+$ Transfer Membrane, dried 3MM filter paper, a stack of paper towels, glass plate, and a weight. After blotting, the nucleic acids were immobilized on the membrane by exposing to 120 mJ ultraviolet light. Then, the membrane was pre-hybridized with DIG Easy Hyb (Roche) at 48°C for an hour followed by hybridization at 48°C for 16 hours with DIG-labeled probes synthesized by PCR DIG Probe Synthesis Kit (Roche) with primers listed in Supplementary Table S3. The membrane was washed with 50 rpm

agitation by emerging in the following orders (except high stringency buffer, all other buffers were used at room temperature): low stringency buffer (2x SSC containing 0.1% SDS) for 5 minutes twice, high stringency buffer (0.1x SSC containing 0.1% SDS) for 15 minutes twice at 60°C, Washing Buffer (Roche) for 2 minutes, Blocking Solution (Roche) for 30 minutes, Anti-Digoxigenin-AP (Roche) solution (1:10000 dilution in Blocking Solution) for 30 minutes, Washing Buffer for 15 minutes twice, and Detection Buffer for 3 minutes. The DIG signal was developed by alkaline phosphatase reacting with chromogen bCIP/tNBT solution (Merck-Millipore).

6. Transcriptional and translational fusion

6.1. Generation of destination vector pGWYFP for C-terminal tagged protein cloning

pEarleyGate 101 and pEarleyGate 301 were reacted with both *Nco*I and *Xba*I (New England Biolabs). The resulting YFP fragment coming from pEarleyGate 101 and the backbone without promoter from pEarleyGate 301 were purified by extracting from agarose gel with Gel/PCR DNA Fragment Extraction Kit (Geneaid). These fragments were ligated T4 DNA ligase (New England Biolab) to generate destination vector pGWYFP (Figure 2-2).

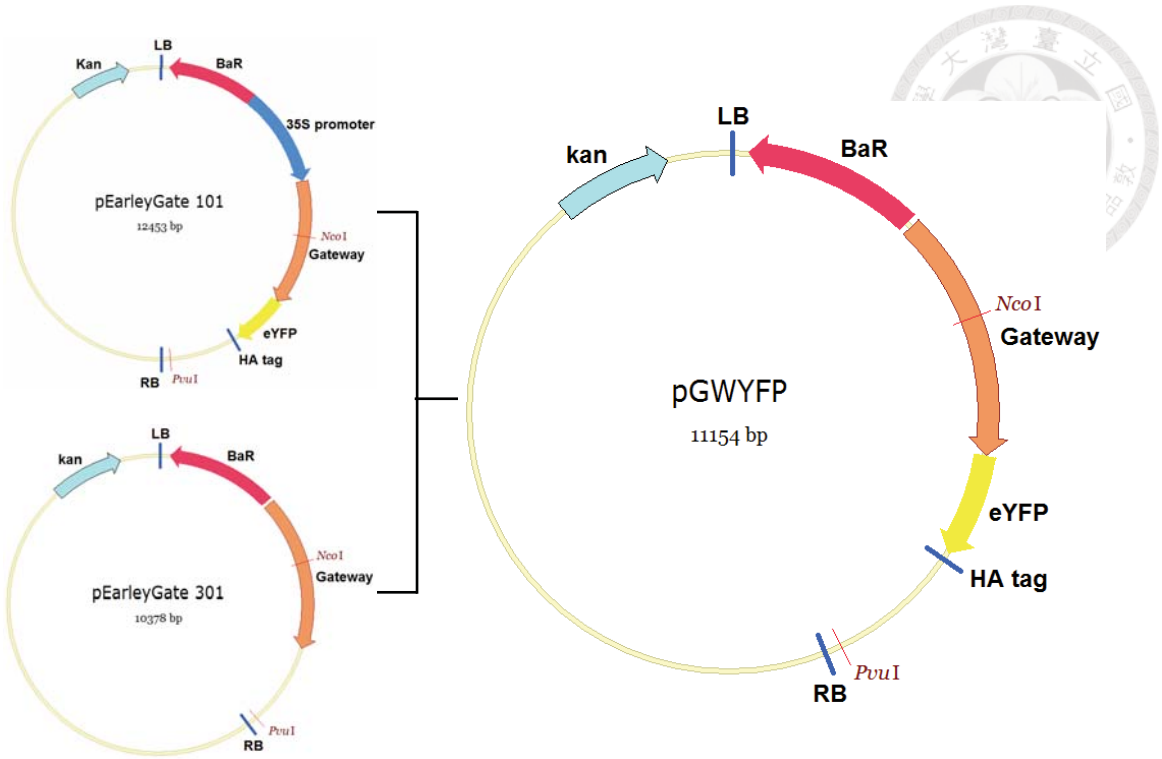

Figure 2-2 pGWYFP vector for *rol* gene complement. pEarleyGate 101 and pEarleyGate 301 were reacted with both endonucleases *Nco*I and *Pvu*I respectively. The resulting eYFP containing fragment from pEarleyGate 101 and backbone sequences from pEarleyGate 301 were purified by gel extraction and were ligated together by T4 DNA ligase to generate pGWYFP. This vector lacks a promoter, so it could be applied in expressing transcriptional or translational fusion to eYFP driven by interested promoter.

6.2. Expression clones establishment

To establish C-terminal YFP fused with RolB or RolC protein driven by native promoter, *rolB/C* promoters (p*rolB*/*C*) with corresponding coding genes were amplified respectively by Phusion High Fidelity DNA Polymerase (Thermo Scientific) with primers listed in Supplementary Table S3. p*rolB*/*C* without coding genes were also amplified to fuse with YFP as control. The amplified fragments were cloned into pCR8/GW/TOPO TA Cloning Vector (Life technologies) to create entry clones respectively. The expression clones, *prolB*-YFP-hemagglutinin tag (HA), *prolC*-YFP-HA, *prolB*-RolB-YFP-HA, and *prolC*-RolC-YFP-HA, were established

by reacting the respective entry clones with pGWYFP using Gateway cloning system (Life Technologies).

For N-terminal YFP fusion, we performed SOEing PCR with Phusion High Fidelity DNA Polymerase (Thermo Scientific) and primers listed in Supplementary Table S3 to create the following constructs *prolB*::HA::YFP, *prolC*::HA::YFP, *prolB*::HA::YFP::RolB, and *prolC*::HA::YFP::RolC. These fragments were firstly cloned into pCR8/GW/TOPO TA Cloning Vector to create entry clones, and the resulting entry clones were reacted with pEarleyGate 302 in Gateway cloning system to create expression clones.

The YFP control constructs were transformed into wild type *A. rhizogenes*, and the other four YFP fusion constructs were individually transformed into corresponding *rolB* or *rolC* gene deficient *A. rhizogenes*. These transformants were used to induce hairy roots to characterize the phenotypic effects caused by *rol* genes, to address the promoter regulations and protein localizations, and to identify the associated proteins in plant.

7. Hairy root induction

7.1. *N. tabacum* W38 growing

N. tabacum L. var W38 seeds were surface-sterilized by 70% EtOH followed by 1% bleach containing 0.01% Tween-20. The seeds were repeatedly washed by sterile deionized water to remove bleach and surfactant. The surface sterilized seeds were spread onto 1/2 Murashige and Skoog (MS) plate (1/2 MS medium consists of 3% sucrose in half-strength MS medium; pH was adjusted to 5.8 by KOH; 1/2 MS plate was 1/2 MS liquid medium gelled with 0.3% w/v phytagel (Sigma)). The seeds were

germinated and grew under 400 lux light intensity with 14/10 light/dark cycle at 22°C for 8 weeks.

7.2. Hairy root induction

A. rhizogenes was incubated in YEB (if *Agrobacterium* harbored the binary vector, appropriate antibiotics were added to the bacterial culture) at 26°C until the cells reached stationary phase (OD_{600} is approximately at 6). The cells were diluted to 0.1 unit of OD_{600} in dilution medium (which was consist of 1/2 MS medium with 0.5 g/l MES and 20 g/l sucrose; pH was adjusted to 5.8 by KOH). The 8-week-old tobacco leaves which contain the main veins were cut into 1 square centimeter. One side of vein section was slightly dipped into the diluted bacteria culture and then the leaf disc was sticked from the opposite side of vein section onto 1/2 MS plate. The leaves and the bacteria were co-incubated at 22°C in the dark. Three days later, the leaves were washed by sterilization medium (1/2 MS medium containing 200 ppm cefotaxime) for 3 times, and then sticked onto the sterilization plate (1/2 MS medium containing 300 ppm of cefotaxime, and solidified with 0.3% w/v phytagel) to remove bacterial contaminations. The hairy roots were subcultured 3 weeks after induction by cutting 1.5 cm tissues measured from root tip and transferring to a new sterilization plate. To keep the hairy root clones, these subculture procedures were taken every two to three weeks. If massive biomass is required, the hairy root will be cultured in 1/2 liquid MS medium. The induction process is shown in Figure 2-3.

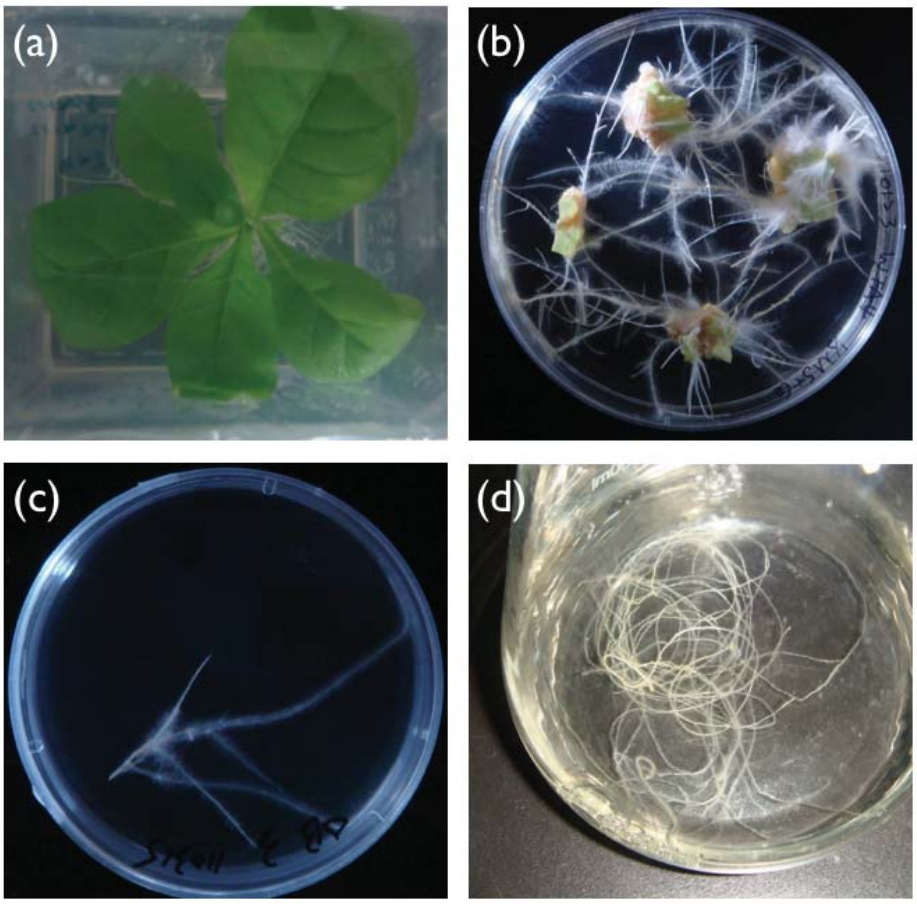

Figure 2-3 Inducing tobacco hairy root. (a) 8-week-old aseptic tobacco plant; (b) leaf discs inoculated with *A. rhizogenes* and hairy roots emerging from infected position. After root emerging, the hairy root was cultured to maintain on (c) the half-strength MS solid medium or in (d) the half-strength MS liquid medium.

7.3. Hairy root confirmation

The hairy roots induced by wild-type or *rol* gene deficient *A. rhizogenes* A4 were confirmed by PCR. A small fragment of hairy root was placed in PCR tube, and the DNA was extracted from the tissue by adding 10 μl of UniversAll Tissue Extraction Buffer (Yeastern Biotech) and incubated at 95°C for 10 minutes. Then, 10 μl of PCR reaction mixture containing 5 μl of *Taq* DNA Polymerase Master Mix Red (Ampliqon), 1 μl of DNA extractant, and 4 μl of each 0.5 μM primers (final 0.2 μM each) were prepared. *rolB* or *rolC* was used for hairy root confirmation, and tobacco

actin-9 was used as a positive control and *A. rhizogenes virA* was used as a negative control. In addition, hairy roots induced by transcriptional or translational complementary strains were selected by incubating the clones on 1/2 MS plates with addition of 10 μg/ml of basta for 3 weeks. The clones which could survive on the plates were further confirmed for the *rol* genes integration by the same procedure.

8. Microarray assay and data analysis

Each hairy root clone was cut 1.5 cm from the root tip, and the root tip was grown in a 250 ml flask containing 50 ml of half-strength liquid MS medium containing 3% sucrose. The 14-day-old tissue was frozen by liquid nitrogen and ground into for powder in a mortar. Before thawing, 1 ml of TRIzol reagent (Life Technologies) per 100 mg of tissue powder was added to the mortar to cover the sample. Samples from 24 independent clones of each hairy root group in TRIzol reagent were then pooled to create a sample mixture (50 μl each). Total RNA was extracted with a Direct-zol RNA MiniPrep kit (Zymo Research) described above. Moreover, RNA from a fast-growing hairy root clone (clone 9) was extracted at 14th day with the same procedure, and RNA from intact roots was extracted and pooled with 24 root samples obtained at one-hour intervals to avoid circadian variation. The RNA quality was determined by an Agilent 2100 bioanalyzer (Agilent Technologies). A 0.2 μg sample of total RNA was amplified by a Low-Input Quick-Amp Labeling Kit (Agilent Technologies) and labeled with Cy3 or Cy5 (CyDye, Agilent Technologies) during *in vitro* transcription. The Cy-labeled cRNAs were hybridized to a dual-channel Agilent Tobacco Oligo 4x44K Microarray (Agilent Technologies) that was scanned with an Agilent microarray scanner (Agilent Technologies) at 535 nm for Cy3 and 625 nm for Cy5. The images were analyzed and normalized by the

rank-consistency-filtering LOWESS method with Feature Extraction Software (version 10.5.1.1; Agilent Technologies). The results were analyzed with GeneSpring GX software (Agilent Technologies), and the differentially expressed genes (p value < 0.05) were extracted and sorted using the Gene Ontology (GO) Analysis Toolkit and Database for the Agricultural Community (AgriGO; http://bioinfo.cau.edu.cn/agriGO/) (Du et al. 2010). The GO enrichment analyses were performed by Singular Enrichment Analysis (SEA) using AgriGO with the default settings. The processed of RNA amplification, Cy dye labeling, microarray hybridization, image processing, and GeneSpring analysis were entrusted to Weikeng Industrial CO., LTD, Taiwan.

9. Quantification of alkaloids

Tobacco tissue was ground into fine powders with liquid nitrogen. Every milligram of tissue powders was added with 7.5 μl of extraction buffer, which consists of 1% formic acid aqueous solution spiked with 10 ppm of cotinine. The alkaloid metabolites were extracted by vigorous vortex for approximate 1 minute. Then, cell debris was removed by centrifugation and the supernatant was directly analyzed by high-performance liquid chromatography with diode array detector (HPLC-DAD). Shimadzu 10 AP system containing a binary pump, an autosampler, and a diode array detector was used with Luna HILIC column (Phenomenex; 3 μm, 250 mm x 4.6 mm) attached to its guard column. The solvent were (A) acetonitrile/50 mM ammonium formate (pH 3.2) 90:10 and (B) acetonitrile/water/50 mM ammonium formate (pH 3.2) 50:40:10. The elution program was as follows: 0-2.5 minutes, 0% of B; 2.5-10 minutes, 0-100% of B; 10-12.5 minutes, 100% of B; 12.5-15 minutes, 100-0% of B; 15-25 minutes, 0% of B. The flow rate was 1 ml/minute, and the injection volume was 10 μl. The eluent was monitored at 260 nm.

The concentration of nicotine was calculated with peak area integrated by Class-VP software (Shimadzu).

10. Yeast two-hybrid

10.1. Bait protein construction

The coding regions of individual four *rol* genes were amplified by Phusion High-Fidelity PCR Master Mix. The PCR products were cloned into yT&A cloning vector (Yeastern) and sub-cloned into pGBKT7 vector respectively by restriction-ligation method.

10.2. Poly A^+ RNA purification

Total RNA was extracted from the highest nicotine-containing hairy root clone 9 by Direct-zol RNA MiniPrep Kit (Zymo Research). The procedure was mentioned above. Then, poly A^+ RNA was purified by Oligotex mRNA Mini Kit (Qiagen). 250 μg of total RNA was added to a microcentrifuge tube, and the volume was adjusted to 250 μl with deionized water. Then, 250 μl of Buffer OBB (Qiagen) and 15 μl of Oligotex Suspension (Qiagen) was added to sample. The sample was further incubated at 70°C for 3 minutes followed by incubation at room temperature for 10 minutes to associate poly A^+ RNA with Oligotex beads. The mRNA:Oligotex complex was pelleted by centrifugation at 14,000 x *g* for 2 minutes. The supernatant was discarded, and the mRNA:Oligotex complex was re-suspended in 400 μl of Buffer OW2 (Qiagen). The suspension was loaded onto a small spin column (Qiagen). The column was centrifuged at 14,000 x *g* for 1 minute, and the flow-through was discarded. The complex was washed again with 400 μl of Buffer OW2 with the same centrifugation condition. Then, 20 μl of Buffer OEB (Qiagen) was added to suspended the complex. The spin column was incubated at 70°C for 2

minutes to dissociate mRNA from Oligotex complex. The purified mRNA was collected by centrifugation at 14,000 x *g* for 1 minutes.

10.3. cDNA synthesis and amplification

The cDNA library was generated by using Make Your Own "Mate & Plate" Library System (Clontech). 0.1 μg of poly A^+ RNA of hairy root clone 9 was added to a PCR tube, and 1 μl of CDSIII (Oligo $d(T)_{15}$; Clontech) was added to the PCR tube. The reaction volume was adjusted to 3 μl with RNase-free water, and the reaction mixtures were incubated at 72°C for 2 minutes followed by 4°C for 2 minutes. Then, 2 μl of 5x First-Strand Buffer (Clontech), 1 μl of 100 mM DTT (Clontech), 1 μl of 10 mM dNTP Mix (Clontech), 1 μl of SMART MMLV Reverse Transcriptase (Clontech), and 1 μl of RNasin Ribonuclease Inhibitor (Promega) were added to the mixture. The reverse-transcription reaction was carried out by incubating at 42°C for 10 minutes, and then 1 μl of SMART III-modified oligo (Clontech) was added to the mixture. The reaction was processed with incubating at 42°C for an hour and stopped by incubating at 75°C for 15 minutes. Then, RNA template was removed by adding 1 μl of 2 units/μl RNase H (Clontech) with incubating at 37°C for 10 minutes. The cDNA was then amplified by long distance PCR (LD-PCR). 4 μl of cDNA was aliquoted into two PCR tubes, and each tube was added with 80 μl of deionized water, 10 μl of 10x Advantage 2 PCR Buffer (Clontech), 2 μl of dNTP mix (10 μM each), 2 μl of 5' PCR primer (Clontech), 2 μl of 3' PCR primer (Clontech), and 2 μl of 50x Advantage 2 Polymerase Mix (Clontech). The thermal cycling parameter applied in LD-PCR was described in Supplementary Table S2. The double stranded cDNA was examined by 1.5% agarose gel electrophoresis.

10.4. Gal4 DNA activation domain fused cDNA library of hairy root

The resulting double stranded cDNA was selected by size exclusive chromatography. Two CHROMA SPIN TE-400 columns (Clontech) were drained by centrifuging at 700 x *g* for 5 minutes, and two tubes of LD-PCR product were loaded onto the columns respectively, and the DNA was collected by centrifuging at 700 x *g* for 5 minutes. Then, the DNA solution was combined together and further purified by ethanol precipitation. The DNA was redissolved in 20 μl of deionized water. The resulting library DNA as well as 6 μl of pGADT7-Rec (Clontech) was added to 600 μl of LiAc component cell, and the transformation was processed according to the protocol mentioned above. The resulting transformants were selected by SD/-Leu agar plate.

11. Phosphatase activity assay

To check if RolB has phosphatase activity, RolB, N terminal fusion of glutathione transferase (GST) with RolB (GST-RolB), and C terminal fusion RolB-GST chimeric proteins were respectively cloned into pET-21d vector by restriction-ligation method. Meanwhile, RolC, GST-RolC, RolC-GST, and GST proteins were also respectively cloned into pET-21d as negative controls and GST tag control. The usage of primers were listed in Supplementary Table S3. The vectors were respectively transformed into *E. coli* BL21(DE3) competent cells. Each transformant was pre-cultured respectively in a test tube containing 3 ml of LB broth with 100 mg/l of ampicillin overnight, and 1 ml of the culture was inoculated into a 500 ml Hinton's flask containing 100 ml of LB broth with 100 mg/l of ampicillin. The culture was incubated at 37°C with shaking at 130 rpm. Once OD_{600} reached 0.6 (approximate 2 hours), 0.1 ml of 100 mM isopropyl-β-D-1-thiogalactopyranoside (IPTG) was added

to culture to induce the expression of the recombinant protein overnight at 16°C with shaking at 100 rpm. The cell was then collect by centrifugation, and the cell pellet was resuspended in 5ml of 2x phosphatase assaying buffer (formula of 1x phosphatase assaying buffer: 25 mM HEPES, 0.1 mM EDTA, 5 mM DTT, 0.1 mg/ml BSA, and 0.01% Brij 23). Then, 0.3 ml of the cell resuspension was added to a 1.5 ml centrifuge tube, following by adding 25 units of benzonase (Novagen), 1x protease inhibitor cocktail without EDTA (Roche), 120 μg of lysozyme (Sigma), and water to make a final solution with 1x phosphatase assaying buffer. The cell was broken by ultra-sonication, and the cell debris was removed by centrifugation at 20,000 x g. The protein was quantified by Bradford method as mentioned above. To assay the phosphatase activity, the protein sample was diluted to 5 mg/ml, and 40 μl of protein sample was added to a 1.5 ml centrifuge tube, following by adding 10 μl of 250 mM of *p*-nitrophenyl phosphate (*p*NPP; dissolved in 1x phosphatase assaying buffer). The reaction was then incubated at either 25°C or 37°C for 20 minutes, and the reaction was stopped by adding 1 ml of 7 N sodium hydroxide solution. The phosphatase activity was determined by measuring the optical density at 405 nm.

Chapter 3: Results and Discussion

Transcriptomic analysis reveals that ROS and genes encoding LTPs are associated with tobacco hairy root growth and branch development

Results

1. *rol* genes deficient *A. rhizogenes* mutants grew faster than wild-type.

Numerous reports have indicated that *rol* genes stimulate both rhizogenesis and secondary metabolites. For the past three decades, researches have tried to clarify the functions of *rol* genes by transforming individual genes into different species of calli or intact plants. However, considering the root natural of the *rol* genes, we would like to elucide their functions in hairy roots instead of other plant tissues. To address the individual functions of *rol* genes in promoting rooting and maintaining the root architectures, respective *rol* gene deficient strains by site specific homologous recombination were constructed. The genotypes of the strains were confirmed by Southern blot (Figure 3-1). To understand if each *rol* gene affects the bacterial growth, we compared the growth curve of these *rol* genes deficient strains with the wild-type strain in YEB liquid cultures. Four individual *rol* genes deficient mutants grew faster than the wild-type in the early exponential phase in YEB broth, but these strains grows no difference from middle exponential phase (Figure 3-2); constantly, wild-type strain takes approximate 1 day longer to form colonies on YEB agar plate. Based on this result and those from other studies (Batra et al. 2004; Lee et al. 2007), we used 48 h cultures in the subsequent hairy root induction experiments.

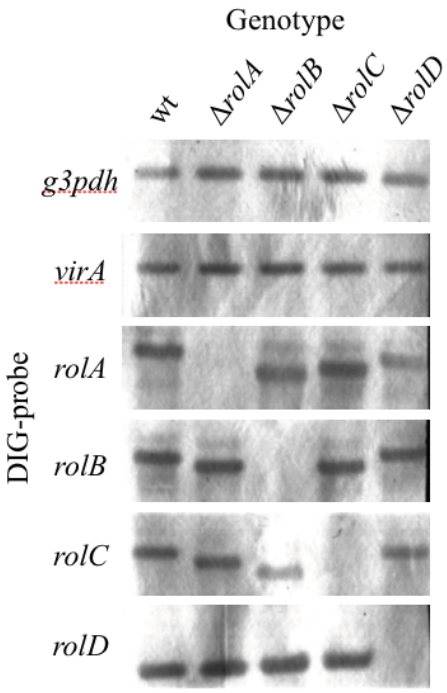

Figure 3-1 Southern blot confirmation of respective *rol* gene deficient strains. 1 μg of total DNA were reacted with *Eco*RI and blotted onto positive charge nylon membrane. The hybridization was performed by DIG-probe and detected by anti-DIG antibody conjugated with alkaline phosphatase. *g3pdh* and *virA* genes, located on the chromosomal DNA and on the pRi plasmid DNA, respectively, were used as the control experiments for DNA extraction and Southern detection. *g3pdh,* glyceraldehyde 3-phosphate dehydrogenase.

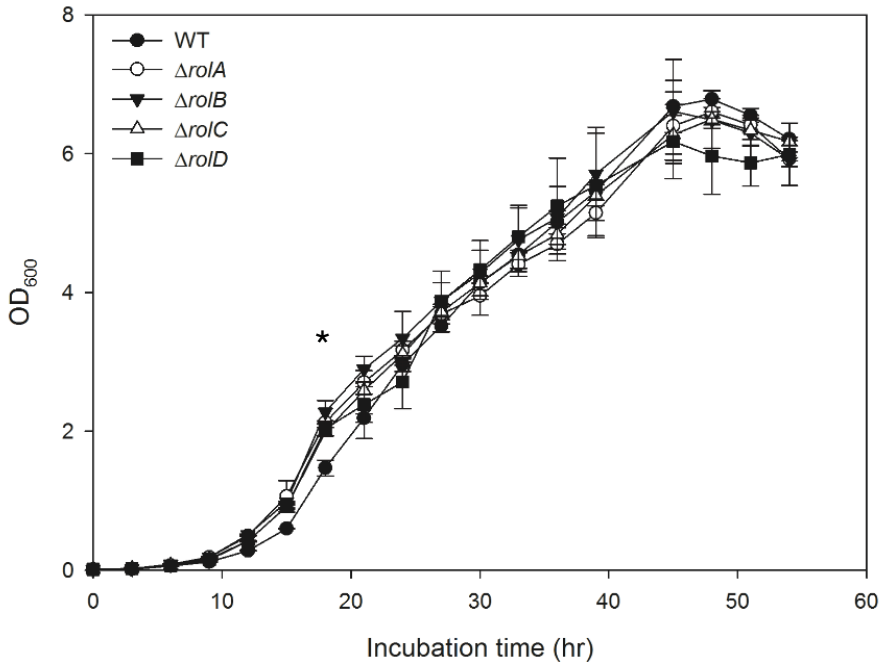

Figure 3-2 The growth curves of wild-type and respective *rol* gene deficient *A. rhizogenes*. The growth curves of four *rol* genes deficient strains are similar during

54-hour liquid cultivation in YEB medium. However, the wild-type strain grows slower than all the mutants at the early logarithm stage (18 hours post inoculation). The standard deviations shown here are represented five independent liquid cultures. The statistical analysis was performed by one-way ANOVA, and significant differences were analyzed by Fisher's least significant difference (LSD). * $p < 0.05$.

rolA is the only gene reported to express in both bacterial and plant cells among the *rol* genes (Pandolfini et al. 2000). However, by our observations, these four *rol* genes might express in the bacterial cells and result in growth-inhibiting during early log phase. Whether they express and what they function in *Agrobacterium* should be further elucidated.

2. Δ*rolB* and Δ*rolC A. rhizogenes* mutants have decreased hairy root induction ability

To evaluate how *rol* genes affect the initiation of hairy roots, we observed leaf discs every day after *Agrobacterium* infection for three weeks to determine the day of first root emergence post-infection (DREPI). Meanwhile, we calculated the primary root number per leaf disc (R/L ratio) at 21 days post-infection (dpi) (Swain et al. 2010). We defined a root-like tissue longer than 0.5 cm as induced hairy root tissue. An earlier DREPI and a higher R/L ratio indicate superior hairy root induction ability.

As shown in Figure 3-3, hairy roots began to emerge at 10 dpi from WTA4-infected tobacco leaf discs, and by 21 dpi, more than 90% of the WT-infected leaf discs had at least one hairy root. A significantly delayed DREPI was observed in Δ*rolB*- or Δ*rolC*-infected leaf discs compared with WT-infected discs ($p = 1.1\text{x}10^{-3}$ and $8.4\text{x}10^{-6}$, respectively); however, this delay was observed neither in Δ*rolA*- nor Δ*rolD*-infected leaf discs ($p = 0.72$ and 0.12, respectively). Δ*rolD*-infected leaf discs showed a lower DREPI prior to but not after 16 dpi, showing no significant difference

compared with WTA4-infected leaf discs. There was little or no difference in the percentage of Δ*rolA*-infected leaf discs showing hairy root emergence compared with WTA4-infected discs. Moreover, as shown in Figure 3-4, statistical analysis of the R/L ratio at 21 dpi revealed significant differences between WTA4-infected leaf discs and either Δ*rolB*-infected leaf discs (p = 1.1x10^{-3}) or Δ*rolC*-infected leaf discs (p = 8.4x10^{-6}), but not Δ*rolA*- or Δ*rolD*-infected leaf discs (p = 0.19 and 1.00, respectively). These results indicate that Δ*rolB*- and Δ*rolC*-infected leaf discs had impaired hairy root initiation ability, whereas Δ*rolA*- or Δ*rolD*-infected leaf discs did not.

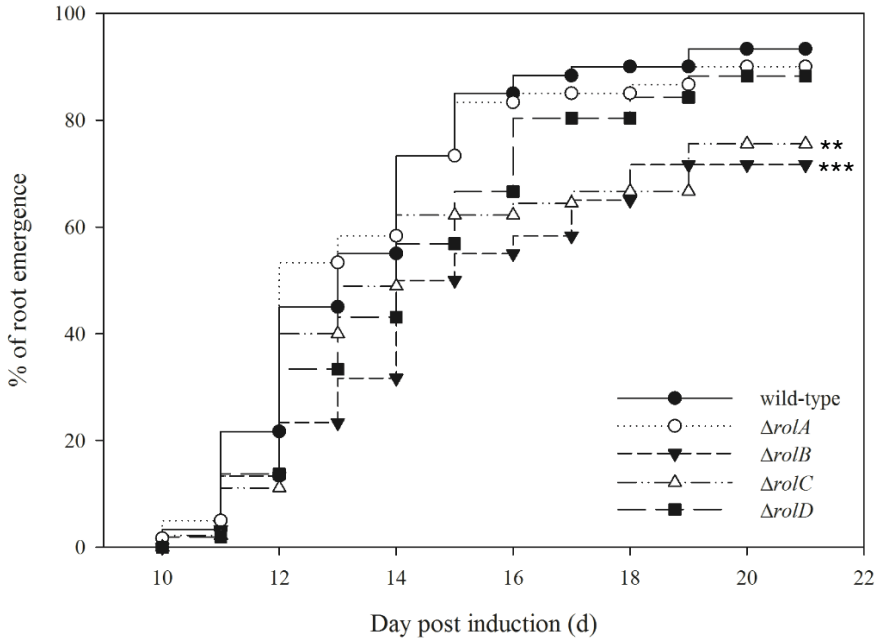

Figure 3-3 The day of the first root emergence post infection (DREPI). Every main vein of leaf were cut into five 1 cm^2 squares, and they were injected 0.4 µl of *A. rhizogenes* culture (OD_{600}=0.1) at a random order. Hairy roots began to emerge at 12 days post-infection (dpi); by 21 dpi, more than 90% of the leaf discs in the wild-type-infected group showed hairy roots. % root emergence indicates the percentage of leaf discs with hairy roots. The test numbers of wild-type, Δ*rolA*, *B*, *C*, and *D* are 60, 60, 60, 45, and 52 replicates were performed for wild-type, Δ*rolA*, Δ*rolB*, Δ*rolC*, and Δ*rolD*, respectively. The statistical analysis was performed by a permutation test using ANOVA with 1000 replicates, and the significant differences were analyzed by Fisher's LSD (** $p < 0.01$, *** $p < 0.001$).

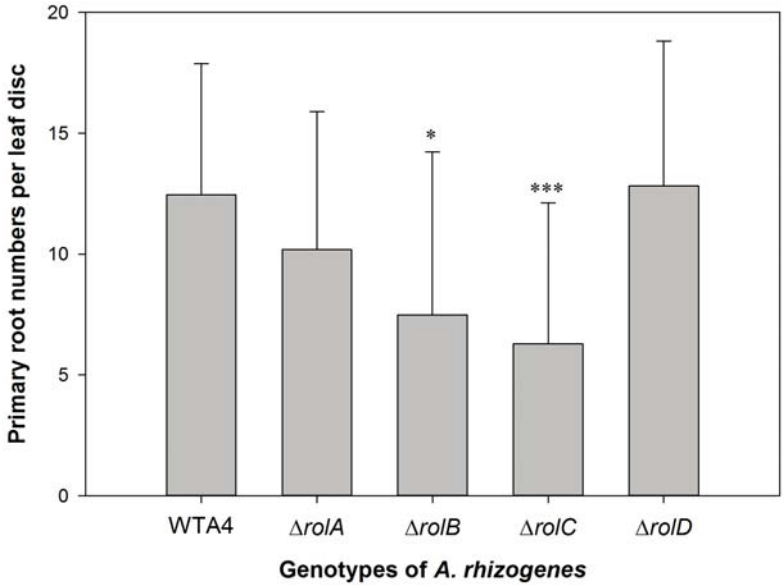

Figure 3-4 Primary root number per leaf disc (R/L ratio). Primary root, emerging from infected leaf disc, numbers were calculated on 21 dpi. The tested leaf disc numbers of WT, Δ*rolA*, *B*, *C*, and *D* were 60, 60, 60, 45, and 51, respectively. The statistical analysis was performed by a permutation test using ANOVA with 1000 replicates, and the significant differences were analyzed by Fisher's LSD (* $p < 0.05$, *** $p < 0.001$).

3. Aberrant hairy roots induced by *rol*-deficient *A. rhizogenes* mutants

To understand how the *rol* genes affect hairy root growth, we established five groups of hairy roots by induction with wild-type *A. rhizogenes* and each *rol*-deficient *A. rhizogenes* clone; these groups were named HRWT, HRΔ*rolA*, HRΔ*rolB*, HRΔ*rolC*, and HRΔ*rolD*. We then evaluated four parameters to determine the morphology at 18 days post-subculture: the main root length (MRL), branch root number (BRN), branch root density (BRD), and total branch root length (TBRL). MRL is defined as the length that the root grew from the root tip after subculture, BRN is the number of primary branch roots that emerged from the main root, BRD is the average number of branch roots per centimeter of main root, and TBRL is the sum of the root length of the whole hairy root culture except for the main root. MRL and

TBRL are respectively used to evaluate root growth ability of the original and new-forming root apical meristems. BRD and BRN describe lateral root emergence rate, which stands for new meristem formation. To select representative hairy root clones, all the hairy root clones of each group were sorted by their MRL from the longest to the shortest, and one representative clone with an MRL in each of the 1st, 25th, 50th, 75th, and 100th percentiles was photographed. As shown in Figure 3-5, in which representative clones from the 1st to 100th percentile are arranged from left to right, HRΔ*rolB* and HRΔ*rolC* clearly showed growth retardation.

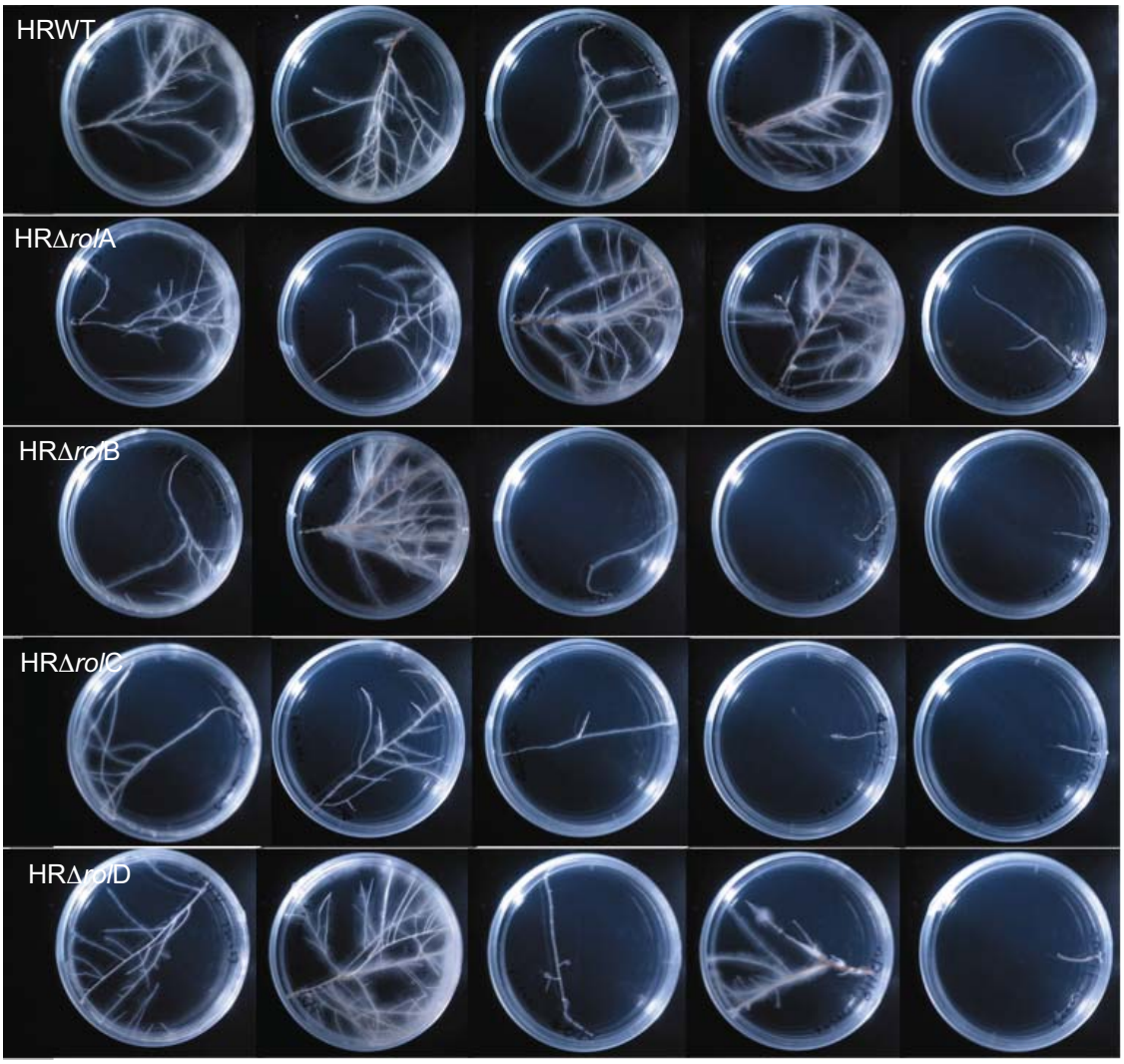

Figure 3-5. Morphology of hairy roots at 18 days post-subculture. Each hairy root was cut 1.5 cm from the root tip, and this segment was placed in fresh medium. After 18 d, all the clones were sorted and photographed according to the main root length

from the longest to the shortest. The figure shows a representative clone (mutant or HRWT) with a main root length in each of the 1st, 25th, 50th, 75th, and 100th percentiles (arranged left to right). The number of independent clones examined was 84 for HRWT, 93 for HRΔ*rolA*, 65 for HRΔ*rolB*, 82 for HRΔ*rolC*, and 58 for HRΔ*rolD*. These photos were taken by Hsiao-Han Lin.

We performed a permutation test using analysis of variance (ANOVA) with 1000 replications to evaluate the differences among these hairy root groups, as statistical analyses revealed that none of the groups showed a normal distribution (Figure 3-6). The results of the MRL analysis (Figure 3-7A) showed significant differences between HRWT and HRΔ*rolC* (p = 9.99x10^{-4}) and between HRWT and HRΔ*rolD* (p = 9.99x10^{-3}). In contrast, there was a slight but not significant difference between HRWT and HRΔ*rolA* (p = 7.79x10^{-2}) and between HRWT and HRΔ*rolB* (p = 0.125), indicating that all four of these genes contribute to the growth of the main root to different degrees. In the analyses of BRN (Figure 3-7B), there was a significant difference between HRWT and HRΔ*rolB* (p = 7.99x10^{-3}) and between HRWT and HRΔ*rolC* (p = 9.99x10^{-4}); however, there was no significant difference between HRWT and either HRΔ*rolA* (p = 0.865) or HRΔ*rolD* (p = 0.549). To examine branch formation activity, we determined BRD, the number of branch roots per centimeter of main root (Figure 3-7C). We found a significant difference between HRWT and HRΔ*rolC* (p = 9.99x10^{-4}) and a slight difference between HRWT and HRΔ*rolB* (p = 7.89x10^{-2}), with no significant difference between HRWT and either HRΔ*rolA* (p = 0.169) or HRΔ*rolD* (p = 0.387). In terms of TBRL, which was the other parameter used to estimate branch root architecture development (Figure 3-7D), a significant difference was observed between HRWT and HRΔ*rolB* (p = 4.39x10^{-2}) and between HRWT and HRΔ*rolC* (p = 9.99x10^{-4}), whereas there was a slight difference between

HRWT and HRΔ*rolA* (p = 5.69x10^{-2}) and between HRWT and HRΔ*rolD* (p = 5.39x10^{-2}). Combining the MRL and TBRL results, all four of these genes can enhance both main root and branch root elongation to different degrees; however, the BRN and BRD results showed that *rolB* and *rolC* are important for promoting branch formation, and *rolC* is more effective than *rolB*. In addition, after subculturing every two weeks for eight months, the clone survival rates (number of surviving clones/total clones) for HRΔ*rolB* and HRΔ*rolC* were only 12.5% and 4.17%, respectively, whereas those for HRΔ*rolA* and HRΔ*rolD* were 87.5% and 95.8%, respectively. This result indicates that *rolB* and *rolC* are essential for maintaining hairy root growth.

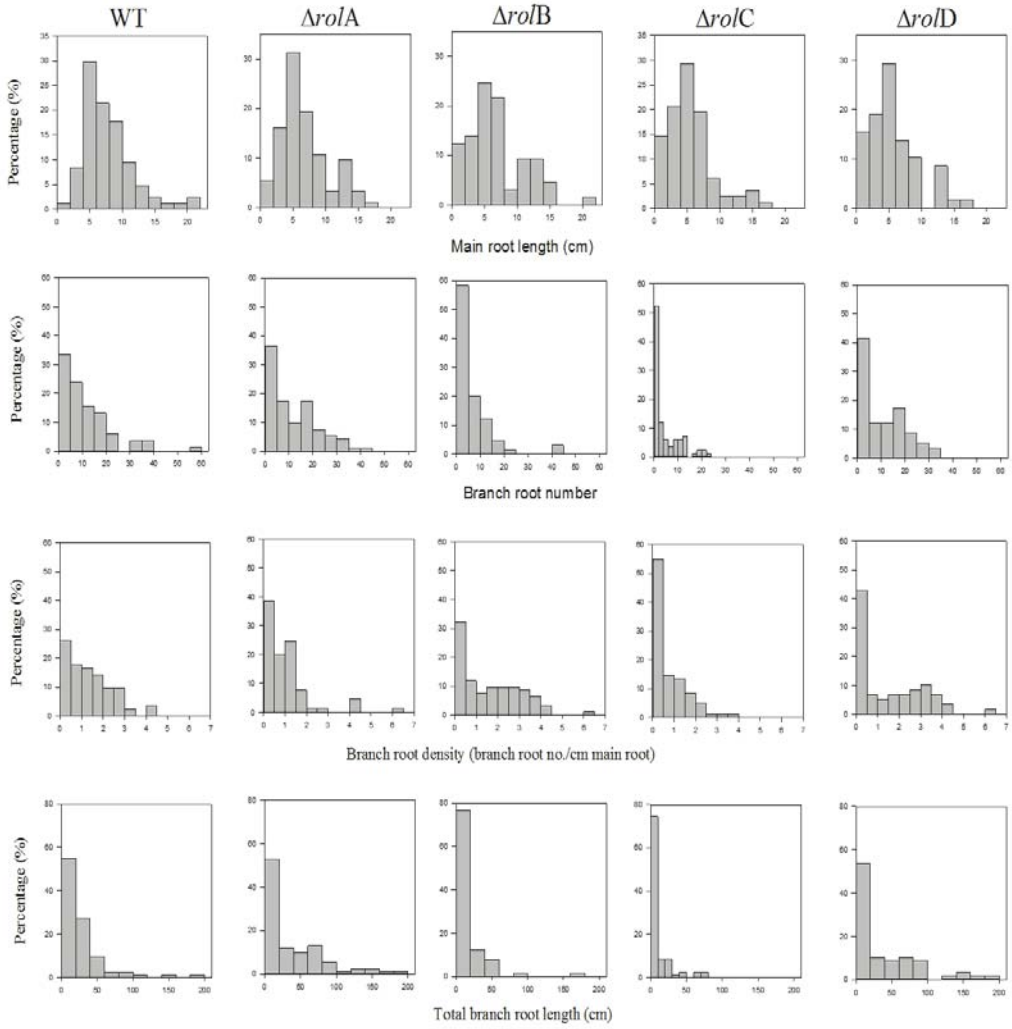

Figure 3-6 Population distribution of the different hairy root architecture parameters. From top to bottom, the panels show the main root length, number of branch roots, branch root density, and total branch root length, and each column shows the indicated genotype. The hairy roots were cut 1.5 cm from the root tip, and the segment was transferred to a new plate. The parameters were measured at 18 days post-subculture. A total of 84, 93, 65, 82, and 58 independent clones of HRWT, HRΔ*rolA*, HRΔ*rolB*, HRΔ*rolC*, and HRΔ*rolD* were examined, respectively.

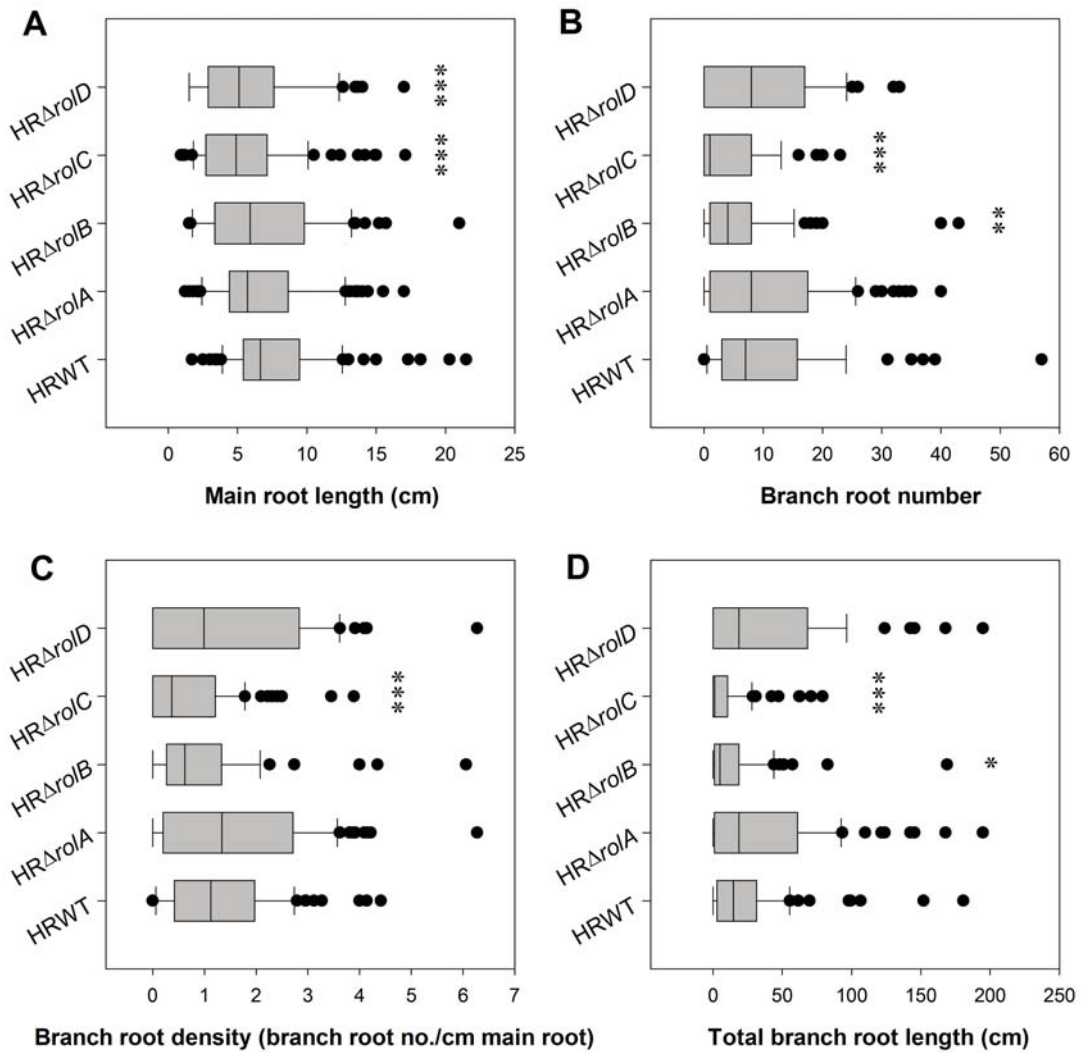

Figure 3-7 Box plot analysis of hairy root architecture. A 1.5 cm section of each hairy root from the root tip was removed and subcultured. At 18 days post-subculture, the following parameters were measured: main root length (A), number of branch roots (B), total branch root length (C), and branch root density (D). Significant differences were determined by Fisher's LSD, which is analyzed by permutation test using ANOVA with 1000 replications against HRWT. (* $p < 0.05$, ** $p < 0.01$, *** $p < 0.001$).

Taken together, these data show that *rolC*- and *rolD*-deficient hairy roots exhibited greater growth retardation in the main root, whereas *rolB*- or *rolC*-deficient hairy roots exhibited decreased hairy root initiation, branch root formation and elongation, and long-term growth ability.

4. Microarray data analysis (Please refer to the Master Thesis of Hsiao-Han Lin for detail information of this portion)

To further elucidate how *rolB* and *rolC* enhance hairy root branching and growth, we compared the transcriptomic differences between HRWT and HRΔ*rolB* and between HRWT and HRΔ*rolC*. We performed two-channel dye-swap microarray assays with two biological replicates. To reduce the variations between different clones, we randomly selected and pooled 24 hairy root clones with the same tissue weight and extracted RNA for the microarray hybridization. Based on the results of statistical analysis, the pooled samples had similar medians and similar variation in the four parameters; therefore, differences in the transcriptomes as shown in the microarray data were due to the gene deficiencies rather than phenotypic variations. Genes consistently showing greater than a two-fold difference in expression can be downloaded at http://apsjournals.apsnet.org/doi/suppl/10.1094/MPMI-12-13-0369-R/suppl_file/MPMI-12-13-0369-RE1.xls, which is attached to the article we have published on Molecular Plant-Microbe Interactions (on-line resource). Compared to HRWT, there were 6 genes in HRΔ*rolB* that showed a more than 2-fold increase in expression and 242 genes that were decreased to less than 0.5-fold; the corresponding numbers for HRΔ*rolC* were 42 and 208, respectively.

Gene ontology (GO) enrichment analysis was performed using agriGO with the default settings (Du et al. 2010). In total, 101 of the 242 genes that were down-

regulated in HRΔ*rolB* and 88 of the 208 genes that were down-regulated in HRΔ*rolC* were annotated. The GO terms with a *p*-value less than 0.05 are shown in Supplementary Table S2-1 and 3-2. Interestingly, the gene sets showing lower expression levels in HRΔ*rolB* and HRΔ*rolC* were quite similar, demonstrating that branch root density and hairy root growth are regulated by these genes. The gene sets that showed lower expression levels in HRΔ*rolB* and HRΔ*rolC* mainly contained LTP genes as well as genes annotated with the GO terms "response to wounding" and "responses to chemical stimuli". Genes annotated with the GO terms "responses to wounding" and "responses to chemical stimuli" have been shown to generate reactive oxygen species (ROS) (reviewed by Bhattacharjee 2012). Moreover, based on molecular function analysis, HRΔ*rolB* and HRΔ*rolC* had decreased oxidoreductase activity, indicating that the ROS levels were altered. Additionally, genes involved in ion balance, carbon and nitrogen metabolism, and molecular transport and localization were down-regulated in HRΔ*rolB/*HRΔ*rolC* roots compared with normal hairy roots. We hypothesize that lipid signals, ROS, ions, metabolism, and molecular transport and localization are important for promoting branch growth and maintaining growth activities in hairy roots.

Table 3-1. GO results for transcripts down-regulated in HRΔ*rolB* compared with HRWT ($p < 0.05$).

Description	*p*-value	FDR
Lipid transport	1.8×10^{-15}	3.0×10^{-13}
Lipid localization	3.1×10^{-15}	3.0×10^{-13}
Lipid binding	2.8×10^{-11}	2.1×10^{-9}
Macromolecule localization	1.7×10^{-6}	1.1×10^{-4}
Response to wounding	2.8×10^{-6}	1.4×10^{-4}
Hydrolase activity, hydrolyzing O-glycosyl compounds	7.3×10^{-6}	2.8×10^{-4}
Hydrolase activity, acting on glycosyl bonds	2.6×10^{-5}	6.6×10^{-4}
Endomembrane system	3.3×10^{-5}	1.8×10^{-3}
Response to chemical stimulus	1.8×10^{-4}	6.8×10^{-3}
Oxidoreductase activity, acting on peroxide as an acceptor	2.5×10^{-4}	3.8×10^{-3}
Peroxidase activity	2.5×10^{-4}	3.8×10^{-3}
Response to stimulus	2.6×10^{-4}	8.0×10^{-3}
Response to stress	2.9×10^{-4}	8.0×10^{-3}
Response to external stimulus	4.0×10^{-4}	9.5×10^{-3}
Electron carrier activity	5.0×10^{-4}	6.4×10^{-3}
Antioxidant activity	8.9×10^{-4}	9.7×10^{-3}
Extracellular region	9.6×10^{-4}	2.6×10^{-2}
Oxidoreductase activity	1.0×10^{-3}	9.7×10^{-3}
Lyase activity	1.3×10^{-3}	1.1×10^{-2}
Transport	1.5×10^{-3}	3.1×10^{-2}
Establishment of localization	1.6×10^{-3}	3.1×10^{-2}
Cation binding	2.0×10^{-3}	1.4×10^{-2}
Ion binding	2.0×10^{-3}	1.4×10^{-2}
Cellular amino acid derivative biosynthetic process	2.1×10^{-3}	3.4×10^{-2}
Localization	2.2×10^{-3}	3.4×10^{-2}
Response to endogenous stimulus	2.3×10^{-3}	3.4×10^{-2}
Oxidoreductase activity, acting on the CH-OH group of donors, NAD, or NADP as an acceptor	2.6×10^{-3}	1.7×10^{-2}
Response to hormone stimulus	3.4×10^{-3}	4.4×10^{-2}
Response to ethylene stimulus	3.5×10^{-3}	4.4×10^{-2}
Oxidoreductase activity, acting on the CH-OH group of donors	4.5×10^{-3}	2.7×10^{-2}
Cellular amino acid derivative metabolic process	6.7×10^{-3}	8.0×10^{-2}
Response to organic substances	1.3×10^{-2}	1.4×10^{-1}
Carbohydrate metabolic process	2.3×10^{-2}	2.4×10^{-1}
Transition metal ion binding	3.0×10^{-2}	1.6×10^{-1}
Metal ion binding	3.1×10^{-2}	1.6×10^{-1}

Table 3-2. GO results for transcripts downregulated in HRΔ*rolC* compared with HRWT ($p < 0.05$).

Description	*p*-value	FDR
Lipid transport	6.0×10^{-12}	6.4×10^{-10}
Lipid localization	9.1×10^{-12}	6.4×10^{-10}
Hydrolase activity, hydrolyzing O-glycosyl compounds	4.4×10^{-10}	2.6×10^{-8}
Hydrolase activity, acting on glycosyl bonds	3.0×10^{-9}	8.7×10^{-8}
Lipid binding	2.1×10^{-7}	4.0×10^{-6}
Extracellular region	8.0×10^{-6}	8.4×10^{-4}
Endomembrane system	1.8×10^{-5}	9.5×10^{-4}
Macromolecule localization	5.2×10^{-5}	2.4×10^{-3}
Transport	1.4×10^{-4}	4.1×10^{-3}
Establishment of localization	1.5×10^{-4}	4.1×10^{-3}
Response to chemical stimulus	1.9×10^{-4}	4.1×10^{-3}
Localization	2.2×10^{-4}	4.1×10^{-3}
Response to stimulus	2.3×10^{-4}	4.1×10^{-3}
Copper ion binding	2.7×10^{-4}	4.0×10^{-3}
Apoplast	4.4×10^{-4}	1.6×10^{-2}
Response to wounding	5.2×10^{-4}	8.1×10^{-3}
Carbohydrate metabolic process	1.1×10^{-3}	1.5×10^{-2}
Ion binding	1.5×10^{-3}	1.4×10^{-2}
Cation binding	1.5×10^{-3}	1.4×10^{-2}
Chloroplast thylakoid	4.9×10^{-3}	8.8×10^{-2}
Plastid thylakoid	4.9×10^{-3}	8.8×10^{-2}
Organelle subcompartment	5.0×10^{-3}	8.8×10^{-2}
Thylakoid part	6.1×10^{-3}	9.2×10^{-2}
Ion transport	6.3×10^{-3}	7.5×10^{-2}
Response to metal ion	6.4×10^{-3}	7.5×10^{-2}
Response to inorganic substance	9.5×10^{-3}	1.0×10^{-1}
Lyase activity	1.0×10^{-2}	8.6×10^{-2}
Response to hormone stimulus	1.1×10^{-2}	1.1×10^{-1}
Response to stress	1.2×10^{-2}	1.1×10^{-1}
Response to external stimulus	1.2×10^{-2}	1.1×10^{-1}
Response to endogenous stimulus	1.8×10^{-2}	1.5×10^{-1}
Thylakoid	2.0×10^{-2}	2.6×10^{-1}
Metal ion binding	2.9×10^{-2}	2.1×10^{-1}
Transition metal ion binding	3.2×10^{-2}	2.1×10^{-1}

To confirm the above-mentioned hypothesis, we compared the transcriptomes between a fast-growing HRWT and tobacco intact roots by dye-swap two-channel

microarray. The transcripts showing an expression change of more than two fold are listed in the on-line resource. The dominant GO enrichment terms ($p < 10^{-6}$) found in hairy roots are listed in Table 3-3, and details regarding which GO terms were upregulated or down-regulated ($p < 0.05$) are listed in the on-line resource. We found that hairy roots expressed more transcripts related with cell replication, which includes genes involved in the cell cycle, cell wall biogenesis, cell component biogenesis, DNA replication, and carbon and nitrogen metabolism; these findings are in agreement with the finding that hairy roots grew much faster than intact roots. We also found that the ROS-related transcripts and genes encoding LTPs were upregulated in HRWT compared with tobacco intact roots, and this result was consistent with the finding that HRΔ*rolB* and HRΔ*rolC* showed growth retardation and had lower LTP and ROS-related gene expression. These results strengthen the hypothesis that LTPs and ROS-related genes play important roles in hairy root development. We therefore aimed to confirm and discuss the relationship among hairy root growth, LTPs, and ROS below.

Table 3-3. GO results for transcripts up-regulated in HRWT compared with tobacco intact roots ($p < 10^{-5}$).

Description	*p*-value	FDR
Cell cycle	6.2×10^{-11}	1.3×10^{-7}
Lipid localization	2.7×10^{-9}	2.8×10^{-6}
Hydrolase activity, acting on glycosyl bonds	2.9×10^{-9}	1.8×10^{-6}
Lipid transport	7.5×10^{-9}	5.2×10^{-6}
Cell cycle process	1.6×10^{-8}	8.1×10^{-6}
Endomembrane system	2.1×10^{-8}	6.7×10^{-6}
Plant-type cell wall	4.2×10^{-8}	6.7×10^{-6}
External encapsulating structure	4.7×10^{-8}	6.7×10^{-6}
Hydrolase activity, hydrolyzing O-glycosyl compounds	8.6×10^{-8}	2.6×10^{-5}
Cell wall	2.2×10^{-7}	2.3×10^{-5}
Antioxidant activity	3.1×10^{-7}	6.1×10^{-5}

Intracellular non-membrane-bounded organelle	6.8×10^{-7}	4.8×10^{-5}
Non-membrane-bounded organelle	6.8×10^{-7}	4.8×10^{-5}
Chromosomal part	8.0×10^{-7}	4.9×10^{-5}
Regulation of cell cycle	1.3×10^{-6}	5.3×10^{-4}
Enzyme regulator activity	1.5×10^{-6}	1.8×10^{-4}
Xyloglucan:xyloglucosyl transferase activity	1.5×10^{-6}	1.8×10^{-4}
Carboxylesterase activity	1.8×10^{-6}	1.8×10^{-4}
Protein-DNA complex	3.0×10^{-6}	1.6×10^{-4}
Pectinesterase activity	9.5×10^{-6}	8.2×10^{-4}
Cytokineses during cell cycle	9.7×10^{-6}	3.3×10^{-3}

5. The expression levels of genes encoding LTPs were related to hairy root growth

There have been few indications that genes encoding LTPs are essential for hairy root growth and branch development. First, we confirmed that the expression of genes encoding LTPs in HRWT and HRΔ*rolB*/*rolC* is consistent with the results of the microarray (data not shown). Because HRΔ*rolB*/*rolC* showed decreased expression of genes encoding LTPs and branch growth, we questioned whether branch development is related to LTPs. We selected three HRWT clones with different BRDs and measured the expression of root growth promoting-*rolB*/*rolC* genes and LTP genes by qRT-PCR. As shown in Table 3-4, hairy roots with higher BRD showed increased LTP, *rolB,* and *rolC* gene expression. Additionally, the expression levels of *rolB* and *rolC* showed a highly positive correlation (correlation coefficient = 0.988), suggesting that the T-DNA integration locus determines the expression levels of the *rolB* and *rolC* genes. These data strongly suggest that *rolB*, *rolC,* and genes encoding LTPs promote branch development. We then compared the expression levels of genes encoding LTPs in tobacco roots and leaves (Table 3-4). We

discovered that the expression profiles of these LTP genes in tobacco roots and leaves were dramatically different from the profile in hairy roots, indicating that genes encoding LTPs are expressed differently in hairy root tissues compared with normal tissue. This evidence indicates that hairy root growth and branch development are related to regulate the expression of genes encoding LTPs.

Table 7. The expression levels of *rolB*/*C* and LTPs in hairy root clones with different branch root densities.

BRD/genes/NCBI accession number	HRWT Clone 115	HRWT Clone 87	HRWT Clone 106	Tobacco Root	Tobacco leaf
Branch root density	2.30 ± 0.60[a]	3.06 ± 0.20[a]	3.79 ± 0.07[b]		
rolB	0.00374 ± 0.00065[a]	0.0139 ± 0.0013[b]	0.0197 ± 0.0068[b]		
rolC	0.464 ± 0.196[a]	1.25 ± 0.17[b]	2.05 ± 0.31[c]		
BQ842876	3.24 ± 1.36[a]	4.88 ± 0.19[a]	7.74 ± 2.00[b]	0.951 ± 0.106	0.990 ± 0.075
EH618856/AB041519	8.40 ± 2.98[a]	12.3 ± 1.35[ab]	16.7 ± 3.4[b]	0.954 ± 0.045	1.02 ± 0.06
EB443656	0.00680 ± 0.00596[a]	0.0134 ± 0.0036[a]	0.0378 ± 0.0137[b]	1.06 ± 0.02	1.20 ± 0.05
EB450585	4.78 ± 0.84[a]	8.56 ± 3.05[a]	15.0 ± 3.6[b]	0.909 ± 0.006	1.07 ± 0.04
D86629	4.86 ± 0.71[a]	8.79 ± 3.25[a]	14.5 ± 2.5[b]	0.925 ± 0.008	1.10 ± 0.06
DV157577	0.0336 ± 0.0120	0.0679 ± 0.0212	0.106 ± 0.047	1.05 ± 0.02	1.17 ± 0.04
BQ842956	0.0340 ± 0.0095[a]	0.0581 ± 0.0220[ab]	0.0807 ± 0.0190[b]	1.05 ± 0.02	1.18 ± 0.05
AF043554	1.02 ± 0.16[a]	2.41 ± 1.18[ab]	3.62 ± 0.61[b]	0.950 ± 0.014	1.09 ± 0.03
AB035125	0.141 ± 0.030[a]	0.637 ± 0.316[b]	1.17 ± 0.20[c]	1.00 ± 0.06	1.22 ± 0.00
DW003388	0.142 ± 0.100	0.324 ± 0.160	0.418 ± 0.098	1.02 ± 0.03	1.20 ± 0.01
FG191218	0.0384 ± 0.0117[a]	0.0957 ± 0.0266[b]	0.147 ± 0.036[b]	1.12 ± 0.01	1.02 ± 0.05
FG137954	0.111 ± 0.018[a]	0.204 ± 0.049[a]	0.453 ± 0.070[b]	1.05 ± 0.02	1.03 ± 0.05

* The relative expression level of each gene is standardized with that of *Tac-9*. The statistical analysis was performed by one-way ANOVA, and significant differences were analyzed by b's least significant difference (LSD).

6. ROS accumulate in hairy roots but decrease when either *rolB* or *rolC* is knocked out

ROS have been considered as side-products in growing tissue, although they have recently been considered as growth regulators in roots (Tsukagoshi et al. 2010). Previous research indicated that ROS levels were dramatically decreased in both CaMV35S-*rolB*- and CaMV35S-*rolC*-transformed cell suspension cultures (Bulgakov et al. 2008; Bulgakov et al. 2012); however, these results conflict with our microarray data. To examine how ROS are regulated in HRWT, HRΔ*rolB,* and HRΔ*rolC*, we measured *in situ* ROS levels by staining with CM-H_2DCFDA. We observed that in both the main roots and branch roots, ROS levels were much higher in HRWT than in HRΔ*rolB* or HRΔ*rolC* (Figure 3-8). These results are consistent with the microarray results, indicating that HRΔ*rolB* and HRΔ*rolC* produce less ROS compared with HRWT. We hypothesize that the expression of *rolB* and *rolC* in different tissue types or the use of different promoters caused the differences in ROS levels. Further studies should be performed to clarify the relationship between hairy root growth and ROS accumulation.

Based on the findings, we concluded the hairy root growth and branch development promoted by *A. rhizogenes rolB* and *rolC* genes are associated with altering the expression of plant genes encoding LTPs and with ROS.

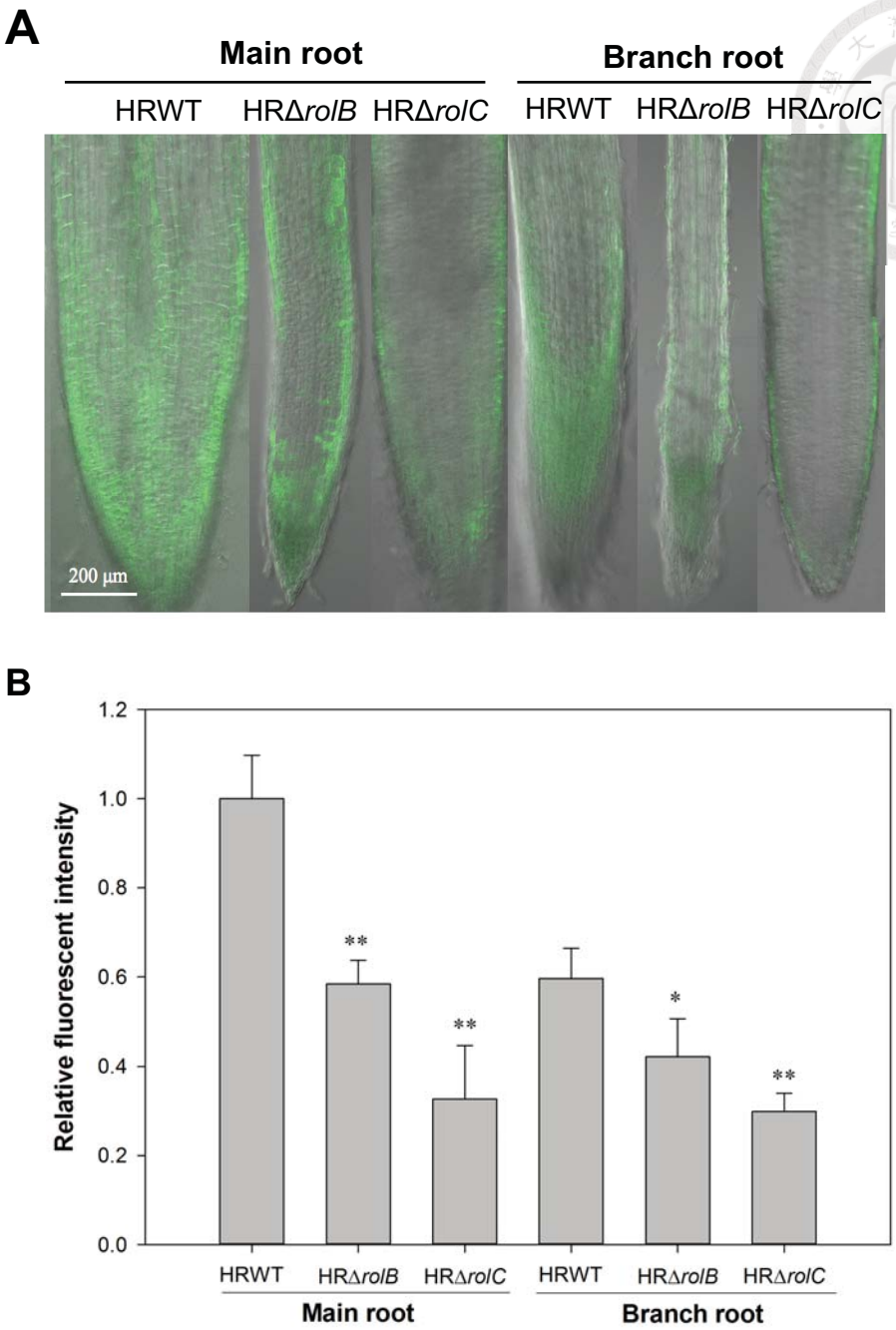

Figure 3-8 ROS content of HRWT, HRΔ*rolB*, and HRΔ*rolC*. A, The ROS was stained by CM-H_2DCFDA and the fluorescence was observed under a confocal microscope. B, Fluorescent signals were quantified in 3 biological replicates using ImageJ. The fluorescence intensities of the main roots and branch roots were compared with those of HRWT, and the significant differences were determined by Fisher's LSD using ANOVA . (* $p < 0.05$, ** $p < 0.01$).

Discussion

Over the past two decades, functional studies of the *rol* genes have been performed using transgenic plants, cell suspensions, and callus cultures, but seldom using hairy roots (Casanova et al. 2005). Because the *rol* genes are "root loci" genes and they encode proteins causing hairy root disease, we chose hairy root tissue to characterize the functions of the *rol* genes. Here, we found that *A. rhizogenes* lacking *rolB* or *rolC* showed decreased hairy root initiation ability (Figure 3-3 ~ 3-4) and that hairy roots lacking *rolB* or *rolC* showed decreased numbers of branch roots and impaired elongation (Figure 3-5 ~ 3-7). Moreover, *rolB* and *rolC* were important for hairy root survival in long-term subculture. These data suggest that *rolB* and *rolC* play crucial roles in regulating hairy root meristem activities, including enhancing branch formation and promoting branch root elongation. In contrast, *rolA* and *rolD* had minor effects on root initiation, branch root growth, and growth in long-term subculture. To our knowledge, this is the first study examining how *rol* genes function in hairy root branch development and long-term maintenance.

Compared with non-infected roots, hairy roots showed increases in various growth parameters, including growth rate, branch root number, and long-term maintenance of growth. These growth parameters were decreased in HRΔ*rolB* and HRΔ*rolC*. Based on the microarray analysis, HRΔ*rolB* and HRΔ*rolC* have similar transcriptomic profiles, which include genes encoding LTPs, ROS-related genes, and genes related to cellular metabolism and ion balance (Table 3-1 and 3-2). These data are consistent with the finding that *rolB* and *rolC* have similar effects on hairy roots. However, they are not redundant genes because they could not complement each other with respect to growth promotion (Figure 3-3 ~ 3-7). Previous studies have also

shown that the expression of *rolB* is induced by auxin and auxin-independent transcription factors, whereas the expression of *rolC* is induced by sucrose (DePaolis et al., 1996; Filetici et al., 1997). In addition, their sites of expression are different: the *rolB* promoter is activated in the root apical meristem and lateral primordia, whereas the *rolC* promoter is activated in the root apical meristem and phloem tissue (Maurel et al., 1994). These observations support the idea that *rolB* and *rolC* are separately regulated in roots and act synergistically to induce hairy root branch development and to maintain hairy root architecture.

Microarray analysis suggested that the biological function of *rolB* and *rolC* is linked to that of LTPs, which might function together to promote hairy root growth. qRT-PCR results showed that branch root densities and LTP expression levels were highly positively correlated (Table 7). Tobacco leaves and roots have similar LTP gene expression profiles; however, in hairy roots, these genes are either dramatically upregulated or down-regulated (Table 7). Genes encoding LTPs are abundant in the plant kingdom, and the functions of most of them are known. In this study, genes were classified as LTPs based on sequence annotations, and we found that regulating the expression levels of these LTP genes is important for mediating hairy root growth. In addition to our findings, there are several lines of evidence implying that the expression of RolB and LTPs are related. First, LTPs translocate lipid molecules intercellulary or intracellularly, and lipids play a key role in determining cell differentiation, proliferation, and tissue development (Kader 1996). The cellular functions of these lipids overlap with those of RolB. Second, both RolB and LTPs are expressed in the same regions of the root, including the apical meristem and branch root primordia (Capone et al. 1991; Thoma et al. 1994). Third, RolB is an auxin-

inducible protein, and *rolB*-transformed cells show enhanced auxin perception (Maurel et al. 1994). In addition, LTPs respond to auxin treatment in both hyacinth and rice plants (EMBL database and RiceXPro database). Therefore, we hypothesized that RolB enhances auxin signals, stimulating LTP expression. Here, we propose that RolB/C and LTPs may act synergistically or sequentially to regulate the fate of the hairy root; however, the molecular mechanisms remain to be elucidated.

ROS are not merely side products of cell growth but key factors for modulating root differentiation and proliferation (Tsukagoshi et al. 2010). However, the means by which ROS are produced by cellular enzymes and the mechanism by which the plant cell regulates its ROS levels to influence growth are still unknown. Our microarray results showed that the expression of ROS-related genes was lower in HRΔ*rolB* and HRΔ*rolC* than in HRWT, and these results were further confirmed by fluorescence staining (Figure 3-8). HRΔ*rolB* and HRWT had a similar MRL, but HRΔ*rolB* had lower ROS levels in the main root. This finding excludes the possibility that hairy root elongation contributes to ROS accumulation, although it suggests that RolB regulates cellular ROS levels to promote cell differentiation and thus generate branch roots. In contrast, HRΔ*rolC* was significantly different from HRWT in terms of both main root growth and branch root growth. However, HRΔ*rolB* and HRΔ*rolC* had similar growth characteristics, and microarray analysis revealed that both mutants had fewer ROS generation-related transcripts than HRWT, suggesting that *rolB* and *rolC* have a similar effect on ROS promotion and similar biological functions. We therefore hypothesize that *rolB* and *rolC* increase cellular ROS levels to promote branch root growth, which is adapted to hairy root growth needs.

Aside from LTPs and ROS, other gene sets showing lower expression levels in HRΔ*rolB* and HRΔ*rolC* compared with HRWT were also enriched in GO terms including "macromolecular localization", "hydrolase activity", "endomembrane system", "carbohydrate metabolic process", and "ion binding" (Table 3-1 and 3-2). In this article, we discussed LTPs and ROS because they were the dominant gene sets and they have not been reported to be related to hairy root growth regulation. The relationships between hairy root growth and the functions of other genes will be further studied.

None of the hairy root architecture parameters measured in this study showed a normal distribution. We hypothesized that this was due to two factors: different T-DNA integration sites and different T-DNA copy numbers. These factors determine the level of expression of the T-DNA genes and the plant genes around the T-DNA. To eliminate these effects, we performed microarray analyses on 2 different batches, each consisting of a different pool of 24 hairy root clones. From the two-batch microarray, only approximately 20% of the transcripts with a more than 2-fold difference were found in both microarray replicates, and we are confident that these genes are regulated by the *rol* genes, although the T-DNA insertion sites and copy numbers may differ.

Some authors have reported that cell suspension cultures expressing either *rolB* or *rolC* driven by the CaMV35S promoter show reduced cellular ROS levels compared with untransformed controls (Bulgakov et al. 2008; Bulgakov et al. 2012). In contrast, we found that hairy roots lacking *rolB* or *rolC* had lower ROS levels compared with HRWT (Figure 3-8). Our data therefore suggest that *rolB* and *rolC* increase cellular ROS levels in hairy roots. The difference between these results may

be explained by the different tissue types in which ROS levels were measured or the different promoters used in each experiment. These data suggest that *rolB* and *rolC* increase ROS levels when driven by their own promoters in hairy root tissue but decrease ROS levels when driven by the CaMV35S promoter in cell suspension cultures.

Hairy roots are very useful for studying root biology and for the production of plant secondary metabolites for the pharmaceutical industry. An understanding of how *Agrobacterium* initiates and prolongs hairy root growth in host plants is a key step toward expanding the application of hairy root technology to other plant species. Although T-DNA transformation can be achieved using *Agrobacterium tumefaciens* in some monocots, the plants cannot produce hairy roots. We hypothesize that hairy root generation is the result of T-DNA-dependent re-programming of the infected cell. In this study, we used tobacco, which can be infected and grow hairy roots easily, to understand how the plant participates in hairy root formation. The finding that either *rolB* or *rolC* alone can induce hairy root formation indicates that hairy root formation mechanisms are tightly linked with the cellular functions of RolB and RolC (Spena et al. 1987). By understanding the biochemical and molecular functions of RolB and RolC in hairy roots, we might expand the application of hairy root technology to plants that are resistant to *A. rhizogenes* infection. In this study, we found that hairy roots lost their indefinite growth ability when *rolB* or *rolC* was knocked out. We conclude that *rolB* and *rolC* play important roles in maintaining root meristem activity. This is a promising result because the means by which the plant retains root meristem activity might be revealed by time-course assays of differential gene expression in HRWT, HRΔ*rolB*, and HRΔ*rolC* hairy roots.

Fast-growing *Nicotiana tabacum* hairy roots accumulate more nicotine than slow-growing hairy roots due to systematic up-regulation of nicotine biosynthetic genes

Results

1. Nicotine accumulated in *N. tabacum* hairy roots

To test whether a higher level of nicotine occurred in *N. tabacum* L. var. Wisconsin 38 (W38) hairy roots than in un-infected intact roots, we measured the nicotine contents of un-infected intact roots, un-infected excised roots, and 19 independent tobacco hairy root clones using a high-performance liquid chromatography-diode array detector (HPLC-DAD) system. As shown in Figure 3-9, the nicotine levels of the un-infected intact roots and excised root cultures were below the detection limits, whereas the hairy root tissues accumulated a relatively higher amount of nicotine. These data are consistent with the results of previous studies that reported a higher level of nicotine accumulation in hairy root culture (Parr and Hamill, 1987).

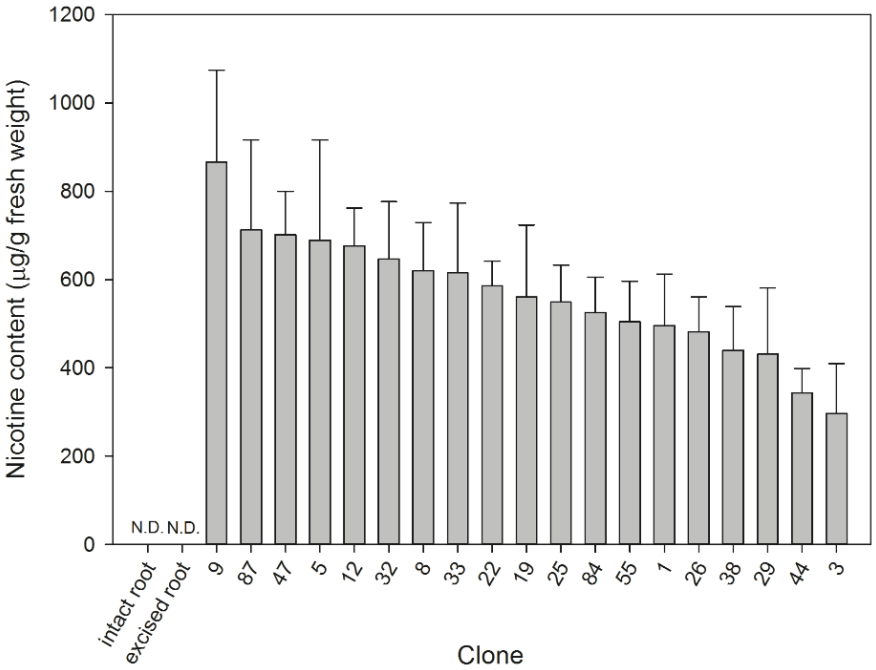

Figure 3-9 Nicotine contents in intact roots, excised roots, and hairy roots. Intact roots are the root tissues that were cut from 8-week-old tobacco plants, and excised roots are the roots that were cut from 8-week-old plants with an additional 2-week cultivation in 1/2 MS liquid medium, and the other roots are hairy root clones that were excised in 0.02 g from root tips and grown in 1/2 MS liquid medium for 2 weeks. The error bars represent 6 to 7 biological replicates.

2. Positive correlations were found between the contents of nicotine and nornicotine and between the contents of nicotine and anabasine in hairy roots

A number of studies have indicated that diverse secondary metabolites accumulate in hairy roots. Therefore, we hypothesized that the increased flux toward secondary metabolism in the hairy root contributes to the production of secondary metabolites. To elucidate this hypothesis, we determined the contents of nornicotine and anabasine to determine whether other substances in addition to nicotine were highly produced in hairy roots. Nornicotine, which is de-methylated nicotine, is the first product of nicotine catabolism (Alworth and Rapoport, 1965). Anabasine is an alkaloid that shares the same intermediate with nicotine biosynthesis, although the production of these compounds are regulated separately (Saitoh et al., 1985). Neither nornicotine nor anabasine could be detected in non-infected intact tobacco roots or excised tobacco roots. However, we observed a moderate to strong correlation (R = 0.6151) (a moderate correlation is defined as a correlation coefficient R = 0.3-0.6) between the nicotine and nornicotine contents and a moderate correlation (R = 0.3847) between the nicotine and anabasine contents (Figure 3-10).

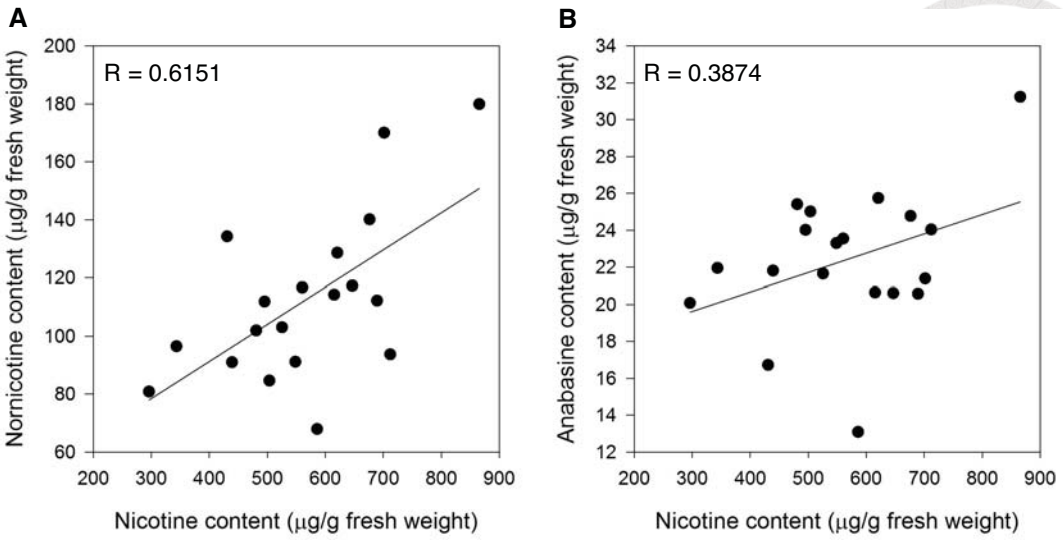

Figure 3-10 The correlation between the contents of (A) nicotine and nornicotine and (B) nicotine and anabasine in tobacco hairy roots. The contents shown here are the average results of 6 to 7 biological replicates.

3. Transcripts of the nicotine biosynthetic gene were up-regulated in hairy roots

The nicotine content in hairy roots was higher than that in both the un-infected intact roots and excised roots. Therefore, we hypothesized that the structural genes of the nicotine biosynthetic pathway are up-regulated in hairy roots. Before analyzing these genes by quantitative reverse transcription PCR (qRT-PCR), we sought a suitable reference gene that is stably expressed in every hairy root and non-infected tobacco intact root. Nine candidate genes that were stably expressed during tobacco development were selected (Schmidt and Delaney, 2010). These genes included the 18S rRNA, actin-9 (TAC-9), elongation factor 1α, L25 ribosomal protein, *α-tubulin*, *β-tubulin* (β-TUB), ubiquitin-conjugating enzyme E2, protein phosphatase 2A, and circadian genes. RNA was isolated from the non-infected intact roots and hairy root clones 9, 22, and 3, which had high, moderate and low nicotine contents, respectively

(Figure 3-9). TAC-9 was the most stable in the hairy roots and non-infected intact roots (Supplementary Table S1); therefore, it was selected as the reference gene for qRT-PCR.

We then quantified the transcripts of nicotine biosynthetic structural genes, including ornithine decarboxylase (ODC), putrescine N-methyltransferase (PMT), N-methylputrescine oxidase 1 (MPO1), MPO2, aspartate oxidase (AO), quinolinic acid synthase (QS), quinolinic acid phosphoribosyltransferase (QPT), and putative nicotine synthase gene *A622* in hairy roots and non-infected intact roots. Except for that of ODC, the transcripts of the nicotine biosynthetic genes were significantly up-regulated in hairy roots compared with those of intact roots (Figure 3-11). Moreover, a positive correlation was observed between the nicotine contents and expression levels of genes of the nicotine biosynthetic pathway: hairy root clone 3 had the lowest nicotine level and showed significantly lower transcript levels of MPO1, MPO2, and AO compared hairy root clone 9, which had the highest nicotine. The other nicotine biosynthetic genes, including *PMT*, *OS*, *QPT*, and *A622*, also showed slightly lower expression levels in clone 3 than in clone 9. In addition, except for *PMT* and *QPT*, the genes were expressed at moderate levels in clone 22. In addition to the nicotine biosynthetic genes, we monitored the storage-related root vacuole transporter multidrug and toxic compound extrusion type transporters 1 and 2 (MATE1/2) and leaf vacuole transporter jasmonate-inducible alkaloid transporter 1 (NtJAT1) (Morita *et al.*, 2009; Shoji and Hashimoto, 2008). As shown in Figure 3-11, MATE1/2 showed a higher expression level in all of the hairy root clones than in un-infected intact roots; however, NtJAT1 did not show a difference between these two root tissues,

indicating that hairy roots promote nicotine biosynthesis and root vacuole storage, resulting in higher nicotine contents.

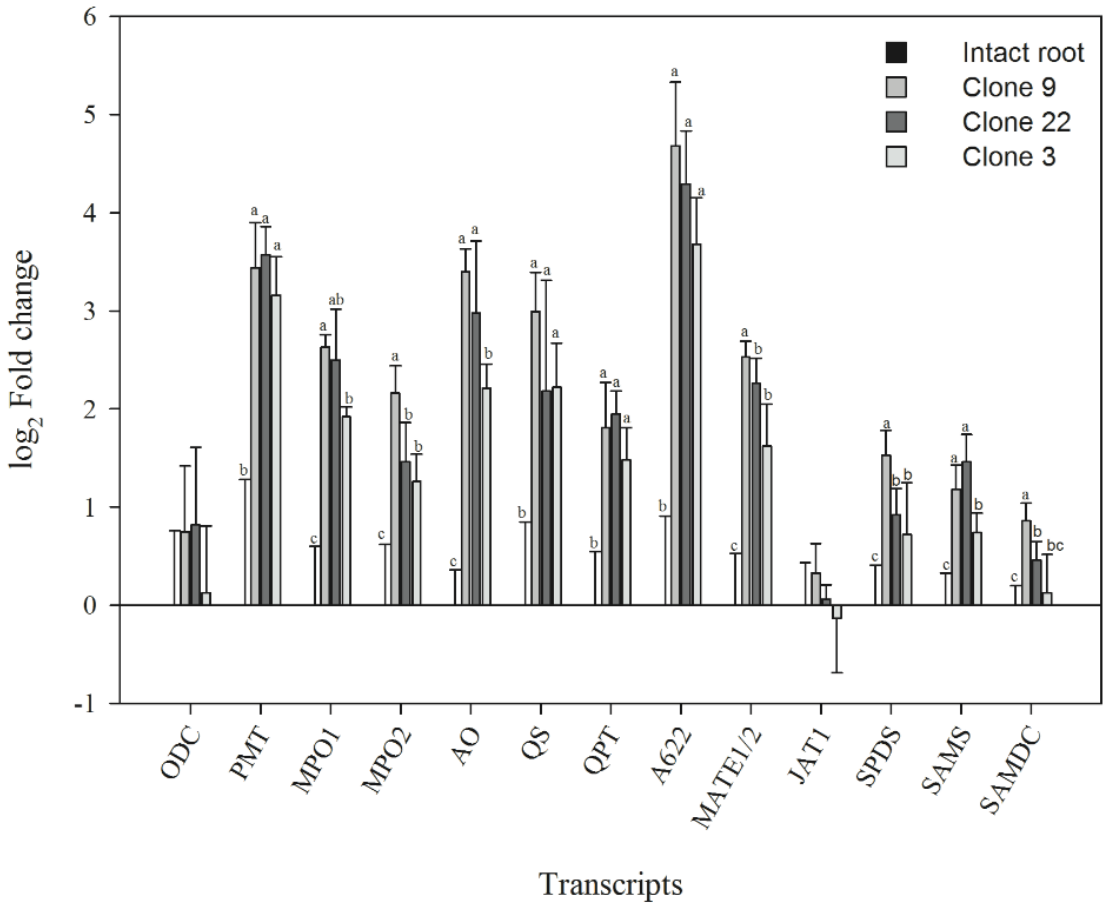

Figure 3-11 Transcript analysis of nicotine biosynthetic genes. The full gene names were shown in figure 1-3. The expression levels were normalized to that of NtTAC-9, which is constantly expressed in hairy root tissues. The fold change is compared to the expression level in the intact root. The standard deviations that are shown here represent 5 biological replicates as analyzed by a one-way analysis of variance. The statistically significant differences were determined at $p < 0.05$ by Fisher's Least Significant Difference test.

In addition to nicotine biosynthesis and storage, we also assayed transcripts that are involved in polyamine biosynthesis, which shares the same intermediates, ornithine and putrescine, with nicotine biosynthesis. The expression levels of spermidine synthase (SPDS), S-adenosylmethionine synthase (SAMS), and S-

adenosylmethionine decarboxylase (SAMDC) were up-regulated in hairy roots (Figure 3-11). We then monitored the contents of polyamines, including putrescine, spermidine, and spermine; however, there was no significant difference among the hairy root clones (data not shown), suggesting that the contents of polyamine did not increase in hairy root tissues.

4. Growth rate and nicotine content were positively correlated in hairy roots

The genes on *A. rhizogenes* T-DNA were considered secondary metabolite regulators, and their over-expression individually or in combination with *rolA*, *rolB*, or *rolC* in plants resulted in higher contents of secondary metabolites (reviewed by Bulgakov, 2008). Our previous study indicated that the deletion of any of the above *rol* genes resulted in aberrant hairy root growth of varying severity (Wang et al., 2014). To verify the relationship between growth and nicotine in tobacco hairy roots, we measured the fresh weight of 2-week-old liquid-cultured hairy roots and constructed a scatter plot using the nicotine contents. The growth and nicotine contents showed a moderate positive correlation (R = 0.5351) (Figure 3-12A), indicating that nicotine accumulation is associated with hairy root growth. We then investigated the relationship between growth and *rolC* expression, and we noted that the clones with higher growth rates revealed higher levels of *rolC* transcripts (R = 0.6335) (Figure 3-12B). In addition, the transcript levels of *rolB* and *rolC* were highly correlated (R = 0.9610) (Figure 3-12C), indicating that the expression of T-DNA genes was simultaneously regulated. Collectively, growth promotion and nicotine acceleration may be synergistic effects of the genes encoded by T-DNA. We then determined the nicotine content of *rolB*- or *rolC*-deficient hairy roots as previously established (Wang *et al.*, 2014). However, there were no significant differences in

nicotine content between the *rol*-gene-deficient hairy roots and general hairy roots (data not shown), indicating that the regulation of nicotine production did not occur from a single *rolB* or *rolC* gene.

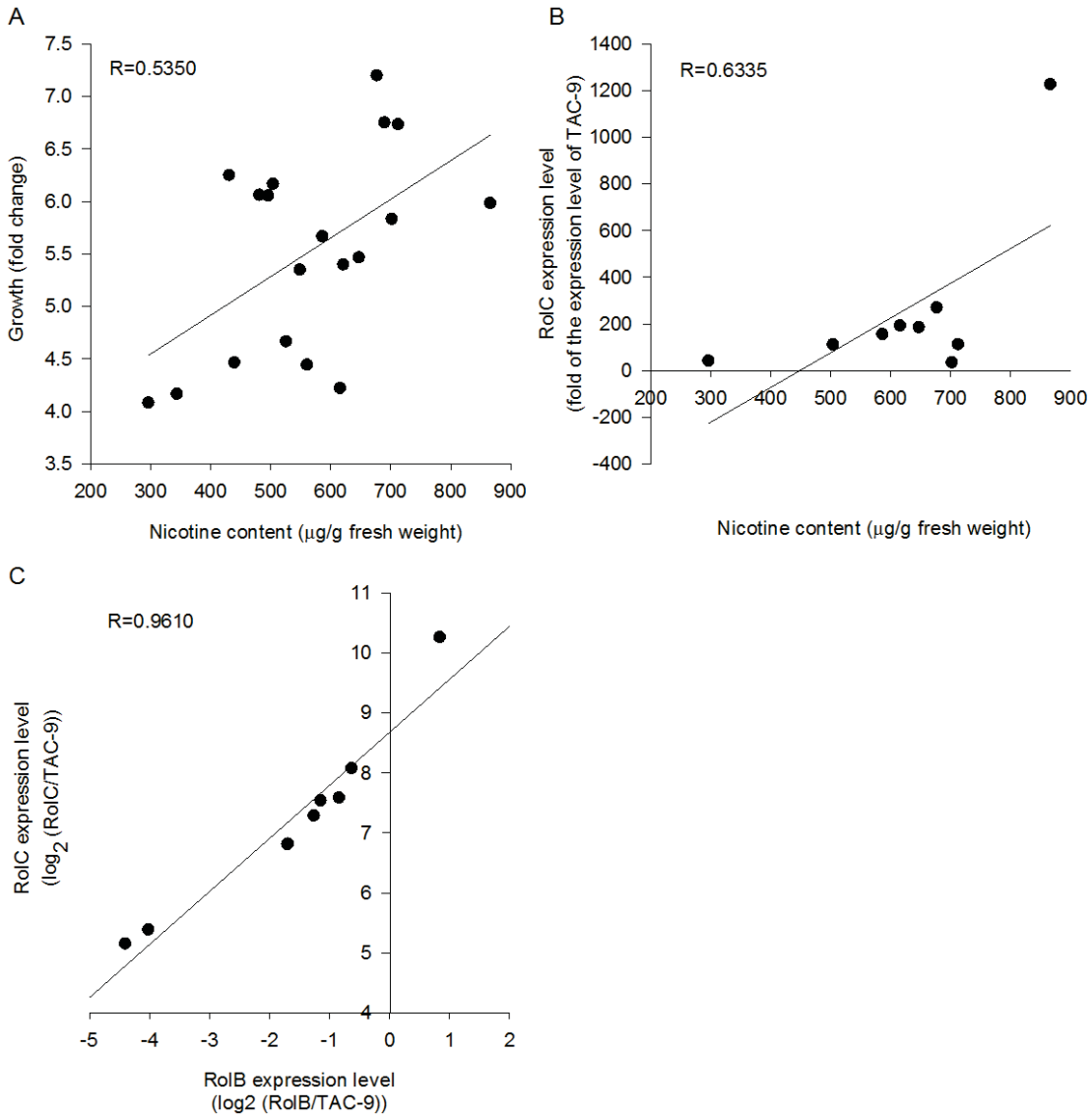

Figure 3-12 The relationship between (A) nicotine content and growth, (B) the expression levels of *rolC* and growth, and (C) expression levels of *rolB* and *rolC*. (A) The growth rate was determined by the fold changes of the tissue fresh weight after two-week liquid cultivations with the same inoculation of 0.02 g of root tips. The growth shown here is the average of 6 to 7 biological replicates. (B)(C) The expression levels of *rolB* and *rolC* shown here are the average of 3 biological replicates.

5. The jasmonic acid pathway is not the activator of nicotine biosynthesis in hairy roots

As previously reported, JA elicits nicotine biosynthesis by up-regulating the expression levels of *ODC*, *PMT*, *MPO*, *AO*, *QS*, *QPT*, *A622*, *NtMATE1/2*, *NtJAT1* and almost all of the known enzymes that are involved in nicotine biosynthesis (Goossens et al., 2003; Imanishi et al., 1998; Shoji, Yamada & Hashimoto, 2000; Xu and Timko, 2004). In addition, the RNA levels of AP2/ERF transcription factors were positively regulated by JA in the *NIC2* mutant tobacco (Shoji et al., 2010). To determine whether nicotine accumulation in tobacco hairy roots occurs by up-regulating the JA-responsive AP2/ERF associated genes, we analyzed their gene expression levels. As shown in Figure 3-13, ERF189 and ERF199 were expressed at significantly higher levels in hairy roots than in un-infected intact roots. ERF189 and ERF199 are transcriptional activators of the key enzymes PMT and QPT (De Boer et al., 2011; Shoji and Hashimoto, 2011b; Zhang et al., 2011). However, except for these two ERFs, there was either no difference in expression among the remaining ERFs or the expression was even lower in hairy roots compared with that of the un-infected intact roots. Moreover, the expression of these AP2/ERFs did not show an obvious correlation with the nicotine contents in hairy roots. We previously analyzed the gene profiles of clone 9 by microarray and ontology analyses, significant differences in JA signaling were not observed between clone 9 and the un-infected intact roots (Wang et al., 2014). In summary, we hypothesize that the accumulation of nicotine in hairy roots occurs via a JA-independent pathway.

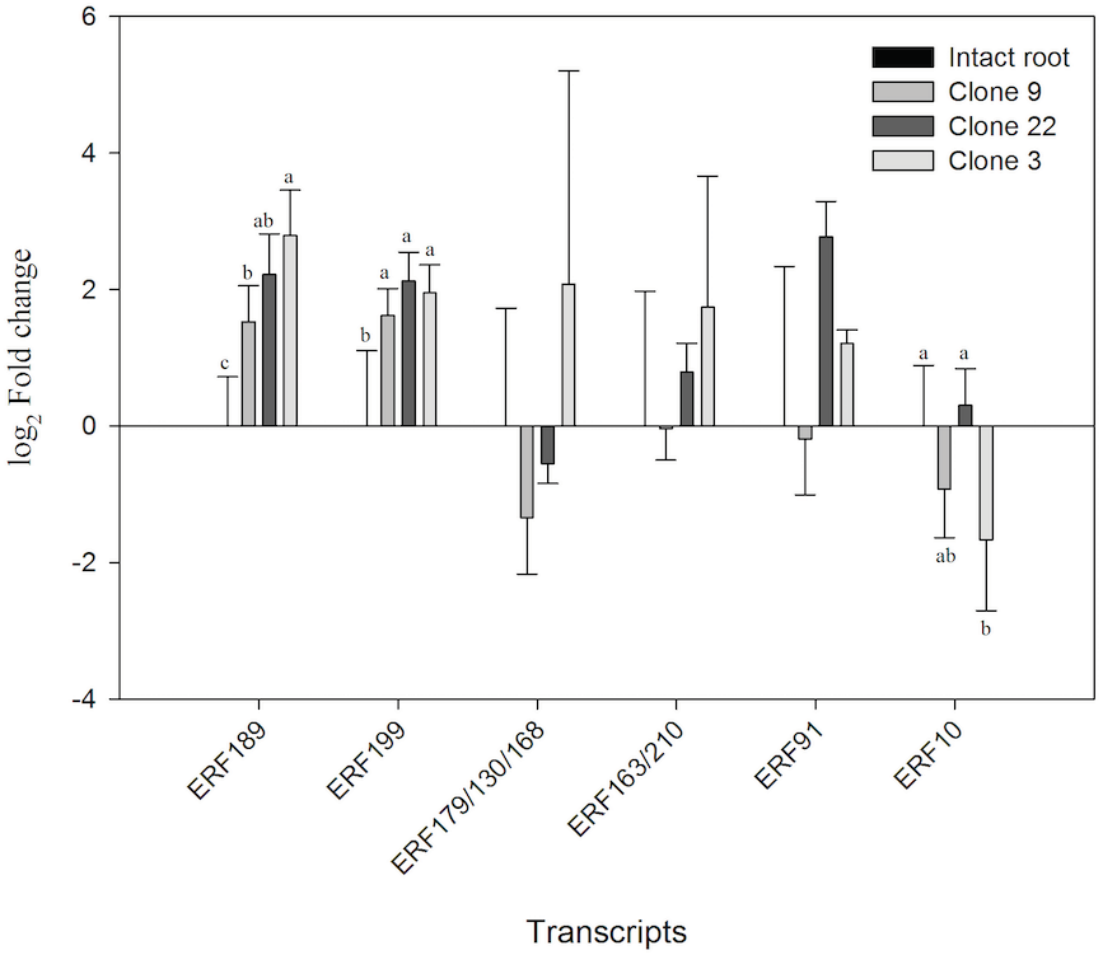

Figure 3-13 The transcript levels of AP2/ERFs in intact roots and hairy root clones 9, 22, and 3. The fold changes represent a comparison with the expression level in intact roots. The standard deviations represent 5 biological replicates as analyzed by a one-way analysis of variance. The statistically significant differences were determined at $p < 0.05$ by Fisher's Least Significant Difference test.

Discussion

For three decades, hairy root tissues have been reported to accumulate higher levels of secondary metabolites than non-infected intact roots. To determine how secondary metabolites are up-regulated in hairy roots, we used tobacco hairy roots as the study model. In this report, we demonstrated that tobacco hairy roots accumulate much more nicotine than do un-infected intact roots and excised roots (Figure 3-9). The nicotine contents in hairy roots were positively correlated with the contents of

both nornicotine and anabasine (Figure 3-10). In tobacco hairy roots, the massive production of nicotine is caused by abundant transcripts of both nicotine biosynthetic genes and storage-related genes (Figure 3-11). Moreover, the nicotine contents were positively correlated with growth and the expression levels of genes located on T-DNA (Figure 3-12). The up-regulation of nicotine is not likely to occur through the JA signaling pathway (Figure 3-13). We deduced that the genes encoded by T-DNA promote nicotine accumulation in tobacco hairy roots by up-regulating the biosynthetic pathway. However, additional studies are required to elucidate the plant signaling pathways that are involved.

In tobacco, nicotine is synthesized in roots but is stored in leaves (Dawson and Solt, 1959); therefore, the low nicotine content in un-infected intact roots is expected. In addition, we hypothesized that nicotine synthesized in the excised root accumulates *in situ* because of the lack of aerial tissue. However, cultivation of the excised roots in hormone-free medium produced undetectable amounts of nicotine (Figure 3-9). We speculated that this result was caused by a lack of above-ground signals that promote nicotine biosynthesis, such as hormones and other unknown signals. However, although tobacco hairy roots lack an aerial portion of the plant, they can synthesize and store massive amounts of nicotine, indicating that hairy roots are self-sufficient for both nicotine biosynthesis and storage. Therefore, we suggest that the regulatory mechanisms of secondary metabolism in hairy roots are different from that of un-infected plant tissues. This idea is supported by other studies. For instance, the malaria drug artemisinin is synthesized in leaves and stored in the leaves and flowers in *Artemisia annua* and cannot be synthesized in suspension cells, calli, or root tissues. However, this drug accumulates in significant amounts in hairy root

tissues (Weathers et al. 1994; Liu et al. 2011). In addition, the regulatory mechanism may be universal because of the diverse secondary metabolites that are stimulated in corresponding plant hairy roots.

Parr and Hamill reported that nicotine and other alkaloid metabolites, including anabasine and anatabine, are more abundant in hairy roots than in un-transformed normal roots (1987). We considered two possibilities for the regulation of secondary metabolite in hairy roots: first, tobacco hairy roots increase the overall flux of secondary metabolism, resulting in a richness of nicotine and all other metabolites; and second, tobacco hairy roots specifically stimulate the production of different metabolites. To verify these possibilities, we determined the contents of nornicotine and anabasine in tobacco hairy roots. Nornicotine is the first intermediate of nicotine catabolism (Robinson, 1974). Therefore, the contents of nicotine and nornicotine are expected to correlate. However, the contents of nicotine and anabasine are separately regulated (Saitoh et al., 1985). The contents of both nornicotine and anabasine showed a moderate positive correlation with nicotine content (Figure 3-10), indicating that nicotine and anabasine are up-regulated simultaneously in hairy roots. This result also suggests that hairy roots have a more active metabolic flux that does not simply promote a specific metabolite.

We then investigated the regulatory mechanism involved in nicotine accumulation by qRT-PCR analysis. Almost all of the nicotine biosynthetic genes were dramatically up-regulated in hairy roots, and surprisingly, gene expression showed a positive correlation with the nicotine content (Figure 3-11), indicating that the genes located on *A. rhizogenes* T-DNA positively regulate nicotine biosynthesis. Moreover, we previously compared the transcriptome between non-infected intact

roots and hairy root clone 9 that produces the highest amount of nicotine via a microarray and found that more than 4000 transcripts have an at least 2-fold difference in expression between these tissues (Wang et al., 2014). These results indicate that the regulatory mechanism of nicotine in hairy roots differs from that of non-infected intact roots. Notably, the secondary metabolism-initiating enzymes PMT and AO were dramatically up-regulated in hairy roots (Figure 3-11). PMT is the first-step enzyme between primary and secondary metabolism (reviewed by Biastoff et al., 2009). Up-regulating PMT indicates a more active secondary metabolic flux in hairy roots. Therefore, tobacco hairy roots greatly accumulate nicotine because of increased activity in the secondary metabolism pathway. In addition to the nicotine pathway, increased polyamine biosynthesis was also observed in hairy roots (Figure 3-11). Polyamine is an elicitor that stimulates lateral root growth and secondary metabolite production (Bais et al., 2000; Wei et al., 2007; Kumar et al., 2008). However, putrescine, spermine, and spermidine showed similar amounts in clones 9, 3, and 22, which might have been caused by higher accumulations of the joint intermediate putrescine, which is shared with the nicotine biosynthetic pathway, or the additional requirements of polyamine to meet the needs of hairy root growth.

Numerous reports have indicated that plants that are separately or simultaneously transformed with *rolA*, *rolB*, and *rolC* genes contain higher secondary metabolites than un-transformed plants (reviewed by Bulgakov, 2008). In *Rubia cordifolia* callus culture, the expression levels of *rolB* and *rolC* were positively correlated with the contents of anthraquinone, a phenolic secondary metabolite, although a negative correlation occurred with callus growth (Shkryl et al., 2008). In this study, we demonstrated that hairy root clones with a higher expression level of

rol genes not only had a higher growth rate but also showed abundant nicotine production (Figure 3-12A). In addition, the expression levels of *rol* genes showed the same tendency among the different clones (Figure 3-12C), indicating that the T-DNA genes promote hairy root growth accompanied by nicotine production. We also found that the effects of T-DNA genes on the growth and production of secondary metabolites may vary between calli and hairy roots; however, it is difficult to identify the importance and effect on metabolic regulation of single T-DNA genes. Therefore, we have proposed that the growth and metabolites in hairy roots are regulated by the same mechanism, which might be mediated by a gene on the T-DNA. Nicotine is up-regulated by the JA pathway but down-regulated by both ethylene and auxin signals. JA elicits nicotine production in tobacco by activating the expression of all of the genes involved in the nicotine biosynthetic pathway (Goossens et al., 2003; Imanishi et al., 1998; Shoji et al., 2000; Xu and Timko, 2004). In tobacco, JA stimulates the expression of PMT and QPT by regulating the Apetla2/ERF (AP2/ERF) family of transcription factors (Shoji *et al.*, 2010; De Boer et al., 2011; Shoji and Hashimoto, 2011b; Zhang et al., 2011). In addition, treatment with ethylene decreases nicotine production by down-regulating the expression of nicotine biosynthetic genes and AP2/ERF transcription factors (Shoji *et al.*, 2000; Shoji et al., 2010). The tobacco parasite *M. sexta* induces ethylene production to prevent nicotine production (von Dahl et al., 2007). In addition, treatment with auxin reduces nicotine levels via an unknown mechanism (Tabata et al., 1971; Takahashi and Yamada, 1973). Nicotine is up-regulated by the JA pathway but is down-regulated by both ethylene and auxin signals. In this study, the transcript levels of ERF189 and ERF199 were up-regulated in hairy roots as expected, but significant differences were not observed in the other

AP2/ERFs or were down-regulated in the hairy roots (Figure 3-13), suggesting that ERF189 and ERF199 are involved in nicotine accumulation in tobacco hairy roots and up-regulation is independent of JA elicitation. Moreover, in our previous study, we compared the transcriptomes between hairy root clone 9 and un-infected intact roots. This analysis showed that at least 4000 genes present a two-fold difference between hairy root clone 9 and un-infected intact roots. However, JA signaling, ethylene signaling, or responsive elements were not significantly changed (Wang et al., 2014). Thus, the nicotine content in hairy roots was regulated by a JA-independent pathway.

In addition to JA signaling, ROS are early responses to stress and act as signal molecules in many aspects of physiology (reviewed by Bhattacharjee, 2012). ROS also stimulate plant secondary metabolites (reviewed by Ferrari, 2010). We previously found that hairy root clone 9 has higher gene expression of the reactive oxygen species (ROS)-related genes and accumulates a greater amount of ROS than do non-infected intact roots; in addition, the ROS levels were significantly reduced in the hairy roots induced by the *rolB* or *rolC* null mutant compared with those induced by wild-type plants (Wang et al., 2014). However, the nicotine contents of *rolB*- or *rolC*-deficient hairy roots were similar to those of the general hairy roots. Therefore, we excluded the possibility that hairy roots accumulate ROS, resulting in nicotine over-production.

In this work, we found that the growth and secondary metabolites in hairy roots were under the control of the same regulator. However, JA signaling, which is the only known factor, was not activated by the expression levels of responsive factors or microarray analysis. In addition, we did not observe potential regulators in the

microarray data, which may have been because the regulators were not annotated or were unclarified genes and/or pathways.

In general, secondary metabolites are stimulated to adapt to environmental stress, which also suppresses growth (reviewed by Ramakrishna and Ravishankar, 2011). However, we found that a large amount of nicotine accumulated in the fast-growing hairy roots. This finding provides a novel screening strategy because hairy roots with higher growth rates have higher secondary metabolite productivity, extending the possibilities to produce high amounts of important secondary metabolites in hairy roots. In addition, because almost all of the enzymes involved in nicotine biosynthesis are activated transcriptionally, hairy roots may provide excellent material for exploring a novel secondary metabolism pathway and its regulation.

Chapter 4: Perspectives

1. Functional exploration of LTPs

To our knowledge, this is the first study indicating that the expression levels of a group of LTPs in hairy roots are higher than in intact roots, and that hairy roots lack of either *rolB* or *rolC* lowers the expression of these LTPs. We also observed that hairy roots lacking either *rolB* or *rolC* lost their meristem maintenance activity in prolong culture, which is also the case in intact roots. Moreover, the expression of LTPs were highly positive correlated to the branch development (Table 7). In previous studies, LTPs are known to play crucial roles in determining cell proliferation and differentiation in plants (reviewed by Kader 1996). We therefore hypothesized the expression levels of LTPs are controlled to promote hairy root initiation and growth.

To verify the hypothesis, we first try to find the possible function of LTPs by analyze the sequences and the ontologies of these genes. The sequence clustering is shown in Figure 4-1. Among the LTPs, only four of them were identified from experiment with biological meaning, including cDNA library from *Agrobacterium* transformed BY-2 cells (BQ842876), cDNA library from senescence leaf (EH618856), suppression substrative hybridization (SSH) cDNA library from non-pathogenic bacterial induced (AB035125), and SSH library of hairy root and normal root (AF043554). The other eight LTPs were expression sequence tag identified by European Sequencing of Tobacco Project. However, none of theseLTPs characterized in their full-length sequence and their biological function. These increase the difficulties to find the function of the LTPs, and how these LTPs regulates hairy root growth.

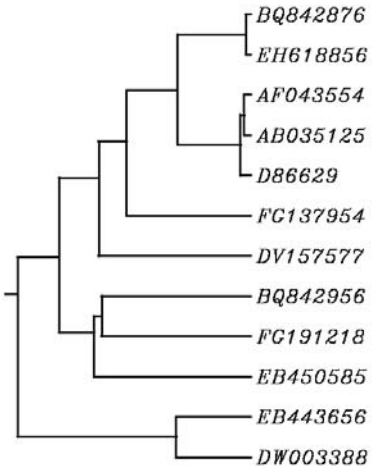

Figure 4-1 Sequence clustering of LTPs identified from microarray. Sequences were download from NCBI database, and the clustering algorithm was performed by ClustalW.

We therefore consider to knock-down each LTPs in hairy root respectively, and address their function by measure the initiation and growth parameters as mentioned in chapter 3 first. To achieve the purpose, we have to ensure the coding sequence of each LTPs. Specifically, we will perform both 5' and 3' rapid amplification of cDNA ends (RACE) to find the mRNA sequences. Then, we plan to clone the full-length antisense RNA of each LTP and transform into tobacco hairy roots. Afterward, we will measure the initiation and growth parameters as mentioned in chapter 3 to see if LTPs is really affecting hairy root growth and maintenance. If the phenotype of these LTP-knock-down hairy root fits the model, we will analyze the biological and molecular function of the LTPs.

2. Exploring the biochemical function of RolB and RolC proteins

Many studies have indicated that *rol* genes affect plant in lots of aspects. In our study, we found that *rolB* and *rolC* are dominant factors among all four *rol* genes in

hairy root initiation, growth promotion, and growth activity maintenance. We hypothesized that RolB and RolC regulate plant physiology via altering plant signaling or transcription process. To understand which pathway(s) may be regulated, we conducted yeast two-hybrid screening to find out the protein(s) associated with RolB or RolC protein.

To perform yeast two-hybrid assay, we constructed chimeric proteins of the respective Rol protein fused with GAL4-DNA binding domain, and we constructed the cDNA library from fast-growing and high nicotine accumulating hairy root clone 9. By screening, we discovered that RolB may interact with three proteins, including a basic leucine zipper domain (bZIP domain)-containing protein NtbZIP, the phosphate-induced gene encoding protein PHI-2, and ORF13a (Sung-Hui Yi, 2014). The first two proteins are found in tobacco, and the ORF13a is encoded by *A. rhizogenes* T-DNA. Notably, all of these three proteins are DNA-associated proteins containing conserved serine/threonine phosphorylation motif (Hansen et al. 1994; Jakoby et al. 2002; Sano and Nagata 2002), and the bZIP containing protein and the PHI-2 protein have been demonstrated as an abscisic acid (ABA) responsive proteins. These hinted RolB may regulate ABA signaling by transcriptional steps.

By sequence analysis, RolB does not contain typical nucleus localization sequence. However, the previous study showed RolB is translocated into nucleus while physical interaction with 14-3-3 proteins (Moriuchi et al. 2004). We expressed eYFP-RolB fusion protein in both *Arabidopsis* and *Nicotiana tabacum* protoplasts, and the eYFP signals were found in nucleus (Ta-Chung Lin, unpublished). Even though RolB does not contain typical nucleus translocation signal peptide, Moriuchi and colleagues discovered that RolB can interact with *Arabidopsis thaliana* 14-3-3

proteins, which resulting in nucleus translocation of RolB-14-3-3 protein complex (2004). In our yeast two-hybrid assay system, we did not found any 14-3-3 proteins that can interact with RolB; however, tobacco 14-3-3ωI can interact with RolB by bimolecular fluorescence complementation (BiFC) assay, and the fluorescent signal appeared clearly in nucleus (Ta-chung Lin, unpublished). Combining these data, we hypothesized that RolB suppresses ABA signaling in transcriptional process to result in an "auxin-like" effect, which increases cell proliferation and differentiation to promote rooting and growing.

In addition to PHI-2 and NtbZIP, ORF13a may also involved in RolB signaling. The early research reported that *rolB* gene and *orf13*, which also contains *orf13a* in their study, can act synergistically to promote rooting more efficiently than *rolB* alone (Aoki and Syõno 1999). Combined the former study, our results suggested RolB and ORF13a may work together to induce rooting. However, the detail mechanism should be further elucidated.

All of NtbZIP, PHI-2, and ORF13a do not have typical tyrosine phosphorylation motif; instead, they have conserved serine/threonine phosphorylation motifs. If these proteins share the similar regulatory mechanism with typical ABA-responsive transcriptional factors, the phosphorylation of these proteins is important to activate down-stream ABA-related transcription processes (reviewed by Fujita et al. 2013). However, Filippini and coworkers found the protein extract from *rolB*-expressing *E. coli* showed significant higher phosphatase activity than non-transformed *E. coli* by using universal phosphatase substrate *para*-nitrophenylphosphatase (*p*NPP). The phosphatase activity can be reduced by adding tyrosine phosphatase inhibitors, but neither serine phosphatase inhibitors nor threonine phosphatase inhibitors was able to

repress the activity. Moreover, they performed RolB phosphatase activity assay with tyrosine-, serine-, threonine-phosphorylated peptides, and RolB can only release free phosphate group from tyrosine-phosphorylated peptide. They concluded that RolB is a tyrosine phosphatase (1996). To confirm whether RolB has phosphatase activity, we expressed a N-terminal GST fused RolB (GST-RolB) in *E. coli*. Neither crude extract nor affinity-purified GST-RolB proteins showed phosphatase activity on the universal phosphatase substrate *p*NPP in our system. We then considered the GST tag may affect the enzymatic activity. To prove this, we construct C-terminal GST fused RolB proteins as well as tag-free RolB proteins to assay the phosphatase activity; nevertheless, none of the crude extracts exhibited phosphatase activity as well. To check with more confidences, we will express RolB in tobacco protoplast and perform the phosphatase assay again by the plant-expressing RolB protein.

In addition to direct de-phosphorylation, RolB might repress the activities of RolB-interacting proteins, including PHI-2, NtbZIP, and ORF13a, via indirect de-phosphorylation or degradation. To prove this, we will mimic the phosphorylation and the de-phosphorylation of PHI-2 and NtbZIP by replacing the predicted Ser/Thr into alanine and glutamic acid, respectively. Then we will assay if the point mutation change the result of protein-protein interaction. It will reveal whether the interaction is phosphorylation dependent or not.

On the other hand, RolC fused with Gal4-DNA binding domain (RolC::DNA-BD) exhibited a strong auto-activation in yeast two-hybrid system. The selection markers include 2 basic nutrients, histidine and adenine, biosynthesis genes *HIS3* and *ADE2*, an antibiotic Aureobasidin A (AbA) resistant gene *AUR1-C*, which encodes inositol phosphorylceramide synthase, and a blue/white selection reporter gene

MEL1, which encoded alpha-galactosidase (Figure 4-2). The auto-activation activity of RolC indicated that RolC might be a transcriptional factor (Figure 4-2). However, Estruch and coworkers discovered that RolC appeared in cytosolic fraction (1991). Also, we expressed eYFP-RolC in both *Arabidopsis* and *Nicotiana tabacum* protoplasts, and the eYFP signals were found in the cytoplasms (Ta-Chung Lin and Ke-Jin Lin, unpublished). These results lowered the possibility that RolC is a transcriptional factor.

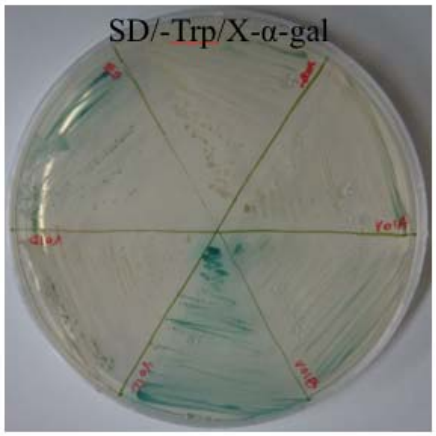

Figure 4-2 RolC has transcriptional activity in yeast. To perform yeast two-hybrid assay, we fused respective *rol* genes with Gal4-DNA binding domain, and we found the *rolC* itself can strongly activate the reporter genes without Gal4 activation domain.

In order to find the RolC interacting proteins, we have to eliminate the auto-activation activity. We have tried to grow the yeast harboring RolC::DNA-BD with histidine and adenine deficient medium and 1.5-fold higher concentration than standard usage of Aureobasidin A; however, it can grow normally. We therefore fuse the RolC with Gal4-DNA activation domain (RolC::DNA-AD) and try to do a screening with the prey fused with Gal4-DNA binding domain. Nevertheless,

RolC::DNA-AD causes yeast lethal. Moreover, RolC is a small protein with approximate 20 kD in molecular weight; therefore, we do not propose to use partial RolC to do the yeast two-hybrid screening. To overcome these problem, we are performing an error-prone PCR to generate a serial mutated *rolC* to find the mutants that cannot auto-activate the reporter. To date, only proline mutation, stop codon incorporation, and frame-shift by nucleotide insertion or deletion mutants have been identified. We hope we can got more diverse kinds of mutants. Then, we will apply some of mutated RolC to yeast two-hybrid screening to find out the putative protein candidates, and we will do co-immunoprecipitation assay and bimolecular complementation assay to check if the candidates can interact with native RolC.

3. The mechanism of secondary metabolite accumulation in hairy roots

Not only root-specific but other tissue-specific secondary metabolites can be induced in hairy roots. For examples, the aerial tissue-synthetic metabolites artemisinin, camptothecin, vindoline, menthol, morphine, codeine, thebaine, taxol, withanolides, vinblastine, and vincristine have been reported to be accumulated in corresponding plant hairy roots (reviewed by Sharma et al. 2013). These findings expand the applicabilities of hairy root in production of secondary metabolites, and in studies of the pathway and regulatory machinery of secondary metabolite.

We have found that the hairy root accumulating more nicotine has more active expression of biosynthetic pathway. We then tried to unveil how the nicotine is regulated in different clones of hairy roots. It is known that wounding signals, such as JA and SA, can stimulate secondary metabolites. We therefore hypothesized that the JA and/or SA signals were much activated in hairy root by gene(s) on T-DNA. However, the expression levels of genes responding to JA or SA signals were not

higher in hairy roots than in intact roots. It hinted the regulation of secondary metabolites in hairy roots differs from the known one.

To address the possible mechanism, we compare the transcriptomic differences between high-nicotine hairy root clone 9 and intact root by microarray assay. The results were shown in Table 3-3. Besides light-dark-related genes, the dominant transcriptomic difference between clone 9 and intact root was LTPs. Notably, the greater branched hairy root clone expressed the higher levels of LTPs (Table 3-4). Moreover, the growth rate showed a positive correlation with the nicotine content (Figure 3-12). These hinted nicotine in hairy root may be stimulated by the growth related genes. To proved our hypothesis, we assayed the nicotine contents of *rolB*- and *rolC*-deficient hairy roots; however, we did not find the significant loss of nicotine in "well-grown" *rolB*- and *rolC*-deficient hairy roots. Quantification of nicotine was limited in the hairy root with strong growth retardation. We cannot conclude if the *rolB* and/or *rolC* involve in stimulating nicotine in hairy roots.

To check if the positive correlation of growth and secondary metabolites is universal in plant hairy root systems, we are trying to induce hairy roots of *C. roseus* and *Linum perenne.* Once we have enough hairy root materials, we will assay the growth rate and their secondary metabolites, vinblastine and vincristine in *C. roseus* and podophyllotoxin in *L. perenne*. If the phenomenon is universal, it will offer a simple and reliable method to screen hairy root clones for secondary metabolite production.

We compared the transcriptomics between high-nicotine containing hairy root and un-infected intact roots, and found the differences between these samples were huge. These indicated hairy roots is very different from intact roots. To unveil the

regulation of secondary metabolite production in hairy roots, the most possible way is to compare the transcriptomics among hairy root clones containing high and low levels of secondary metabolites. It may also offer possible mechanism about growth regulation of hairy roots.

Chapter 5: Conclusion

This thesis focuses on growth regulation and nicotine accumulation in tobacco hairy root. In the part of growth regulation, this study is the first one to indicate that *rolB* and *rolC* control hairy root growth and maintenance by influencing the expression of plant lipid transfer proteins (LTP) and reactive oxygen species (ROS). Our data also indicated that RolB might influence ABA signaling to promote rooting and growth; nevertheless, how RolC participates in growth regulation has not yet been identified. In the part of secondary metabolism regulation, we found that the nicotine biosynthetic genes were transcriptionally activated in hairy root tissue, which offers an explanation of why tobacco hairy root accumulates much higher level of nicotine than the un-infected root. Moreover, our data also showed that hairy root growth rate is positively correlated with nicotine content, which suggests hairy root growth and nicotine biosynthesis were regulated synergistically. We also excluded the possibility that nicotine accumulation was led by jasmonic acid signaling. Overall, this thesis extends our understanding about the regulations of growth and secondary metabolism in tobacco hairy roots. We hope these results can enhance the applicability of secondary metabolites production in hairy root tissues.

References

Akiyoshi, D.E., Morris R.O., Hinz, R., Kosuge, T., Garfinkel, D.J., Gordon, M.P. and Nester, E.W. Cytokinin/auxin balance in crown gall tumors is regulated by specific loci in the T-DNA. Proc Natl Acad Sci U S A *80*, 407-411.

Aloni, R., Wolf, A., Feigenbaum, P., Avni, A. and Klee, H.J. (1998). The never ripe mutant provides evidence that tumor-induced ethylene controls the morphogenesis of *Agrobacterium tumefaciens*-induced crown galls on tomato stems. Plant Physiol *117*, 841-849.

Altamura, M.M., Capitani, F., Gazza, L., Capone, I. and Costantino, P. (1994). The plant oncogene *rolB* stimulates the formation of flower and root meristemoids in tobacco thin cell-layers. New Phytol *126*, 283-293.

Altamura, M.M., D'Angeli, S. and Capitani, F. (1998). The protein of *rolB* gene enhances shoot formation in tobacco leaf explants and thin cell layers from plants in different physiological stages. J Exp Bot *49*, 1139-1146.

Alworth, W.L. and Rapoport, H. (1965) Biosynthesis of the nicotine alkaloid in *Nicotiana glutinosa*: interrelationships among nicotine, nornicotine, anabasine, and anatabine. Arch Biochem Biophys *112*, 45-53.

Aoki, S. and Syõno, K. (1999). Synergistic function of *rolB*, *rolC*, ORF13 and ORF14 of T_L-DNA of *Agrobacterium rhizogenes* in hairy root induction in *Nicotiana tabacum*. Plant Cell Physiol *40*, 252-256.

Arshad, W., Haq, I.U., Waheed, M.T., Mysore, K.S. and Mirza, B. (2014) *Agrobacterium*-mediated transformation of tomato with *rolB* gene results in enhancement of fruit quality and foliar resistance against fungal pathogens. PLoS ONE *9,* e96979.

Bais, H.P., Madhusudhan, R., Bhagyalakshmi, N., Rajasekaran, T., Ramesh, B.S. and Ravishankar, G.A. (2000) Influence of polyamines on growth and formation of secondary metabolites in hairy root cultures of *Beta vulgaris* and *Tagetes patula*. Act Physiol Plant *22*, 151-158.

Bakó, L., Umeda, M., Tiburcio, A.F., Schell, J. and Koncz, C. (2003). The VirD2 pilot protein of *Agrobacterium*-transferred DNA interacts with the TATA box-binding protein and a nuclear protein kinase in plants. Proc Natl Acad Sci U S A *100*, 10108-10113.

Baque, M.A., H., M.S., Lee, E.J., Zhong, J.J. and Paek, K.Y. (2012). Production of biomass and useful compounds from adventitious roots of high-value added medicinal plants using bioreactor. Biotechnol Adv *30*, 1255-1267.

Batra, J., Dutta, A., Singh, D., Kumar, S. and Sen, J. (2004). Growth and terpenoid indole alkaloid production in *Catharanthus roseus* hairy root clones in relation to left- and right-termini-linked Ri T-DNA gene integration. Plant Cell Rep *23*, 148-154.

Baumann, K., De Paolis, A., Costantino, P. and Gualberti, G. (1999). The DNA binding site of the Dof protein NtBBF1 is essential for tissue-specific and auxin-regulated expression of the *rolB* oncogene in plants. Plant Cell *11*, 323-333.

Beinsberger, S.E.I., Valcke, R.L.M., Deblaere, R.Y., Clijsters, H.M.M., Degreef, J.A. and Vanonckelen, H.A. (1991). Effects of the introduction of *Agrobacterium tumefaciens* T-DNA *ipt* gene in *Nicotiana tabacum* L. cv. Petit Havana Sr1 plant cells. Plant Cell Physiol *32*, 489-496.

Bellincampi, D., Cardarelli, M., Zaghi, D., Serino, G., Salvi, G., Gatz, C., Cervone, F., Altamura, M.M., Costantino, P. and DeLorenzo, G. (1996). Oligogalacturonides prevent rhizogenesis in *rolB*-transformed tobacco explants by inhibiting auxin-induced expression of the *rolB* gene. Plant Cell *8*, 477-487.

Benvenuto, E., Ancora, G., Spanò, L. and Costantino, P. (1983). Morphogenesis and iso peroxidase characterization in tobacco hairy root regenerants. Z Pflanzenphysiol *110*, 239-245.

Bercetche, J., Chriqui, D., Adam, S. and David, C. (1987). Morphogenetic and cellular reorientations induced by *Agrobacterium rhizogenes* (Strain 1855, Strain 2659 and Strain 8196) on Carrot, Pea and Tobacco. Plant Sci *52*, 195-210.

Bettini, P., Michelotti, S., Bindi, D., Giannini, R., Capuana, M. and Buiatti, M. (2003). Pleiotropic effect of the insertion of the *Agrobacterium rhizogenes rolD* gene in tomato (*Lycopersicon esculentum* Mill.). Theor Appl Genet *107*, 831-836.

Bhattacharjee, S., Lee, L.Y., Oltmanns, H., Cao, H.B., Veena, Cuperus, J. and Gelvin, S.B. (2008). IMPa-4, an *Arabidopsis* importin α isoform, is preferentially involved in *Agrobacterium* mediated plant transformation. Plant Cell *20*, 2661-2680.

Bhattacharjee, S. (2012). The language of reactive oxygen species signaling in plants. J Bot *2012*, Article ID 985298, 22 pages. doi:10.1155/2012/985298.

Biastoff, S., Brandt, W. and Dräger, B. (2009) Putrescine N-methyltransferase—the start for alkaloids. Phytochemistry *70*, 1708-1718.

Bonhomme, V., Laurain-Mattar, D. and Fliniaux, M.A. (2000a). Effects of the *rolC* gene on hairy root: induction development and tropane alkaloid production by *Atropa belladonna*. J Nat Prod *63*, 1249-1252.

Bonhomme, V., Laurain-Mattar, D. and Fliniaux, M.A. (2004). Hairy root induction of *Papaver somniferum* var. album, a difficult-to-transform plant, by *Agrobacterium rhizogenes* LBA 9402. Planta *218*, 890-893.

Bonhomme, V., Laurain-Mattar, D., Lacoux, J., Fliniaux, M.A. and Jacquin-Dubreuil, A. (2000b). Tropane alkaloid production by hairy roots of *Atropa belladonna* obtained after transformation with *Agrobacterium rhizogenes* 15834 and *Agrobacterium tumefaciens* containing *rol A*, *B*, *C* genes only. J Biotechnol *81*, 151-158.

Brencic, A. and Winans, S.C. (2005). Detection of and response to signals involved in host-microbe interactions by plant-associated bacteria. Microbiol Mol Biol R *69*, 155-194.

Browse, J. (2009). Jasmonate passes muster: a receptor and targets for the defense hormone. Annu Rev Plant Biol 60, 183-205.

Bulgakov, V.P. (2008). Functions of *rol* genes in plant secondary metabolism. Biotechnol Adv *26*, 318-324.

Bulgakov, V.P., Aminin, D.L., Shkryl, Y.N., Gorpenchenko, T.Y., Veremeichik, G.N., Dmitrenok, P.S. and Zhuravlev, Y.N. (2008). Suppression of reactive oxygen species and enhanced stress tolerance in *Rubia cordifolia* cells expressing the *rolC* oncogene. Mol Plant Microbe Interact *21*, 1561-1570.

Bulgakov, V.P., Gorpenchenko, T.Y., Shkryl, Y.N., Veremeichik, G.N., Mischenko, N.P., Avramenko, T.V., Fedoreyev, S.A. and Zhuravlev, Y.N. (2011). CDPK-

driven changes in the intracellular ROS level and plant secondary metabolism. Bioeng Bugs *2*, 327-330.

Bulgakov, V.P., Gorpenchenko, T.Y., Veremeichik, G.N., Shkryl, Y.N., Tchernoded, G.K., Bulgakov, D.V., Aminin, D.L. and Zhuravlev, Y.N. (2012). The *rolB* gene suppresses reactive oxygen species in transformed plant cells through the sustained activation of antioxidant defense. Plant Physiol 158, 1371-1381.

Bulgakov, V.P., Khodakovskaya, M.V., Labetskaya, N.V., Chernoded, G.K. and Zhuravlev, Y.N. (1998). The impact of plant *rolC* oncogene on ginsenoside production by ginseng hairy root cultures. Phytochemistry *49*, 1929-1934.

Bulgakov, V.P., Kusaykin, M., Tchernoded, G.K., Zvyagintseva, T.N. and Zhuravlev, Y.N. (2002a). Carbohydrase activities of the *rolC* gene transformed and non-transformed ginseng cultures. Fitoterapia *73*, 638-643.

Bulgakov, V.P., Tchernoded, G.K., Mischenkol, N.P., Khodakovskaya, M., Glazunov, V.P., Radchenko, S.V., Zvereva, E.V., Fedoreyev, S.A. and Zhuravlev, Y.N. (2002b). Effect of salicylic acid, methyl jasmonate, ethephon and cantharidin on anthraquinone production by Rubia cordifolia callus cultures transformed with the *rolB* and *rolC* genes. J Biotechnol *97*, 213-221.

Camilleri, C. and Jouanin, L. (1991) The T_R-DNA region carrying the auxin synthesis genes of the *Agrobacterium rhizogenes* agropine-type plasmid pRiA4: nucleotide sequence analysis and introduction into tobacco plants. Mol Plant Microbe Interact *4*, 155-162

Capone, I., Cardarelli, M., Mariotti, D., Pomponi, M., Depaolis, A. and Costantino, P. (1991). Different promoter regions control level and tissue-specificity of

expression of *Agrobacterium rhizogenes rolB* Gene in Plants. Plant Mol Biol *16*, 427-436.

Capone, I., Frugis, G., Costantino, P. and Cardarelli, M. (1994). Expression in different populations of cells of the root-meristem is controlled by different domains of the *rolB* promoter. Plant Mol Biol *25*, 681-691.

Capone, I., Spanò, L., Cardarelli, M., Bellincampi, D., Petit, A. and Costantino, P. (1989) Induction and growth-properties of carrot roots with different complements of *Agrobacterium rhizogenes* T-DNA. Plant Mol Biol *13*, 43-52.

Cardarelli, M., Mariotti, D., Pomponi, M., Spanò, L., Capone, I. and Costantino, P. (1987). *Agrobacterium rhizogenes* T-DNA genes capable of inducing hairy root phenotype. Mol Gen Genet *209*, 475-480.

Carmi, N., Salts, Y., Dedicova, B., Shabtai, S. and Barg, R. (2003). Induction of parthenocarpy in tomato via specific expression of the *rolB* gene in the ovary. Planta *217*, 726-735.

Carneiro, M. and Vilaine, F. (1993). Differential expression of the *rolA* plant oncogene and its effect on tobacco development. Plant J *3*, 785-792.

Casanova, E., Trillas, M.I., Moysset, L. and Vainstein, A. (2005). Influence of *rol* genes in flori culture. Biotechnol Adv 23, 3-29.

Casanova, E., Valdés, A.E., Zuker, A., Fernández, B., Vainstein, A., Trillas, M.I. and Moysset, L. (2004). *rolC*-transgenic carnation plants: adventitious organogenesis and levels of endogenous auxin and cytokinins. Plant Sci *167*, 551-560.

Casanova, E., Zuker, A., Trillas, M.I., Moysset, L. and Vainstein, A. (2003). The *rolC* gene in carnation exhibits cytokinin- and auxin-like activities. Sci Hortic Amsterdam *97*, 321-331.

Cascales, E. and Christie, P.J. (2003). The versatile bacterial type IV secretion systems. Nat Rev Microbiol *1*, 137-149.

Cecchetti, V., Pomponi, M., Altamura, M.M., Pezzotti, M., Marsilio, S., D'Angeli, S., Tornielli, G.B., Costantino, P. and Cardarelli, M. (2004). Expression of *rolB* in tobacco flowers affects the coordinated processes of anther dehiscence and style elongation. Plant J *38*, 512-525.

Chen, I., Christie, P.J. and Dubnau, D. (2005). The ins and outs of DNA transfer in bacteria. Science *310*, 1456-1460.

Chen, L.S., Li, C.M. and Nester, E.W. (2000). Transferred DNA (T-DNA)-associated proteins of *Agrobacterium tumefaciens* are exported independently of *virB*. Proc Natl Acad Sci U S A *97*, 7545-7550.

Cheng, Y.F. and Zhao, Y.D. (2007). A role for auxin in flower development. J Integr Plant Biol *49*, 99-104.

Chilton, M.D., Tepfer, D.A., Petit, A., David, C., Cassedelbart, F. and Tempe, J. (1982). *Agrobacterium rhizogenes* inserts T-DNA into the genomes of the host plant-root cells. Nature *295*, 432-434.

Christey, M.C. (2001). Use of Ri-mediated transformation for production of transgenic plants. In Vitro Cell Dev Biol- Plant *37*, 687-700.

Christie, P.J., Atmakuri, K., Krishnamoorthy, V., Jakubowski, S. and Cascales, E. (2005). Biogenesis, architecture, and function of bacterial type IV secretion systems. Annu Rev Microbiol *59*, 451-485.

Costantino, P., Capone, I., Cardarelli, M., Depaolis, A., Mauro, M.L. and Trovato, M. (1994). Bacterial plant oncogenes- the *rol* Genes Saga. Genetica *94*, 203-211.

Costerton, J.W., Lewandowski, Z., Caldwell, D.E., Körber, D.R. and Lappin-Scott, H.M. (1995). Microbial biofilms. Annu Rev Microbiol *49*, 711-745.

Crane, Y.M. and Gelvin, S.B. (2007). RNAi-mediated gene silencing reveals involvement of *Arabidopsis* chromatin-related genes in *Agrobacterium*-mediated root transformation. Proc Natl Acad Sci U S A *104*, 15156-15161.

Dawson, R.F. and Solt, M.L. (1959). Estimated contributions of root and shoot to the nicotine content of the tobacco plant. Plant Physiol *34*, 656-661.

De Boer, K., Tilleman, S., Pauwels, L., Vanden Bossche, R., De Sutter, V., Vanderhaeghen, R., Hilson, P., Hamill, J.D. and Goossens, A. (2011). APETALA2/ETHYLENE RESPONSE FACTOR and basic helix-loop-helix tobacco transcription factors cooperatively mediate jasmonate-elicited nicotine biosynthesis. Plant J *66*, 1053-1065.

Dehio, C., Grossmann, K., Schell, J. and Schmülling, T. (1993). Phenotype and hormonal status of transgenic tobacco plants overexpressing the *rolA* gene of *Agrobacterium rhizogenes* T-DNA. Plant Mol Biol *23*, 1199-1210.

Delbarre, A., Muller, P., Imhoff, V., Barbierbrygoo, H., Maurel, C., Leblanc, N., Perrotrechenmann, C. and Guern, J. (1994). The *rolB* gene of *Agrobacterium rhizogenes* does not increase the auxin sensitivity of tobacco protoplasts by modifying the intracellular auxin concentration. Plant Physiol *105*, 563-569.

Deng, W., Chen, L., Wood, D.W., Metcalfe, T., Liang, X., Gordon, M.P., Comai, L. and Nester, E.W. (1998). *Agrobacterium* VirD2 protein interacts with plant host cyclophilins. Proc Natl Acad Sci U S A *98*, 10954-10959.

DePaolis, A., Sabatini, S., DePascalis, L., Costantino, P. and Capone, I. (1996). A *rolB* regulatory factor belongs to a new class of single zinc finger plant proteins. Plant J *10*, 215-223.

Douglas, C., Halperin, W. and Nester, E.W. (1982). *Agrobacterium tumefaciens* mutants affected in attachment to plant cells. J Bacteriol *152*, 1265-1275.

Du, Z., Zhou, X., Ling, Y., Zhang, Z. and Su, Z. (2010). argiGO: a GO analysis toolkit for the agricultural community. Nucleic Acids Res 38, W64-70.

Dubrovina, A.S., Kiselev, K.V., Veselova, M.V., Isaeva, G.A., Fedoreyev, S.A. and Zhuravlev, Y.N. (2009). Enhanced resveratrol accumulation in *rolB* transgenic cultures of *Vitis amurensis* correlates with unusual changes in CDPK gene expression. J Plant Physiol *166*, 1194-1206.

Dubrovsky, J.G., Sauer, M., Napsucialy-Mendivil, S., Ivanchenko, M.G., Friml, J., Shishkova, S., Celenza, J. and Benková, E. (2008). Auxin acts as a local morphogenetic trigger to specify lateral root founder cells. Proc Natl Acad Sci U S A *105*, 8790-8794.

Duckely, M. and Hohn, B. (2003). The VirE2 protein of *Agrobacterium tumefaciens*: the Yin and Yang of T-DNA transfer. FEMS Microbiol Lett *223*, 1-6.

Duckely, M., Oomen, C., Axthelm, F., van Gelder, P., Waksman, G. and Engel, A. (2005). The VirE1VirE2 complex of *Agrobacterium tumefaciens* interacts with single-stranded DNA and forms channels. Mol Microbiol *58*, 1130-1142.

Dumas, F., Duckely, M., Pelczar, P., Van Gelder, P. and Hohn, B. (2001). An *Agrobacterium* VirE2 channel for transferred-DNA transport into plant cells. Proc Natl Acad Sci U S A *98*, 485-490.

Durandtardif, M., Broglie, R., Slightom, J. and Tepfer, D. (1985). Structure and expression of Ri T-DNA from *Agrobacterium rhizogenes* in Nicotiana tabacum. Organ and phenotypic specificity. J Mol Biology *186*, 557-564.

Estruch, J.J., Chriqui, D., Grossmann, K., Schell, J. and Spena, A. (1991a). The plant oncogene *rolC* is responsible for the release of cytokinins from glucoside conjugates. EMBO J *10*, 2889-2895.

Estruch, J.J., Paretssoler, A., Schmülling, T. and Spena, A. (1991b). Cytosolic localization in transgenic plants of the RolC peptide from *Agrobacterium rhizogenes*. Plant Mol Biol *17*, 547-550.

Estruch, J.J., Schell, J. and Spena, A. (1991c). The protein encoded by the *rolB* plant oncogene hydrolyses indole glucosides. EMBO J *10*, 3125-3128.

Faiss, M., Strnad, M., Redig, P., Dolezal, K., Hanus, J., VanOnckelen, H. and Schmülling, T. (1996). Chemically induced expression of the *rolC*-encoded β-glucosidase in transgenic tobacco plants and analysis of cytokinin metabolism: *rolC* does not hydrolyze endogenous cytokinin glucosides in planta. Plant J *10*, 33-46.

Ferrari, S. (2010) Biological elicitors of plant secondary metabolites: mode of action and use in the production of nutraceutics. Adv Exp Med Biol *698*, 152-166.

Filetici, P., Moretti, F., Camilloni, G. and Mauro, M.L. (1997). Specific interaction between a *Nicotiana tabacum* nuclear protein and the *Agrobacterium rhizogenes rolB* promoter. J Plant Physiol *151*, 159-165.

Filippini, F., Loschiavo, F., Terzi, M., Costantino, P. and Trovato, M. (1994). The plant oncogene *rolB* alters binding of auxin to plant-cell membranes. Plant Cell Physiol *35*, 767-771.

Filippini, F., Rossi, V., Marin, O., Trovato, M., Costantino, P., Downey, P.M., Lo Schiavo, F. and Terzi, M. (1996). A plant oncogene as a phosphatase. Nature *379*, 499-500.

Fladung, M. (1990). Transformation of diploid and tetraploid potato clones with the *rolC* gene of *Agrobacterium rhizogenes* and characterization of transgenic plants. Plant Breed *104*, 295-304.

Flemming, H.G. and Wingender, J. (2010). The biofilm matrix. Nat Rev Microbiol *8*, 623-633.

Fujii, N. and Uchimiya, H. (1991). Conditions favorable for the somatic embryogenesis in carrot cell-culture enhance expression of the *rolC* promoter-GUS fusion gene. Plant Physiol *95*, 238-241.

Fujii, N., Yokoyama, R. and Uchimiya, H. (1994). Analysis of the *rolC* promoter region involved in somatic embryogenesis-related activation in carrot cell cultures. Plant Physiol *104*, 1151-1157.

Fujishige, N.A., Kapadia, N.N., De Hoff, P.L. and Hirsch, A.M. (2006). Investigations of *Rhizobium* biofilm formation. FEMS Microbiol Ecol *56*, 195-206.

Fujita Y., Yoshida, T. and Yamaguchi-Shinozaki, K. (2013) Pivotal role of the AREB/ ABF-SnRK2 pathway in ABRE-mediated transcription in response to osmotic stress in plants. Physiol Plant *147*, 15-27.

Garfinkel, D.J. and Nester, E.W. (1980). *Agrobacterium tumefaciens* mutants affected in crown gall tumorigenesis and octopine catabolism. J Bacteriol *144*, 732-743.

Garfinkel, D.J., Simpson, R.B., Ream, L.W., White, F.F., Gordon, M.P. and Nester, E.W. (1981). Genetic analysis of crown gall: fine structure map of the T-DNA by site-directed mutagenesis. Cell *27*, 143-153.

Gaspar, Y.M., Nam, J., Schultz, C.J., Lee, L.Y., Gilson, P.R., Gelvin, S.B. and Bacic, A. (2004). Characterization of the *Arabidopsis* Lysine-rich arabinogalactan-protein *AtAGP17* Mutant (*rat1*) that results in a decreased efficiency of *Agrobacterium* transformation. Plant Physiol *135*, 2162-2171.

Gaudin, V. and Jouanin, L. (1995). Expression of *Agrobacterium rhizogenes* auxin biosynthesis genes in transgenic tobacco plants. Plant Mol Biol *28*, 123-136

Gaudin, V., Vrain, T. and Jouanin, L. (1994). Bacterial genes modifying hormonal balances in plants. Plant Physiol Biochem *32*, 11-29.

Gelvin, S.B. (2010a). Finding a way to the nucleus. Curr Opin Microbiol *13*, 53-58.

Gelvin, S.B. (2010b). Plant proteins involved in *Agrobacterium* mediated genetic transformation. Annu Rev Phytopathol *48*, 3.1-3.24.

Gheysen, G., Villarroel, R. and Van montagu, M. (1991). Illegitimate recombination in plants: a model for T-DNA integration. Gene Dev *5*, 287-297.

Giri, A. and Narasu, M.L. (2000). Transgenic hairy roots: recent trends and applications. Biotechnol Adv *18*, 1-22.

Goossens, A., Häkkinen, S.T., Laakso, I., Seppänen-Laakso, T., Biondi, S., De Sutter, V., Lammertyn, F., Nuutila, A.M., Söderlund, H., Zabeau, M., Inzé, D. and Oksman-Caldentery K.M. (2003). A functional genomics approach toward the understanding of secondary metabolism in plant cells. Proc Natl Acad Sci U S A *100*, 8595-8600.

Gorpenchenko, T.Y., Kiselev, K.V., Bulgakov, V.P., Tchernoded, G.K., Bragina, E.A., Khodakovskaya, M.V., Koren, O.G., Batygina, T.B. and Zhuravlev, Y.N. (2006). The *Agrobacterium rhizogenes rolC* gene-induced somatic embryogenesis and shoot organogenesis in *Panax ginseng* transformed calluses. Planta *223*, 457-467.

Grange, W., Duckely, M., Husale, S., Jacob, S., Engel, A. and Hegner, M. (2008). VirE2: a unique ssDNA-compacting molecular machine. PLoS Biol *6*, e44.

Grémillon, L., Helfer, A., Clément, B. and Otten, L. (2004). New plant growth-modifying properties of the *Agrobacterium* T-6b oncogene revealed by the use of a dexamethasone-inducible promoter. Plant J *37*, 218-228.

Guillon, S., Trémouillaux-Guiller, J., Pati, P.K., Rideau, M. and Gantet, P. (2006). Hairy root research: recent scenario and exciting prospects. Curr Opin Plant Biol *9*, 341-346.

Guivarc'h, A., Carneiro, M., Vilaine, F., Pautot, V. and Chriqui, D. (1996). Tissue-specific expression of the *rolA* gene mediates morphological changes in transgenic tobacco. Plant Mol Biol *30*, 125-134.

Gundlach, H., Müller, M.J., Kutchan, T.M. and Zenk, M.H. (1992). Jasmonic acid is a signal transducer in elicitor-induced plant cell cultures. Proc Natl Acad Sci U S A *89*, 2389-2393.

Hamill, J.D., Parr, A.J., Robins, R.J. and Rhodes, M.J.C. (1986). Secondary product formation by cultures of *Beta vulgaris* and *Nicotiana rustica* transformed with *Agrobacterium rhizogenes*. Plant Cell Rep *5*, 111-114.

Hansen, G., Larribe, M., Vaubert, D., Tempé, J., Biermann, B.J., Montoya, A.L., Chilton, M.D. and Brevet, J. (1991) *Agrobacterium rhizogenes* pRi8196 T-

DNA: mapping and DNA sequence of functions involved in mannopine synthesis and hairy root differentiation. Proc Natl Acad Sci U S A *88*, 7763-7767.

Hansen, G., Vaubert, D., Clérot, D. and Brevet, J. (1997) Wound-inducible and organ-specific expression of ORF13 from *Agrobacterium rhizogenes* 8196 T-DNA in transgenic tobacco plants. Mol Gen Genet *254*, 337-343.

Hansen, G., Vaubert, D., Clérot, D., Tempé, J. and Brevet, J. (1994). A new open reading frame, encoding a putative regulatory protein, in *Agrobacterium rhizogenes* T-DNA. Comptes rendus de I'Academie des sciences Serie III, Sciences de la vie *317*, 49-53.

Hansen G., Vaubert, D., Héron, J.N., Clérot, D., Tempe, J. and Brevet, J. (1993) Phenotypic effects of overexpression of *Agrobacterium rhizogenes* T-DNA *orf13* in transgenic tobacco plants are mediated by diffusible factor(s). Plant J *4*, 581-585.

Hodges, L.D., Lee, L.Y., McNett, H., Gelvin, S.B. and Ream, W. (2009). The *Agrobacterium rhizogenes* GALLS gene encodes two secreted proteins required for genetic transformation of plants. J Bacteriol *191*, 355-364.

Hodges, L.D., Vergunst, A.C., Neal-McKinney, J., den Dulk-Ras, A., Moyer, D.M., Hooykaas, P.J. and Ream, W. (2006). *Agrobacterium rhizogenes* GALLS protein contains domains for ATP binding, nuclear localization, and type IV secretion. J Bacteriol *188*, 8222-8230.

Hoekema, A., Hirsch, R.P., Hooykaas, P.J.J. and Schilperoort, R.A. (1983). A binary plant vector strategy based on separation of *vir*- and T-region of the *Agrobacterium tumefaciens* Ti-plasmid. Nature *303*, 179-180.

Hong, S.B., Hwang, I., Dessaux, Y., Guyon, P., Kim, K.S. and Farrand, S.K. (1997). A T-DNA gene required for agropine biosynthesis by transformed plants is functionally and evolutionarily related to a Ti plasmidd gene required for catabolism of agropine by *Agrobacterium* strains. J Bacteriol *179*, 4831-4840.

Horton, R.M. (1995). PCR-mediated recombination and mutagenesis. SOEing together tailor-made genes. Mol Biotechnol *3*, 93-99.

Hussain, M.S., Fareed, S., Ansari, S., Rahman, M.A., Ahmad, I.Z. and Saeed, M. (2012) Current approaches toward production of secondary plant metabolites. J Pharm Bioallied Sci *4*, 10-20.

Imanishi, S., Hashizume, K., Nakakita, M., Kojima, H., Matsubayashi, Y., Hashimoto, T., Sakagami, Y., Yamada, Y. and Nakamura, K. (1998). Differential induction by methyl jasmonate of genes encoding ornithine decarboxylase and other enzymes involved in nicotine biosynthesis in tobacco cell cultures. Plant Mol Biol *38*, 1101-1111.

Inyushkina, Y.V., Kiselev, K.V., Bulgakov, V.P. and Zhuravlev, Y.N. (2009). Specific genes of cytochrome P450 monooxygenases are implicated in biosynthesis of caffeic acid metabolites in *rolC*-transgenic culture of *Eritrichium sericeum*. Biochemistry (Moscow) *74*, 917-924.

Ionkova, I. and Fuss, E. (2009). Influence of different strains of *Agrobacterium rhizogenes* on induction of hairy roots and lignan production in *Linum tauricum* ssp. tauricum. Pharmacogn Mag *5*, 14-18.

Jakoby, M., Weisshaar, B., Dröge-Laser, W., Vicente-Carbajosa, J., Tiedemann, J., Kroj, T., Parcy, F. and bZIP Research Group. (2002). bZIP transcription factors in *Arabidopsis*. Trends Plant Sci *7*, 106-111.

Joos, H., Timmerman, B., Van Montagu, M. and Schell, J. (1983). Genetic analysis of transfer and stabilisation of Agrobacterium DNA in plant cell. EMBO J *2*, 2151-2160.

Kader, J.C. (1996). Lipid-transfer proteins in plant. Annu Rev Plant Physiol Plant Mol Biol *47*, 627-654.

Kaneyoshi, J. and Kobayashi, S. (1999). Characteristics of transgenic trifoliate orange (*Poncirus trifoliata*) possessing the *rolC* gene of *Agrobacterium rhizogenes* Ri plasmid. J Jpn Soc Hortic Sci *68*, 734-738.

Kiselev, K.V., Dubrovina, A.S. and Bulgakov, V.P. (2009). Phenylalanine ammonia-lyase and stilbene synthase gene expression in *rolB* transgenic cell cultures of *Vitis amurensis*. Appl Microbiol Biotechnol *82*, 647-655.

Kiselev, K.V., Dubrovina, A.S., Veselova, M.V., Bulgakov, V.P., Fedoreyev, S.A. and Zhuravlev, Y.N. (2007). The *rolB* gene-induced overproduction of resveratrol in *Vitis amurensis* transformed cells. J Biotechnol *128*, 681-692.

Kiselev, K.V., Kusaykin, M.I., Dubrovina, A.S., Bezverbny, D.A., Zvyagintseva, T.N. and Bulgakov, V.P. (2006). The *rolC* gene induces expression of a pathogenesis-related β-1,3-glucanase in transformed ginseng cells. Phytochemistry *67*, 2225-2231.

Koltunow, A.M., Johnson, S.D., Lynch, M., Yoshihara, T. and Costantino, P. (2001). Expression of *rolB* in apomictic *Hieraclum piloselloides* Vill. causes ectopic meristems in planta and changes in ovule formation, where apomixis initiates at higher frequency. Planta *214*, 196-205.

Koncz, C., Martini, N., Mayerhofer, R., Koncz-Kalman, Z., Körber, H., Redei, G.P. and Schell, J. (1989). High-frequency T-DNA-mediated gene tagging in plants. Proc Natl Acad Sci U S A *86*, 8467-8471.

Körber, H., Strizhov, N., Staiger, D., Feldwisch, J., Olsson, O., Sandberg, G., Palme, K., Schell, J. and Koncz, C. (1991). T-DNA gene *5* of *Agrobacterium* modulates auxin response by autoregulated synthesis of a growth hormone antagonist in plants. EMBO J *10*, 3983-3991.

Koshita, Y., Nakamura, Y., Kobayashi, S. and Morinaga, K. (2002). Introduction of the *rolC* gene into the genome of the genome of the japanese persimmon causes dwarfism. J Jpn Soc Hortic Sci *71*, 529-531.

Kumar, V., Giridhar, P., Chandrashekar, A. and Ravishankar, G.A. (2008) Polyamines influence morphogenesis and caffeine biosynthesis in *in vitro* cultures of *Coffea canephora* P. ex Fr. Acta Physiol Plant *30*, 217-223.

Lacroix, B., Tzfira, T., Vainstein, A. and Citovsky, V. (2006). A case of promiscuity: *Agrobacterium's* endless hunt for new partners. Trends Genet *22*, 29-37.

Lacroix, B., Vaidya, M., Tzfira, T. and Citovsky, V. (2005). The VirE3 protein of *Agrobacterium* mimics a host cell function required for plant genetic transformation. EMBO J *24*, 428-437.

Leach, F. and Aoyagi, K. (1991). Promoter analysis of the highly expressed *rolC* and *rolD* root-inducing genes of *Agrobacterium rhizogenes*. Enhancer and tissue-specific DNA determinants are dissociated. Plant Sci *79*, 69-76.

Lee, K.T., Chen, S.C., Chiang, B.L. and Yamakawa, T. (2007). Heat-inducible production of β-glucuronidase in tobacco hairy root cultures. Appl Microbiol Biotechnol *73*, 1047-1053.

Lee, K.W., Bode, A.M. and Dong, Z.G. (2011). Molecular targets of phytochemicals for cancer prevention. Nat Rev Cancer *11*, 211-218.

Leemans, J., Deblaere, R., Willmitzer, L., de Greeve, H. and Hernalsteens, J.P. (1982). Genetic identification of functions of T_L-DNA transcripts in octopine crown galls. EMBO J *1*, 147-152.

Lemcke, K. and Schmülling, T. (1998) Gain of function assays identify non-*rol* genes from *Agrobacterium rhizogenes* T_L-DNA has tryptophan 2-monooxygenase activity. Mol Plant Microbe Interact *13*, 787-790.

Levesque, H., Delepelaire, P., Rouzé, P., Slightom, J. and Tepfer, D. (1988). Common evolutionary origin of the central portions of the Ri T_L-DNA of *Agrobacterium rhizogenes* and the Ti T-DNA of *Agrobacterium tumefaciens*. Plant Mol Biol *11*, 731-744.

Li, W., Li, M., DL., Y., Xu, R. and Zhang, R. (2009). Production podophyllotoxin by root culture of *Podophyllum hexandrum* Royle. Elect J Biol *5*, 34-39.

Liu, B.Y., Wang, H., Du, Z.G., Li, G.F. and Ye, H.C. (2011). Metabolic engineering of artemisinin biosynthesis in *Artemisia annua* L. Plant Cell Rep *30*, 689-694.

Magrelli, A., Langenkemper, K., Dehio, C., Schell, J. and Spena, A. (1994). Splicing of the *rolA* transcript of *Agrobacterium rhizogenes* in *Arabidopsis*. Science *266*, 1986-1988.

Malamy, J.E. and Benfey, P.N. (1997). Organization and cell differentiation in lateral roots of *Arabidopsis thaliana*. Development *124*, 33-44.

Martin-Tanguy, J., Corbineau, F., Burtin, D., Ben-Hayyimt, G. and Tepfer, D. (1993). Genetic transformation with a derivative of *rolC* from *Agrobacterium rhizogenes* and treatment with α-aminoisobutyric acid produce similar

phenotypes and reduce ethylene production and the accumulation of water-insoluble polyamines hydroxycinnamic acid conjugates in tobacco flowers. Plant Sci *93*, 63-76.

Matthysse, A.G. (2014). Attachment of *Agrobacterium* to plant surfaces. Front Plant Sci *5*, 252.

Matthysse, A.G. (1983). Role of bacterial cellulose fibrils in *A. tumefaciens* infection. J Bacteriol *154*, 906-915.

Matthysse, A.G., Holmes, K.V. and Gurlitz, R.H.G. (1981). Elaboration of cellulose fibrils by *Agrobacterium tumefaciens* during attachment to carrot cells. J Bacteriol *145*, 583-595.

Matthysse, A.G., Marry, M., Krall, L., Kaye, M., Ramey, B.E., Fuqua, C. and White, A.R. (2005). The effect of cellulose overproduction on binding and biofilm formation on roots by *Agrobacterium tumefaciens*. Mol Plant Microbe Interact *18*, 1002-1010.

Maurel, C., Barbierbrygoo, H., Spena, A., Tempé, J. and Guern, J. (1991). Single *rol* Genes from the *Agrobacterium rhizogenes* T_L-DNA alter some of the cellular-responses to auxin in *Nicotiana tabacum*. Plant Physiol *97*, 212-216.

Maurel, C., Brevet, J., Barbier-Brygoo, H., Guern, J. and Tempé, J. (1990). Auxin regulates the promoter of the root-inducing *rolB* gene of *Agrobacterium rhizogenes* in transgenic tobacco. Mol Gen Genet *223*, 58-64.

Maurel, C., Leblanc, N., Barbier-Brygoo, H., Perrot-Rechenmann, C., Bouvier-Durand, M. and Guern, J. (1994). Alterations of auxin perception in rolB-transformed tobacco protoplasts. Time course of *rolB* mRNA expression and

increase in auxin sensitivity reveal multiple control by auxin. Plant Physiol *105*, 1209-1215.

Mauro, M.L., De Lorenzo, G., Costantino, P. and Bellincampi, D. (2002). Oligogalacturonides inhibit the induction of late but not of early auxin-responsive genes in tobacco. Planta *215*, 494-501.

Mauro, M.L., Trovato, M., DePaolis, A., Gallelli, A., Costantino, P. and Altamura, M.M. (1996). The plant oncogene *rolD* stimulates flowering in transgenic tobacco plants. Dev Biol *180*, 693-700.

McCullen, C.A. and Binns, A.N. (2006). *Agrobacterium tumefaciens* and plant cell interactions and activities required for interkingdom macromolecular transfer. Annu Rev Cell Dev Biol *22*, 101-127.

Mehrotra, S., Kukreja, A.K., Khanuja, S.P.S. and Mishra, B.N. (2008). Genetic transformation studies and scale up of hairy root culture of *Glycyrrhiza glabra* in bioreactor. Electron J Biotechnol North America, 1115 04.

Mehrotra, S., Rahman, L.U. and Kukreja, A.K. (2010). An extensive case study of hairy-root cultures for enhanced secondary-metabolite production through metabolic-pathway engineering. Biotechnol Appl Biochem *56*, 161-172.

Messens, E., Lenaerts, A., van Montagu, M. and Hedges, R.W. (1985). Genetic basis for opine secretion from crown gall tumor cells. Mol Gen Genet *199*, 344-348.

Michael, T. and Spena, A. (1995). The plant oncogenes *rolA, B*, and *C* from *Agrobacterium rhizogenes.* Effects on morphology, development, and hormone metabolism. Methods Mol Biol *44*, 207-222.

Morita, M., shitan, N., Sawada, K., Van Montagu, M.C.E., Inzé, D., Rischer, H., Goossens, A., Oksman-Caldentey, K.M., Moriyama, Y. and Yazaki, K. (2009).

Vacuolar transport of nicotine is mediated by a multidrug and toxic compound extrusion (MATE) transporter in *Nicotiana tabacum*. Proc Natl Acad Sci U S A *106*, 2447-2452.

Moritz, T. and Schmülling, T. (1998). The gibberellin content of *rolA* transgenic tobacco plants is specifically altered. J Plant Physiol *153*, 774-776.

Moriuchi, H., Okamoto, C., Nishihama, R., Yamashita, I., Machida, Y. and Tanaka, N. (2004). Nuclear localization and interaction of RolB with plant 14-3-3 proteins correlates with induction of adventitious roots by the oncogene *rolB*. Plant J *38*, 260-275.

Mothes, K. (1954). Physiology of alkaloids. Annu Rev Plant Physiol *6*, 393-432.

Nam, J., Mysore, K.S. and Gelvin, S.B. (1998). *Agrobacterium tumefaciens* transformation of the radiation hypersensitive *Arabidopsis thaliana* mutants *uvh1* and *rad5*. Mol Plant Microbe Interact *11*, 1136-1141.

Namdeo, A.G. (2007) Plant cell elicitation for production of secondary metabolites: a review. Pharmacogn Rev *1*, 69-79.

Nilsson, O., Crozier, A., Schmülling, T., Sandberg, G. and Olsson, O. (1993a). Indole-3-acetic acid homeostasis in transgenic tobacco plants expressing the *Agrobacterium rhizogenes rolB* gene. Plant J *3*, 681-689.

Nilsson, O., Moritz, T., Imbault, N., Sandberg, G. and Olsson, O. (1993b). Hormonal characterization of transgenic tobacco plants expressing the *rolC* gene of *Agrobacterium rhizogenes* T_L-DNA. Plant Physiol *102*, 363-371.

Nilsson, O., Moritz, T., Sundberg, B., Sandberg, G. and Olsson, O. (1996). Expression of the *Agrobacterium rhizogenes rolC* Gene in a deciduous forest

tree alters growth and development and leads to stem fasciation. Plant Physiol *112*, 493-502.

Nilsson, O. and Olsson, O. (1997). Getting to the root: the role of the *Agrobacterium rhizogenes rol* genes in the formation of hairy roots. Physiol Plant *100*, 463-473.

Okada, K., Ueda, J., Komaki, M.K., Bell, C.J. and Shimura, Y. (1991). Requirement of the auxin polar transport-system in early stages of *Arabidopsis* floral bud formation. Plant Cell *3*, 677-684.

Ono, N.N. and Tian, L. (2011). The multiplicity of hairy root cultures: prolific possibilities. Plant Sci *180*, 439-446.

Oono, Y., Kanaya, K. and Uchimiya, H. (1990). Early flowering in transgenic tobacco plants possessing the *rolC* gene of *Agrobacterium rhizogenes* Ri plasmid. Jpn J Genet *65*, 7-16.

Otten, L. and Helfer, A. (2001) Biological activity of the *rolB*-like 5' end of the A4 *orf8* gene from the *Agrobacterium rhizogenes* T_L-DNA. Mol Plant Microbe Interact *14*, 405-411.

Ouartsi, A., Clérot, D., Meyer, A.D., Dessaux, Y., Brevet, J. and Bonfill, M. (2004) The T-DNA ORF8 of the cucumopine-type *Agrobacterium rhizogenes* Ri plasmid is involved in auxin response in transgenic tobacco. Plant Sci *166*, 557-567.

Ouyang, L., Luo, Y., Tian, M., Zhang, S.Y., Lu, R., Wang, J.H., Kasimu, R. and Li, X. (2014) Plant natural products: from traditional compounds to new emerging drugs in cancer therapy. Cell Proliferat *47*, 506-515.

Palazón, J., Cusidó, R.M., Gonzalo, J., Bonfill, M., Morales, C. and Piñol, M.T. (1998a). Relation between the amount of *rolC* gene product and indole alkaloid accumulation in *Catharanthus roseus* transformed root cultures. J Plant Physiol *153*, 712-718.

Palazón, J., Cusidó, R.M., Roig, C. and Piñol, M.T. (1998b). Expression of the *rolC* gene and nicotine production in transgenic roots and their regenerated plants. Plant Cell Rep *17*, 384-390.

Palazón, J., Cusidó, R.M., Roig, C. and Piñol, M.T. (1997). Effect of *rol* genes from *Agrobacterium rhizogenes* T_L-DNA on nicotine production in tobacco root cultures. Plant Physiol Biochem *35*, 155-162.

Palmer, A.G., Gao, R., Maresh, J., Erbil, W.K. and Lynn, D.G. (2004). Chemical biology of multi-host/pathogen interaction: chemical perception and metabolic complementation. Annu Rev Phytopathol *42*, 439-464.

Pandolfini, T., Storlazzi, A., Calabria, E., Defez, R. and Spena, A. (2000). The spliceosomal intron of the *rolA* gene of *Agrobacterium rhizogenes* is a prokaryotic promoter. Mol Microbiol *35*, 1326-1334.

Parr, A.J. and Hamill, J.D. (1987). Relationship between *Agrobacterium rhizogenes* transformed hairy roots and intact, uninfected *Nicotiana* plants. Phytochemistry *26*, 3241-3245.

Petit, A., David, C., Dahl, G.A., Ellis, J.G., Guyon, P., Casse-Delbart, D. and Tempé, J. (1983). Further extension of the opine concept: plasmids in *Agrobacterium rhizogenes* cooperate for opine degradation. Mol Gen Genet *190*, 204-214.

Pitzschke, A. and Hirt, H. (2010). New insights into an old story: *Agrobacterium*-induced tumour formation in plants by plant transformation. EMBO J *29*, 1021-1032.

Ramakrishna, A. and Ravishankar, G.S. (2011) Influence of abiotic stress signals on secondary metabolites in plants. Plant Signal Behav *6*, 1720-1731.

Rigden, D.J. and Carneiro, M. (1999). A structural model for the *rolA* protein and its interaction with DNA. Proteins *37*, 697-708.

Robinson, T. (1974). Metabolism and function of alkaloids in plants. Science *184*, 430-435.

Rodriguez-Navarro, D.N., Dardanelli, M.S. and Ruiz-Sainz, J.E. (2007). Attachment of bacteria to the roots of higher plants. FEMS Microbiol Lett *272*, 127-136.

Ruffing A.M. and Chen, R.R. (2012). Transcriptome profiling of a curdlan-producing *Agrobacterium* reveals conserved regulatory mechanisms of exopolysaccharide are involved in biofilm formation by *Rhizobium leguminosarum*. J Bacteriol *188*, 4474-4486.

Sano, T. and Nagata, T. (2002). The possible involvement of a phosphate-induced transcription factor encoded by *phi-2* gene from tobacco in ABA-signaling pathways. Plant Cell Physiol *43*, 12-20.

Saitoh, F., Noma, M. and Kawashima, N. (1985) The alkaloid contents of sixty *Nicotiana* species. Phytochemistry *24*, 477-480.

Saunders, J.A. (1979). Investigations of vacuoles isolated from tobacco: quantitation of nicotine. Plant Physiol *64*, 74-78.

Schäfer, A., Tauch, A., Jäger, W., Kalinowski, J., Thierbach, G. and Pühler, A. (1994). Small mobilizable multi-purpose cloning vectors derived from the

Escherichia coli plasmids pK18 and pK19: selection of defined deletions in the chromosome of *Corynebacterium glutamicum*. Gene *145*, 69-73.

Schmidt, G.W. and Delaney, S.K. (2010). Stable internal reference genes for normalization of real-time RT-PCR in tobacco (*Nicotiana tabacum*) during development and abiotic stress. Mol Genet Genomics *283*, 233-241.

Schmülling, T., Fladung, M., Grossmann, K. and Schell, J. (1993). Hormonal content and sensitivity of transgenic tobacco and potato plants expressing single *rol* genes of *Agrobacterium rhizogenes* T-DNA. Plant J *3*, 371-382.

Schmülling, T., Schell, J. and Spena, A. (1988). Single genes from *Agrobacterium rhizogenes* influence plant development. EMBO J *7*, 2621-2629.

Schmülling, T., Schell, J. and Spena, A. (1989). Promoters of the *rolA*, *B*, and *C* genes of *Agrobacterium rhizogenes* are differentially regulated in transgenic plants. Plant Cell *1*, 665-670.

Schrammeijer, B., Risseeuw, E., Pansegrau, W., Regensburg-Tuïnk, T.J.G., Crosby, W.L. and Hooykaas, P.J.J. (2001). Interaction of the virulence protein VirF of *Agrobacterium tumefaciens* with plant homologs of the yeast Skp1 protein. Curr Biol *11*, 258-262.

Schröder, G., Waffenschmidt, S., Weiler, E.W. and Schröder, J. (1984). The T-region of Ti plasmids codes for an enzyme synthesizing indole-3-acetic acid. Eur J Biochem *138*, 387-391.

Scorza, R., Zimmerman, T.W., Cordts, J.M., Footen, K.J. and Ravelonandro, M. (1994). Horticultural characteristics of transgenic tobacco expressing the *rolC* gene from *Agrobacterium rhizogenes*. J Am Soc Hortic Sci *119*, 1091-1098.

Sevón, N. and Oksman-Caldentey, K.M. (2002). *Agrobacterium rhizogenes*-mediated transformation: root cultures as a source of alkaloids. Planta Med *68*, 859-868.

Sharma, P., Padh, H. and Shrivastava, N. (2013) Hairy root cultures: a suitable biological system for studying secondary metabolic pathways in plants. Eng Life Sci *13*, 62-75.

Shaw, C.H., Watson, M.D., Carter, G.H. and Shaw, C.H. (1984). The right hand copy of the nopaline Ti-plasmid 25 bp repeat is required for tumour formation. Nucleic Acids Res *12*, 6031-6041.

Shen, W.H., Petit, A., Guern, J. and Tempé, J. (1988). Hairy roots are more sensitive to auxin than normal roots. Proc Natl Acad Sci U S A *85*, 3417-3421.

Shkryl, Y.N., Veremeichik, G.N., Bulgakov, V.P., Tchernoded, G.K., Mischenko, N.P., Fedoreyev, S.A. and Zhuravlev, Y.N. (2008). Individual and combined effects of the *rolA, B,* and *C* genes on anthraquinone producution in *Rubia cordifolia* transformed calli. Biotechnol Bioeng *100*, 118-125.

Shoji, T. and Hashimoto, T. (2008). Why does anatabine, but not nicotine, accumulate in jasmonate-elicited cultured tobacco BY-2 cells? Plant Cell Physiol *49*, 1209-1216.

Shoji, T. and Hashimoto, T. (2011a). Nicotine biosynthesis. In Plant Metabolism and Biotechnology. Edited by Ashihara, H., Crozier, A. and Komamine, A. pp. 191–216. John Wiley & Sons, New York.

Shoji, T. and Hashimoto, T. (2011b). Tobacco MYC2 regulates jasmonate-inducible nicotine biosynthesis genes directly and by way of the NIC2-locus ERF genes. Plant Cell Physiol *52*, 1117-1130.

Shoji, T. Kajikawa, M., and Hashimoto, T. (2010). Clustered transcription factor genes regulate nicotine biosynthesis in tobacco. Plant Cell *22*, 3390-3409.

Shoji, T. Nakajima, K., and Hashimoto, T. (2000a). Ethylene suppresses jasmonate-induced gene expression in nicotine biosynthesis. Plant Cell Physiol *41*, 1072-1076.

Shoji, T. Yamada, Y., and Hashimoto, T. (2000b). Jasmonate induction of putrescine N-methyltransferase genes in the root of *Nicotiana sylvestris*. Plant Cell Physiol *41*, 831-839.

Sinkar, V.P., Pythoud, F., White, F.F., Nester, E.W. and Gordon, M.P. (1988). *rolA* locus of the Ri plasmid directs developmental abnormalities in transgenic tobacco plants. Genes Dev *2*, 688-697.

Slightom, J.L., Durandtardif, M., Jouanin, L. and Tepfer, D. (1986). Nucleotide-sequence analysis of T_L-DNA of *Agrobacterium rhizogenes* agropine type plasmid. Identification of open reading Frames. J Biol Chem *261*, 108-121.

Smulders, M.J.M., Janssen, G.F.E., Croes, A.F., Barendse, G.W.M. and Wullems, G.J. (1988). Auxin regulation of flower bud formation in tobacco explants. J Exp Bot *39*, 451-459.

Smulders, M.J.M., Visser, E.J.W., Vanderkrieken, W.M., Croes, A.F. and Wullems, G.J. (1990). Effects of the developmental state of the tissue on the competence for flower bud regeneration in pedicel explants of tobacco. Plant Physiol *92*, 582-586.

Sonti, R.V., Chiurazzi, M., Wong, D., Davies, C.S., Harlow, G.R., Mount, D.W. and Signer, E.R. (1995). *Arabidopsis* mutants deficient in T-DNA integration. Proc Natl Acad Sci U S A *92*, 11786-11790.

Spanò, L., Mariotti, D., Cardarelli, M., Branca, C. and Costantino, P. (1988). Morphogenesis and auxin sensitivity of transgenic tobacco with different complements of Ri T-DNA. Plant Physiol *87*, 479-483.

Spena, A., Schmülling, T., Koncz, C. and Schell, J.S. (1987). Independent and synergistic activity of *rol A*, *B* and *C* loci in stimulating abnormal growth in plants. EMBO J *6*, 3891-3899.

Sprunck, S., Jacobsen, J.J. and Reinard, T. (1995). Indole-3-lactic acid is a weak auxin analogue but not an anti-auxin. J Plant Growth Regul *14*, 191-197.

Srivastava, S. and Srivastava, A.K. (2007). Hairy root culture for mass-production of high-value secondary metabolites. Crit Rev Biotechnol *27*, 29-43.

Stachel, S.E., Messens, E., Vanmontagu, M. and Zambryski, P. (1985). Identification of the signal molecules produced by wounded plant-cells that activate T-DNA transfer in *Agrobacterium tumefaciens*. Nature *318*, 624-629.

Stachel, S.E. and Nester, E.W. (1986). The genetic and transcriptional rrganization of the *vir* region of the A6-Ti plasmid of *Agrobacterium* tumefaciens. EMBO J *5*, 1445-1454.

Stähelin, H. (1970). 4'-Demethyl-epipodophyllotoxin thenylidene glucoside (VM-26), a podophyllum compound with a new mechanism of action. Eur J Cancer *6*, 303-311.

Stähelin, H. (1973). Activity of a new glycosidic lignan derivative (VP 16-213) related to podophyllotoxin in experimental tumors. Eur J Cancer *9*, 215-221.

Steppuhn, A., Gase, K., Krock, B., Halitschke, R. and Baldwin, I.T. (2004). Nicotine's defensive function in nature. PLoS Biol *2*, E217.

Stieger, P.A., Meyer, A.D., Kathmann, P., Frundt, C., Niederhauser, I., Barone, M. and Kuhlemeier, C. (2004) The *orf13* T-DNA gene of *Agrobacterium rhizogenes* confers meristematic competence to differentiated cells. Plant Physiol *135*, 1798-1808.

Sugaya, S. and Uchimiya, H. (1992). Deletion analysis of the 5'-upstream region of the *Agrobacterium rhizogenes* Ri plasmid *rolC* gene required for tissue-specific expression. Plant Physiol *99*, 464-467.

Sun, L.Y., Monneuse, M.O., Martin-Tanguy, J. and Tepfer, D. (1991). Changes in flowering and the accumulation of polyamines and hydroxycinnamic acid-polyamine conjugates in tobacco plants transformed by the *rolA* locus from the Ri T_L-DNA of *Agrobacterium rhizogenes*. Plant Sci *80*, 145-156.

Swain, S.S., Sahu, L., Barik, D.P. and Chand, P.K. (2010). *Agrobacterium* x plant factors influencing transformation of 'Joseph's coat' (*Amaranthus tricolor* L.). Sci Hortic-Amsterdam *125*, 461-468.

Szechtman, A.D., Salts, Y., Carmi, N., Shabtai, S., Pilowsky, M. and Barg, R. (1997). Seedless fruit setting in response to NAM treatment of transgenic tomato expressing the *iaaH* gene specifically in the ovary. Acta Hort *447*, 597-598.

Tabata, M., Yamamoto, H., Hiraoka, N., Marumoto, Y. and Konoshim.M (1971). Regulation of nicotine production in tobacco tissue culture by plant growth regulators. Phytochemistry *10*, 723-729.

Takahashi, M. and Yamada, Y. (1973). Regulation of nicotine production by auxins in tobacco cultured cells in vitro. Agr Biol Chem Tokyo *37*, 1755-1757.

Taneja, J., Jaggi, M., Wankhede, D.P. and Sinha, A.K. (2010) Effect of loss of T-DNA genes on MIA biosynthetic pathway gene regulation and alkaloid

accumulation in *Catharanthus roseus* hairy roots. Plant Cell Rep *29*, 1119-1129.

Tepfer, D. (1984). Transformation of several species of higher plants by *Agrobacterium rhizogenes*- sexual transmission of the transformed genotype and phenotype. Cell *37*, 959-967.

Thoma, S., Hecht, U., Kippers, A., Botella, J., Devries, S. and Somerville, C. (1994). Tissue-specific expression of a gene encoding a cell wall-localized lipid transfer protein from *Arabidopsis*. Plant Physiol *105*, 35-45.

Thomashow, L.S., Reeves, S. and Thomashow, M.F. (1984). Crown gall oncogenesis: evidence that a T-DNA gene from the *Agrobacterium* Ti plasmid pTiA6 encodes an enzyme that catalyzes synthesis of indoleacetic acid. Proc Natl Acad Sci U S A *81*, 5071-5075.

Thomashow, M.F., Hughly, S., Buchholz, W.G. and Thomashow, L.S. (1986). Molecular basis for the auxin-independent phenotype of crown gall tumor tissue. Science *231*, 616-618.

Tinland, B., Fournier, P., Heckel, T. and Otten, L. (1992). Expression of a chimeric heat-shock-inducible *Agrobacterium 6b* oncogene in *Nicotiana rustica*. Plant Mol Biol *18*, 921-930.

Tinland, B., Schoumacher, F., Gloeckler, V., Bravoangel, A.M. and Hohn, B. (1995). The *Agrobacterium tumefaciens* virulence D2 protein is responsible for precise integration of T-DNA into the plant genome. EMBO J *14*, 3585-3595.

Tomlinson, A.D., Ramey-Hartung, B., Day, T.W., Merritt, P.M. and Fuqua, C. (2010). *Agrobacterium tumefaciens* ExoR represses succinoglycan biosynthesis and is required for biofilm formation and motility. Microbiology *156*, 2670-2681.

Trovato, M., Maras, B., Linhares, F. and Costantino, P. (2001). The plant oncogene *rolD* encodes a functional ornithine cyclodeaminase. Proc Natl Acad Sci U S A *98*, 13449-13453.

Trovato, M., Mauro, M.L., Costantino, P. and Altamura, M.M. (1997). The *rolD* gene from *Agrobacterium rhizogenes* is developmentally regulated in transgenic tobacco. Protoplasma *197*, 111-120.

Tsukagoshi, H., Busch, W. and Benfey, P.N. (2010). Transcriptional regulation of ROS controls transition from proliferation to differentiation in the root. Cell *143*, 606-616.

Tzfira, T. and Citovsky, V. (2002). Partners-in-infection: host proteins involved in the transformation of plant cells by *Agrobacterium*. Trends Cell Biol *12*, 121-129.

Tzfira, T., Vaidya, M. and Citovsky, V. (2004). Involvement of targeted proteolysis in plant genetic transformation by *Agrobacterium*. Nature *431*, 87-92.

Ulker, B., Li, Y., Rosso, M.G., Logemann, E., Somssich, I.E. and Weisshaar, B. (2008). T-DNA-mediated transfer of *Agrobacterium tumefaciens* chromosomal DNA into plants. Nature Biotechnol *26*, 1015-1017.

Umber, M., Clément, B. and Otten, L. (2005) The T-DNA oncogene A4-*orf8* from *Agrobacterium rhizogenes* A4 induces abnormal growth in tobacco. Mol Plant Microbe Interact *18*, 205-211.

Umber, M., Voll, L., Weber, A., Michler, P. and Otten, L. (2002) The *rolB*-like part of the *Agrobacterium rhizogenes orf8* gene inhibits sucrose export in tobacco. Mol Plant Microbe Interact *15*, 956-962.

Vaishnav, P. and Demain, A.L. (2011). Unexpected applications of secondary metabolites. Biotechnol Adv *29*, 223-229.

van Altvorst, A.C., Bino, R.J., van Dijk, A.J., Lamers, A.M.J., Lindhout, W.H., van der Mark, F. and Dons, J.J.M. (1992). Effects of the introduction of *Agrobacerium rhizogenes rol* genes on tomato plant and flower development. Plant Sci *83*, 77-85.

van der Salm, T.P.M., van der Toorn, C.J.G., Bouwer, R., Charlotte, H., ten Cate, H. and Dons, H.J.M. (1997). Production of *rol* gene transformed plants of *Rosa hybrida* L. and characterization of their rooting ability. Mol Breed *3*, 39-47.

van Onckelen, H., Prinsen, E., Inzé, D., Rüdelsheim, P., van Lijsebettens, M., Follin, A., Schell, J., van Montagu, M. and De Greef, J. (1986). *Agrobacterium* T-DNA gene *1* codes for tryptophan 2-monooxygenase activity in tobacco crown gall cells. FEBS Lett *198*, 357-360.

Vansuyt, G., Vilaine, F., Tepfer, M. and Rossignol, M. (1992). *rolA* modulates the sensitivity to auxin of the proton translocation catalyzed by the plasma membrane H'-ATPase in transformed tobacco. FEBS Lett *298*, 89-92.

Venis, M.A., Napier, R.M., Barbierbrygoo, H., Maurel, C., Perrotrechenmann, C. and Guern, J. (1992). Antibodies to a peptide from the maize auxin-binding protein have auxin agonist activity. Proc Natl Acad Sci USA *89*, 7208-7212.

Veselov, D., Langhans, M., Hartung, W., Aloni, R., Feussner, I., Götz, C., Veselova, S., Schlomski, S., Dickler, C., Bächmann, K. and Ullrich, C.I. (2003). Development of *Agrobacterium tumefaciens* C58-induced plant tumors and impact on host shoots are controlled by a cascade of jasmonic acid, auxin, cytokinin, ethylene and abscisic acid. Planta *216*, 512-522.

Vilaine, F., Charbonnier, C. and Cassedelbart, F. (1987). Further insight concerning the TL region of the Ri plasmid of *Agrobacterium rhizogenes* strain A4:

transfer of a 1.9 kb fragment is sufficient to induce transformed roots on tobacco leaf fragments. Mol Gen Genet *210*, 111-115.

Vilaine, F., Rembur, J., Chriqui, D. and Tepfer, M. (1998). Modified development in transgenic tobacco plants expressing a *rolA*::*gus* translational fusion and subcellular localization of the fusion protein. Mol Plant Microbe Interact *11*, 855-859.

von Dahl, C.C., Winz, R.A., Halitschke, R., Kühnemann, F., Gase, K. and Baldwin, I.T. (2007). Tuning the herbivore-induced ethylene burst: the role of transcript accumulation and ethylene perception in *Nicotiana attenuata*. Plant J *51*, 293-307.

Wabiko, H. and Minemura, M. (1996). Exogenous phytohormone-independent growth and regeneration of tobacco plants transgenic for the *6b* gene of *Agrobacterium tumefaciens* AKE10. Plant Physiol *112*, 939-951.

Wang, J.H., Lin, H.H., Liu, C.T., Lin, T.C., Liu, L.Y. and Lee, K.T. (2014). Transcriptomic analysis reveals that reactive oxygen species and genes encoding lipid transfer protein are associated with tobacco hairy root growth and branch development. Mol Plant Microbe Interact *27*, 678-687.

Wang, K., Herrera-Estrella, L., van Montagu, M. and Zambryski, P. (1984). Right 25 by terminus sequence of the nopaline T-DNA is essential for and determines direction of DNA transfer from *Agrobacterium* to the plant genome. Cell *38*, 455-462.

Weiler, E.W. and Spanier, K. (1981). Phytohormones in the formation of crown gall tumors. Planta *153*, 326-337.

Wasternack, C. (2007). Jasmonates: an update on biosynthesis, signal transduction and action in plant stress response, growth and development. Ann Bot *100*, 681-697.

Wasternack, C. and Hause, B. (2013). Jasmonates: biosynthesis, perception, signal transduction and action in plant stress response, growth and development. An update to the 2007 review in Annals of Botany. Ann Bot *111*, 1021-1058.

Weathers, P.J., Cheetham, R.D., Follansbee, E. and Teoh, K. (1994). Artemisinin production by transformed roots of *Artemisia annua*. Biotechnol Lett *16*, 1281-1286.

Wei, M., Jiang, S.T. and Luo, J.P. (2007) Enhancement of growth and polysaccharide production in suspension cultures of protocorm-like bodies from *Dendrobium huoshanense* by the addition of putrescine. Biotechnol Lett *29*, 495-499.

White, F.F., Taylor, B.H., Huffman, G.A., Gordon, M.P. and Nester, E.W. (1985). Molecular and genetic analysis of the transferred DNA regions of the root-inducing plasmid of *Agrobacterium rhizogenes*. J Bacteriol *164*, 33-44.

Wilson, M., Savka, M.A., Hwang, I., Farrand, S.K. and Lindow, S.E. (1995). Altered epiphytic colonization of mannityl opine-producing transgenic tobacco plants by a mannityl opine-catabolizing strain of *Pseudomonas syringae*. Appl Environ Microbiol *61*, 2151-2158.

Winans, S.C. (1992). Two-way chemical signaling in *Agrobacterium*-plant interactions. Microbiol Rev *56*, 12-31.

Winans, S.C., Kerstetter, R.A. and Nester, E.W. (1988). Transcriptional regulation of the *virA* gene and *virG* gene of *Agrobacterium tumefaciens*. J Bacteriol *170*, 4047-4054.

Xu, B. and Timko, M. (2004). Methyl jasmonate induced expression of the tobacco putrescine N-methyltransferase genes requires both G-box and GCC-motif elements. Plant Mol Biol *55*, 743-761.

Xu, J., Kim, J., Danhorn, T., Merritt, P.M. and Fuqua, C. (2012). Phosphorus limitation increases attachment in *Agrobacterium tumefaciens* and reveals a conditional functional redundancy in adhensin biosynthesis. Res Microbiol *163*, 674-684.

Yadav, N.S., Vanderleyden, J., Bennett, D.R., Barnes, W.M. and Chilton, M.D. (1982). Short direct repeats flank the T-DNA on a nopaline Ti plasmid. Proc Natl Acad Sci U S A 79, 6322-6326.

Yi, H., Mysore, K.S. and Gelvin, S.B. (2002). Expression of the *Arabidopsis* histone H2A-1 gene correlates with susceptibility to *Agrobacterium* transformation. Plant J *32*, 285-298.

Yi, H., Sardesai, N., Fujinuma, T., Chan, C.W., Veena, J.H. and Gelvin, S.B. (2006). Constitutive expression exposes functional redundancy between the *Arabidopsis* histone H2A gene HTA1 and other H2A gene family members. Plant Cell *18*, 1575-1589.

Yokoyama, R., Hirose, T., Fujii, N., Aspuria, E.T., Kato, A. and Uchimiya, H. (1994). The *rolC* promoter of *Agrobacterium rhizogenes* Ri plasmid is activated by sucrose in transgenic tobacco plants. Mol Gen Genet *244*, 15-22.

Yuan, J.S., Reed, A. and Chen, F., Stewart, C.N. (2006). Statistical analysis of real-time PCR data. BMC Bioinformatics *7*, 85-96.

Zhang, H.B., Bokowiec, M.T., Rushton, P.J., Han, S.C. and Timko, M.P. (2012). Tobacco transcription factors NtMYC2a and NtMYC2b form nuclear

complexes with the NtJAZ1 repressor and regulate multiple jasmonate-inducible steps in nicotine biosynthesis. Mol Plant *5*, 73-84.

Zheng, Y., He, X.W., Ying, Y.H., Lu, J.F., Gelvin, S.B. and Shou, H.X. (2009). Expression of the *Arabidopsis thaliana* histone gene AtHTA1 enhances rice transformation efficiency. Mol Plant *2*, 832-837.

Zambryski, P., Depicker, A., Kruger, K. and Goodman, H.M. (1982). Tumor induction by *Agrobacterium tumefaciens*: analysis of the boundaries of T-DNA. J Mol Appl Genet *1*, 361-370.

Zhou, M.L., Zhu, X.M., Shao, J.R., Tang, Y.X. and Wu, Y.M. (2011). Production and metabolic engineering of bioactive substances in plant hairy root culture. Appl Microbiol Biot *90*, 1229-1239.

Zhu, Y., Nam, J., Humara, J.M., Mysore, K.S., Lee, L.Y., Cao, H., Balentine, L., Li, J., Kaiser, A.D., Kopecky, A.L., Hwang, H.H., Bhattacharjee, S., Rao, P.K., Tzfira, T., Rajagopal, J., Yi, H., Veena, J.H., Yadav, B.S., Crane, Y.M., Lin, K., Larcher, Y., Gelvin, M.J.K., Knue, M., Ramos, C., Zhao, X., Davis, S.J., Kim, S.I., Ranjith-Kumar, C.T., Choi, Y.J., Hallan, V.K., Chattopadhyay, S., Sui, X., Ziemienowicz, A., Matthysse, A.G., Citovsky, V., Hohn, B. and Gelvin, S.B. (2004). Identification of *Arabidopsis rat* mutants. Plant Physiol *132*, 494-505.

Ziemienowicz, A. (2001). Odyssey of *Agrobacterium* T-DNA. Acta Biochim Pol *48*, 623-635.

Appendix

Supplementary Table S1. Reference genes for qRT-PCR.

Transcripts	Correlation coefficient of Ct value and log (ssDNA concentration)
18s rRNA	-0.6831
TAC-9	-0.991
EF-1α	-0.9695
L25	-0.9799
TUBA1	-0.9738
β-TUB	-0.9888
NtUBC2	-0.9835
PP2A	-0.9832
NtCP-23	-0.8984

Supplementary Table S2. PCR conditions.

***Taq* DNA Polymerase Master Mix Red (Ampliqon) for general PCR &**

Expand High Fidelity PCR System (Roche) for Southern probe preparation

Stage 1:

95°C	5 minutes

Stage 2 (30 cycles):

95°C	30 seconds
55°C	30 seconds
72°C	1 kb/1 minutes

Stage 3:

72°C	5 minutes

Phusion Flash High-Fidelity PCR Master Mix (Thermo Scientifics) for cloning

Stage 1:

98°C	2 minutes

Stage 2 (30 cycles):

98°C	5 seconds
55°C	15 seconds
72°C	1 kb/15 seconds

Stage 3:

72°C	5 minutes

Advantage 2 Polymerase Mix (Clontech) for cDNA library construction

Stage 1:

95°C 1 minutes

Stage 2 (26 cycles):

95°C 10 seconds

68°C 6 minutes (ramp 5 seconds per cycle)

Stage 3:

68°C 5 minutes

Advantage 2 Polymerase Mix (Clontech) for yeast-two hybrid screening

Stage 1:

95°C 1 minutes

Stage 2 (30 cycles):

95°C 10 seconds

68°C 2 minutes

Stage 3:

68°C 5 minutes

Supplementary Table S3. The primers used in this study.

Purpose	Gene	Forward Primer	Reverse Primer
Upstream of target deleting sequence	*rol*A	AACTGGCTTGTCACCTGGTC	CGAACGCTAGGCAACAGTAA
	*rol*B	CTCATCGCTGCTTGTCACAT	TGTCGTGTTGTTTGGCCTTA
	*rol*C	TAAAATACGGCGTCGGAAAC	AATTAATGGATGCGGCTGTC
	*rol*D	TGTTGAAGCTGAGTGGCATC	TGCTTGGAGGGTACTTTTGG
Downstream of target deleting sequence	*rol*A	ttactgttgcctagcgttcg GCGCGATTGTCCTGTTTTAT	CCAGAAACGATGGGCTCTT
	*rol*B	taaggccaaacaacacgaca CTATGTACCCTCCCGCAGTC	GAAAGGAAATCCGCAATCAA
	*rol*C	gacagccgcatccattaatt GATGGGCTGACGAGTTTGAT	TTGTTCTCCTTGCAGGCTGT
	*rol*D	ccaaaagtaccctccaagca TTCATCGTTTCTCGCAATCA	GCGTATCGAATTCACCGTTT
Probe synthesis for Southern blot	*g3dph*	ATCAAGGCTGCATCGAAC	AAGTGAGGATACGCACG
	*vir*A	TACAAAGCGTGAGAGAGCA	CCAATCTCTTTGATTAGCTCTTCATA
	*rol*A	TGGAATTAGCCGGACTAAACG	GGTCTGAATTTTCACGTCCG
	*rol*B	TGGAGTTAAAAGTGACCAACGT	TTAGGCTTCTTTCTTCAGGTTTAC
	*rol*C	ATGGCTGAAGACGACCTGTG	GAAGCAGAGCATCATCGTCG
	*rol*D	GCGGTATGAAACTGACCCAA	TTAATGCCCGTGTTCCATCG
qRT-PCR for LTPs	BQ842876	GGTTCCATCTGGCTTCCAGTGTGC	CCCTAGACCACCTTGTGCGCT
	EH618856/ AB041519	CCCATCCAAAGGCAAGTGCCCA	AGCAGCCTCAAGGTCAGCAACA
	EB443656	AGTGTCGAGGGCACAGGGAA	CTTGGCTGTAGGCGCCGAGG
	EB450585	CCGCTAGCCCCGCGATCAAG	GCAAGGCAGGTGCCCGAGAG
	D86629	GGCAACGGAGGTGGTTCGGG	CCAGCCCCGCGATCAAGCTG
	DV157577	CCCTGGTAGGCCCCACCCTC	GCCAGGTGGCCTTGTGACCG
	BQ842956	GCCAGGTGGCCTTGTGACCG	CCCTGGTAGGCCCCACCCTC
	AF043554	GCTCTGAAGTTGGGTGTATGTG	TGGCATCGTTGGAGGACTC
	AB035125	AGCCGAAGTACCCGATTA	ATTGGGCTTTACGATCCTG
	DW003388	CACACAACTTGGGTTGGCTGAGT	GCCGTGAGTCCATCATCGCCC
	FG191218	GCTTCAAGTTCCACAAGTC	GTTCCTCCAGTTACACCAT
	FG137954	TTGGTTGTGGATATTGTGGAA	CAGGTGGCAAGTTGATAGG

Supplementary Table S3. The Primers used in this study (*continue).*

Purpose	Gene	Forward Primer	Reverse Primer
Reference genes for qRT-PCR	18S rRNA	GGTGGAGCGATTTGTCTGGT	CAGGCTGAGGTCTCGTTCGT
	TAC-9	CCTGAGGTCCTTTTCCAACCA	GGATTCCGGCAGCTTCCATT
	EF-1α	TGAGATGCACCACGAAGCTC	CCAACATTGTCACCAGGAAGTG
	L25	CCCCTCACCACAGAGTCTGC	AAGGGTGTTGTTGTCCTCAATCTT
	TUB A1	CAAGACTAAGCGTACCATCCA	TTGAATCCAGTAGGGCACCAG
	β-tubulin	GCATCTTTGCGTACACTTTGCT	ACATAAGCCCAAAACTAGCTGGA
	NtUBC2	CTGGACAGCAGACTGACATC	CAGGATAATTTGCTGTAACAGATTA
	PP2A	GTGAAGCTGTAGGGCCTGAGC	CATAGGCAGGCACCAAATCC
	NTCP-23	CACCACAAAGGGCAATCTCA	CCGCCAGTCTTTCGTCTCC
qRT-PCR: nicotine synthetic pathway	ODC	ACTGTGTTTGGGCCCACTTG	CCATATTAGGAAAAACCAGC
	PMT	ATTGGACCAAGATCGAGTC	ATTACTGCAGAATTCTCCTAC
	MPO1	CAGTGATGTTACTGAAACTA	ATAGGCGAGGAGGACTCATG
	MPO2	TCCTCGGGGATGTGACTTG	GCTTGGCCATCAAACTACTGG
	AO	TTAACAAAGTCATCCGTCGG	ATTTAGTCTTGAGGTAGACC
	QS	AATCACTGCTTGATGGTATC	ACTGGCAAGTTCTTGGACTC
	QPT	GACGCATTCCGTGAAAGCAC	AAGTAATGGCGCTCATGCTC
	A622	CATAGCGACATACACTATCG	GGCATATGGCCAAATTAGTC
qRT-PCR: nicotine storage	MATE	CAAGGAATGAAGGTGGTGGC	GACTTCTTTCCCCTTGCATA
	JAT1	AATTTCGAACACTTCGATGG	TACCCCTAAATTCGAACGCC
qRT-PCR: polyamine synthetic pathway	SPDS	AGATGTAGCTGTAGGATACG	ATCGTAAGTTCCTGCAGCAA
	SAMS	ACCAAGGTGGACAGGAGTGG	CATAAGAAACCTGGACAATG
	SAMDC	CAGTGTCCGTGTCTGTCTCTG	ACAAATCCGAACGACACAGC
qRT-PCR: *rol* genes	*rolA*	GGAATTAGCCGGACTAAACG	AAGTCATGGCCAAAGGAGTG
	rolB	GAATGCTTCATCGCCATTTT	GATATCCCGAGGGCATTTTT
	rolC	CAATAGAGGGCTCAGGCAAG	CCTCACCAACTCACCAGGTT
	rolD	TTTCGAGCTCGTCGAAAAGT	CGCAGATAGGACATGCTCAA
Real-time PCR for AP2/ERFs	ERF189	GCAGCTTCGACTGCAGCTTCCT	CTCCTCGGACTCGGAGCACTTC
	ERF199	TTAGCAGCTTCGACTTCGAC	CGGAGTACTTTTCATGGGAT
	ERF115/29	CAGAAAARTARCTTSRAHAYCTC	CCTTYVTTTCCTCCTCRGACTC
	ERF179/130/168	GAAACAACAAYTCTCGAATCTC	KCCTCCAATHTTGCTTCGTG
	ERF163/210	CAGAAAACAACTTTTACTATGGG	TTCATGAAACTTTTCAGTGGC
	ERF91	CTGATCTCTTCCGTCCTTG	GCATTACTAAAACATTGATC
	ERF10	TAGGTCCCAACTGGGTTCTG	AATTCATTACTTCAGCCAAG

Supplementary Table S3. The Primers used in this study (*continue).*

Purpose	Gene	Forward Primer	Reverse Primer
promoter:: YFP::HA	*rol*B	TAACAAAGTAGGAAACAGGTTG	CATTGTGATGTGAGTTGGAT
	*rol*C	TGTGATGTGAGTTGGATAGTTACG	CATGTTAACAAAGTAGGAAA
promoter::*rol*:: YFP::HA	*rolB*	TAACAAAGTAGGAAACAGGTTG	GGCTTCTTTCTTCAGGTTTAC
	rolC	TGTGATGTGAGTTGGATAGTTACG	GCCGATTGCAAACTTGCAC
promoter:: HA::YFP	*rol*B promoter	GTTAACAAAGTAGGAAACAGGTTGC	agcgtaatctggaacatcgtatgggta CATTGTGATGTGAGTTGGATAGTT
	*rol*C promoter	TGTGATGTGAGTTGGATAGTTACG	agcgtaatctggaacatcgtatgggta CATGTTAACAAAGTAGGAAACAGG
	eYFP-forward-HA	tacccatacgatgttccagattacgctgctgaagctgcagcta aagaagctgcagctaaagcagtgagcaagggcgaggag	
	eYFP-reverse		tcaTCACTTGTACAGCTCGTCCATGC
promoter::HA:: YFP::*rol*	*rolB* coding region	gatctggaggtggaggttcaATGGATCCCAAATT GCTATTC	TCATCAGGCTTCTTTCTTCAGGTTTAC TG
	rolC coding region	gatctggaggtggaggttcaATGGCTGAAGACG ACCTGTG	TCATCAGCCGATTGCAAACTTGCAC
Yeast two-hybrid, DNA-binding domain fusion protein	*rol*B	gaattcATGGATCCCAAATTGCTATT	gaattcTTAGGCTTCTTTCTTCAGGTT
	*rol*C	gggaattcATGGCTGAAGACGACCTGTG	agaattcTTAGCCGATTGCAAACTTGCAC
GST-Rol protein by *E. coli* expression	GST	ATGTCCCCTATACTAGGTTATTGG	CAAACTTGTTTGATTCGACC
	rolB	ggtcgaatcaaacaagtttg ATGGATCCCAAATTGCTATT	agctacaagctt TTAGGCTTCTTTCTTCAGGTTT
	rolC	ggtcgaatcaaacaagtttg ATGGCTGAAGACGACCTGTGTTCTCT	agctacaagctt TTAGCCGATTGCAAACTTGCACTC
	GST-control		TTACAAACTTGTTTGATTCGACC

- Capital letters indicate priming sequencing, black small letters indicate sequence for restriction-ligation applications, and gray small letters in downstream of target deleting sequences are the complementary sequences to upstream of targeting sequences.